Stem cell dynamics in *Macrostomum lignano* (Platyhelminthes) during homeostasis and regeneration

Freija Verdoodt

Promoters:

Prof. dr. Wim Bert (UGent)

dr. Maxime Willems (UGent)

Thesis submitted to obtain the degree of doctor in Sciences

Proefschrift voorgelegd tot het bekomen van de graad van doctor in de Wetenschappen

Dit werk werd mogelijk gemaakt door een beurs van het Instituut voor de Aanmoediging van Innovatie door Wetenschap en Technologie in Vlaanderen (IWT-Vlaanderen)

This work was supported by a grant of the Institute for Promotion of Innovation through Science and Technology in Flanders (IWT-Flanders).

Reading Committee:

Prof. dr. Peter Ladurner (University of Innsbruck, Austria)

Dr. Karen Smeets (Hasselt University, Belgium)

Prof. dr. Gerlinde Van de Walle (Ghent University, Belgium)

Dr. Katrien De Mulder (Ghent University, Belgium)

Examination Committee:

Prof. dr. Bart Braeckman (chairman, Ghent University, Belgium)

Prof. dr. Wim Bert (secretary, promoter, Ghent University, Belgium)

Prof. dr. Peter Ladurner (University of Innsbruck, Austria)

Dr. Karen Smeets (Hasselt University, Belgium)

Prof. dr. Gerlinde Van de Walle (Ghent University, Belgium)

Dr. Katrien De Mulder (Ghent University, Belgium)

Prof. dr. Ann Huysseune (Ghent University, Belgium)

Dr. Maxime Willems (promotor, Ghent University, Belgium)

Acknowledgements

Dit is het moment waarnaar ik vier jaar lang heb uitgekeken, stiekem weliswaar. Ik heb namelijk steevast beweerd dat ik niet op de feiten vooruit zou lopen en dat ik mijn onderzoek jaar per jaar, verlenging per verlenging, en artikel per artikel zou aanpakken. De uitdrukking 'We zien wel hoe het afloopt' is mij niet vreemd. Toch zat het schrijven van mijn dankwoord, als een streefdoel ergens diep in mijn achterhoofd. Enerzijds natuurlijk omdat dit samengaat met het voltooien van mijn doctoraatsthesis (zonder dit zou het maar een dun boekje worden), maar vooral omdat ik dan iedereen zou kunnen bedanken die heeft bijgedragen aan dit project. En zo zijn er wel een paar. Zonder twijfel hebben elk van de hieronder vernoemde personen, met behulp van praktische tips en/of kritische (tot zéér kritische) opmerkingen, bijgedragen aan een verbeterd resultaat en dus ook aan een betere 'mentale gezondheid'. Hoewel, dit laatste niet altijd in eerste instantie, maar dan wel in tweede … of toch op zen minst in derde instantie. Want, ja het is een enorm verrijkende, horizon-verruimende en intrigerende ervaring, maar het zal niemand verbazen als ik zeg dat het soms ook een beetje 'irritant' (tot 'zéér irritant') was. Hoedanook, alles in acht genomen, was een onvergetelijke en mooie (tot zéér mooie) tijd.

In eerste instantie, wil ik graag mijn promotor en begeleider **Maxime Willems** bedanken. Jij hebt bij mij het idee opgewekt dat ik, na het werken met Macrostomum lignano tijdens mijn thesis, dit onderzoek zou kunnen voortzetten. Je hebt er dan ook voor gezorgd dat ik een IWT-project kon binnenhalen, door me zeer intensief en vol enthousiasme te begeleiden bij de aanvraag hiervan. Ook tijdens mijn doctoraat leek je enthousiasme vaak onuitputtelijk. Kortom, zonder Willems M. geen Verdoodt F. et al. Hartelijk dank, maxime.

Mijn andere promotor, **Wim Bert**, wil ik eveneens bedanken. Hoewel ik pas laat in jouw groep terecht kwam en mijn onderzoek inhoudelijke weinig raakvlakken heeft met dat van

jou, tonen parametrische (ja, en zelf niet-parametrische) testen aan dat je bijdrage hoogst significant was ($p<0.01$).

Subsequently, I want to thank **Peter Ladurner**, who has invited me to come to Innsbruck for a cooperation. I have learned a great deal from that experience, and, without a doubt, your input has had a major effect on the quality of my study. Furthermore, I sincerely want to thank you for willing to go along with the LRC-idea.

Stijn Mouton wil ik bedanken voor de wetenschappelijke babbels tijdens de voorbije vier jaar. Je was een zeer bereikbaar klankbord waaraan ik mijn hypotheses kon toetsen en dat heb ik ten zeerste kunnen appreciëren. Voorts wil ik ook nog graag vermelden dat, indien er een soundtrack bij mijn doctoraat zou horen, enkele van jouw muzikale invloeden er zeker deel van zouden uitmaken, waarvoor eveneens dank.

Marjolein Couvreur wil ik uitgebreid bedanken. Eerst en vooral voor de fantastische en professionele technische begeleiding van mijn experimenten en culturen. Niet zelden hebben jouw suggesties het verschil gemaakt. Daarnaast wil ik je ook bedanken voor de steun die je voor me was tijdens mijn onderzoek. Ik kon haast altijd bij jou terecht met m'n kleine en grote (en soms ook immense) frustraties, maar ook voor mijn overwinningen was je mijn favoriete klankbord. Je was een ongelooflijke stimulans tijdens mijn onderzoek. Bovendien, heb je me vaak aan het lachen gebracht. Hoewel je echt rotslecht bent in het vertellen van moppen, apprecieer ik de herhaaldelijke pogingen ten zeerste.

Katrien De Mulder wil ik van harte bedanken voor haar opmerkelijke wetenschappelijke ingesteldheid en de bereidheid om dit talent meermaals in te zetten, ten behoeve van mijn onderzoek (en dat van vele anderen!). Je onbeperkte behulpzaamheid, fascinatie en bescheidenheid doen me nog vaak met verstomming slaan en deze zeldzame combinatie maakt jou, in mijn ogen, een top-wetenschapper. Ik wens elke prof dan ook 'een Katrien' in

zijn/haar groep toe. Los daarvan wil ik je eigenlijk voornamelijk bedanken voor je vriendschap, je hardnekkig optimisme, je vrolijkheid en je humor. Dus Katrien, tot snel!

Wouter Houthoofd wil ik bedanken voor het tijdelijk op zich nemen van het promotorschap van mijn doctoraat. De toewijding waarmee je deze taak volbracht, zonder eigenbelang, is opmerkelijk. Hartelijk dank hiervoor.

Ineke Dhondt wil ik bedanken voor haar enorme inzet tijdens haar thesisjaar. Die inzet werd beloond met een zeer goed eindresultaat, waarvan ikzelf ook de vruchten heb kunnen plukken (zie chapter 4).

Pieter Bogaert, Kristel De Meyere en Evelyne Meyer wil ik van harte bedanken voor de professionele begeleiding binnen de wereld van de flow cytometrie. Het is fascinerend om zien hoe jullie, met allerlei 'trucs en kunstjes', een massa aan informatie aan dit toestel weten te ontlokken.

Winnok De Vos wil ik bedanken voor het ontwikkelen van een methode voor colocalisatie-analyse. Via jouw inbreng kregen we toegang tot een -voor ons onbekende- wereld van automatische beeldverwerking.

I would like to thank the **members of the jury** of my PhD: Dr. Karen Smeets, Dr. Peter Ladurner, Dr. Katrien De Mulder, Prof. Gerlinde Van de Walle, Prof. Ann Huysseune. Thank you for your commitment to reading my thesis and for the insightful comments.

Voorts verdienen enkele niet-eerder-vernoemde collega's een bijzondere dank. **Hanne, Pam en Mieke** bedankt voor de gezellige … iedereen weet nu ongetwijfeld wat er volgt … taarten, champagne (!) en naaipatronen. Ha! Ja, en ook voor de gezellige werksfeer natuurlijk ;-)

Maar vooral, wil ik **mijn familie** bedanken. Er is geen twijfel over dat zij, gezamenlijk, de laatste auteur-plaats verdienen in dit dankwoord. Moeke, Vake, Evi, Benson en Ruby(!). Dankjewel voor de kans die ik gekregen heb om te studeren. Bedankt ook voor de onaflatende steun en de warme thuis waar ik altijd met open armen ontvangen wordt. En clichés zijn er om bevestigd te worden, want ik had het echt niet gekund zonder jullie!

Table of Contents

1. GENERAL INTRODUCTION 17

1.1. STEM CELLS 18

1.1.1. WHAT ARE STEM CELLS? 18

1.1.2. PROTECTION MECHANISMS IN STEM CELLS 18

1.1.3. STEM CELL DYNAMICS IN ADULT ORGANISMS 20

1.1.4. STEM CELL DYNAMICS DURING REGENERATION 24

1.1.5. MODELS FOR STEM CELL RESEARCH 25

1.2. FLATWORMS AS STEM CELL MODELS 27

1.2.1. THE PHYLUM PLATYHELMINTHES 27

1.2.2. STEM CELLS IN FLATWORMS 29

1.2.3. *MACROSTOMUM LIGNANO* AS A MODEL FOR THE *IN VIVO* STUDY OF STEM CELL DYNAMICS 30

1.3. AIMS OF THIS STUDY 38

1.4. OUTLINE OF THIS STUDY 40

1.5. REFERENCES 42

2. STEM CELLS PROPAGATE THEIR DNA BY RANDOM SEGREGATION IN THE FLATWORM *MACROSTOMUM LIGNANO* 51

2.1. ABSTRACT 52

2.2. INTRODUCTION 53

2.3. METHODS 59

2.3.1. ANIMAL CULTURE 59

2.3.2. BRDU PULSE LABELING AND IMMUNOCYTOCHEMISTRY IN WHOLE-MOUNT ORGANISMS AND MACERATED CELL SUSPENSIONS 59

2.3.3. DOUBLE LABELING WITH CLDU AND IDU AND IMMUNO-CYTOCHEMISTRY OF WHOLE MOUNTS 61

2.3.4. EdU-pulse labeling, immunocytochemistry in macerated cell suspensions and the use of cytochalasin D 62
2.3.5. EdU-pulse labeling, immunocytochemistry in whole mounts and the use of Macvasa antibody 62
2.3.6. Imaging and quantification of LRCs in whole-mounts 63
2.4. RESULTS 64
2.4.1. Establishment of LRCs in *M. lignano* 64
2.4.2. Label-retaining stem cells are positive for the neoblast marker Macvasa 68
2.4.3. Label-retaining stem cells manifest low proliferative activity 70
2.4.4. The use of cytochalasin D indicates random segregation of DNA strands 73
2.5. DISCUSSION 75
2.6. SUPPLEMENTARY MATERIAL 83
2.7. REFERENCES 85
3. PROLIFERATIVE RESPONSE OF THE STEM CELL SYSTEM DURING REGENERATION OF THE ROSTRUM IN MACROSTOMUM LIGNANO (PLATYHELMINTHES) 91
3.1. ABSTRACT 92
3.2. INTRODUCTION 93
3.3. MATERIALS & METHODS 94
3.3.1. Cultures 94
3.3.2. *In vivo* observations 95
3.3.3. Staining of muscle F-actin and serotonergic nerve cells 95
3.3.4. Scanning electron microscopy 96
3.3.5. BrdU pulse, BrdU pulse-chase, and anti-phos-H3 labelling 96
3.3.6. Quantitative analysis of cellular dynamics 97
3.4. RESULTS 98
3.4.1. Growth curve of the rostrum and morphological study of the regeneration process 98
3.4.2. Stem cell dynamics during regeneration of the rostrum 102
3.4.3. Spatial Distribution of S-phase and Mitotic cells 106

3.4.4. BrdU pulse-chase experiments to study cell cycle parameters and migration of cells 107

3.5. DISCUSSION.....110

3.5.1. Wound healing and blastema formation 110

3.5.2. Biphasic S-phase pattern 110

3.5.3. Migration and proliferation in the rostrum.....111

3.5.6. Cell cycle characteristics 112

3.5.7. Conclusion.....113

3.6. SUPPLEMENTARY MATERIAL.....114

3.7. REFERENCES 118

4. MEASURING S-PHASE DURATION OF ADULT STEM CELLS IN THE FLATWORM *MACROSTOMUM LIGNANO* BY DOUBLE REPLICATION LABELLING AND QUANTITATIVE COLOCALIZATION ANALYSIS122

4.1 ABSTRACT 123

4.2 INTRODUCTION 123

4.3 MATERIALS AND METHODS 125

4.3.1 Animal culture and amputation of the rostrum 125

4.3.2 Accumulation of mitotic cells after colchicine incubation 125

4.3.3 CldU- and IdU-pulse and immunocytochemistry.....126

4.3.4 Image Acquisition.....126

4.3.5 Image Analysis.....127

4.3.6 Statistical Analysis.....128

4.4 RESULTS.....130

4.4.1 Validation of the colocalization analysis.....130

4.4.2 S-phase duration during homeostasis 131

4.4.3 S-phase duration during regeneration.....135

4.5 DISCUSSION.....138

4.6 SUPPLEMENTARY MATERIAL.....143

4.7 REFERENCES.....146

5. CELL CYCLE PARAMETERS OF ADULT STEM CELLS IN *MACROSTOMUM LIGNANO* (PLATY-HELMINTHES) DURING HOMEOSTASIS AND REGENERATION: STUDYING ACTIVELY CYCLING AND LABEL-RETAINING STEM CELLS USING FLOW CYTOMETRY 150

5.1. ABSTRACT 151

5.2. INTRODUCTION 151

5.3. MATERIALS & METHODS 154

5.3.1. ANIMAL CULTURE AND AMPUTATION OF THE ROSTRUM 154
5.3.2. PREPARATION OF SAMPLES FOR UNIPARAMETRIC FLOW CYTOMETRY 155
5.3.3. EDU-LABELLING AND PREPARATION OF SAMPLES FOR BIPARAMETRIC FLOW CYTOMETRY 155
5.3.4. FLOW CYTOMETRY 156
5.3.5. DATA ANALYSIS AND STATISTICS 156

5.4. RESULTS 157

5.4.1. CELL CYCLE DISTRIBUTION OF ASCS DURING HOMEOSTASIS, AND REGENERATION 157
5.4.2. PROGRESSION OF EDU-LABELLED CELLS THROUGH THE CELL CYCLE 161
5.4.3. CYCLING ACTIVITY OF LABEL-RETAINING CELLS DURING HOMEOSTASIS AND REGENERATION 165

5.5. DISCUSSION 168

5.5.1. UNIPARAMETRIC FLOW CYTOMETRY TO STUDY CELL CYCLE DISTRIBUTION OF ASCS IN *M. LIGNANO* 168
5.5.2. PROGRESSION OF EDU-LABELLED CELLS THROUGH THE CELL CYCLE 169
5.5.3. CELL CYCLE DISTRIBUTION OF ASCS DURING REGENERATION 172
5.5.4. QUIESCENT NEOBLASTS PARTICIPATE IN THE REGENERATION PROCESS 174
5.5.6. CONCLUSIONS 175

5.6. REFERENCES 176

6. GENERAL DISCUSSION 180

6.1. ADULT STEM CELLS IN *M. LIGNANO* 181

6.1.1. STUDYING STEM CELL DYNAMICS IN *M. LIGNANO*: AN EXPANDING TOOLBOX 182
6.1.2. STEM CELL PROTECTION IN *M. LIGNANO* 184
6.1.3. NEOBLASTS, A HETEROGENEOUS POPULATION OF ADULT STEM CELLS 186

6.1.4. THE CELL CYCLE IN *M. LIGNANO*: ADVANCES AND FUTURE PROSPECTS 189
6.1.5. QUIESCENT NEOBLASTS IN *M. LIGNANO*: ADVANCES AND FUTURE PROSPECTS 191
6.2. UNIVERSAL RELEVANCE OF STEM CELL RESEARCH IN FLATWORMS 193
6.3. REFERENCES 197
7. APPENDIX 204
7.1. GLOSSARY 205
7.2. LIST OF ABBREVIATIONS 207
7.3. CURRICULUM VITAE 208
7.3.1. PUBLICATION LIST 208
7.3.2. ACTIVE CONTRIBUTION TO INTERNATIONAL CONFERENCES 209
8. SUMMARY / SAMENVATTING 210
8.1. SUMMARY 211
8.2. SAMENVATTING 215

1. General introduction

1.1. Stem Cells

1.1.1. What are stem cells?

Classically, stem cells are distinguished from other cell types by two important characteristics. First, they are unspecialized cells that are able to self-renew through cell division. Second, they can generate differentiated progeny that will fulfill specialized functions within the organism (Morrison and Spradling, 2008). These stem cell features emphasize the primary role of adult stem cells in living organisms as they provide a mechanism for maintenance (tissue homeostasis*) and repair (regeneration) of tissues. Not surprisingly, they have been described as nature's gift to multi-cellular organisms (Fuchs et al., 2004).

However, their responsibility is coupled with the need for a tight control on stem cell proliferation, in order to maintain appropriate numbers of cells within tissues (DeGregori, 2011). This is exemplified by several medical conditions, such as cancer and some birth defects, which are directly linked to abnormal cell division and differentiation (Houghton et al., 2007; Iwashita et al., 2003). Therefore, expanding the knowledge on stem cell proliferation and their transformation into an array of specialized cells, will lead to a better understanding, and possibly correction, of the errors that cause these medical conditions.

1.1.2. Protection mechanisms in stem cells

Given the life-long importance of adult stem cells, there must exist a mechanism or a collection of mechanisms to protect the genetic integrity of these cells, thereby avoiding malignant transformation or premature ageing (Tannenbaum et al., 2005; Park and Gerson, 2005).

The stem cell niche* has been described to create a protective microenvironment in which stem cells reside. Within this niche, a diverse gathering of neighboring differentiated cells secrete and organize a rich milieu of extracellular matrix and other factors, allowing stem

* all terms indicated with an asterisk are explained in the glossary (7.1., p205)

cells to manifest their unique properties while keeping differentiation programs on hold (Fuchs et al., 2004). The importance of the stem cell niche is illustrated by experiments, in which stem cells, when placed in a foreign environment of *in vivo* tissue, were observed to differentiate in multicellular tumor masses (Nussbaum et al., 2007).

Besides the protection provided by extrinsic factors, several intrinsic factors have been described. Stem cells are considered to be equipped with DNA damage response pathways that trigger DNA repair. This is supported by a number of studies showing that mutations in mediators of diverse DNA repair pathways, significantly contribute to premature stem cell depletion (Ito et al., 2004; Rossi et al., 2008 and references therein).

Another intrinsic mechanism for maintaining genome integrity in stem cells was originally proposed by Cairns (1975) as the 'Immortal strand hypothesis'. According to this controversial theory, DNA-strands are non-randomly distributed amongst daughter cells during asymmetric stem cell division. This allows for the newly synthesized DNA copy, which might contain *de novo* mutations, to be segregated to the daughter cell that is destined to differentiate and eventually will wear off due to normal cell turnover*. The original DNA-copy on the other hand, is segregated to the other daughter cells which retains stem cell identity. In this way, the genetic integrity of stem cells is secured. Three decades after this theory has been proposed, the immortal strand hypothesis still remains a matter of intense debate (Rando, 2007; Lansdorp, 2007).

Furthermore, cellular quiescence is widely considered to be an essential protective mechanism within stem cell populations. As new and improved tools become available and new adult stem cell models emerge, it is becoming increasingly apparent that quiescence is a frequent feature of stem cell populations (Fuchs, 2009). By reducing the number of cell divisions, these cells minimize the chance to incorporate mutations into their DNA during the error-prone process of DNA-synthesis, and furthermore avoid cell exhaustion* (Sharpless and Depinho, 2007; Orford and Scadden, 2008). Moreover, as quiescent stem cells appear to be less metabolically active, they may be subjected to lower levels of DNA-damage-inducing metabolic side products such as reactive oxygen species (ROS) (Rossi et al., 2005; Kobayashi and Suda, 2012).

1.1.3. Stem cell dynamics in adult organisms

There can be little dispute that cellular proliferation is one of the most fundamental of biological processes (Hall and Levison, 1990). Although intrinsic properties of stem cells are likely to be similar across stem cell populations, proliferation activity and cycling rate are features that vary considerably (Fuchs, 2009). For example, in mammals, brain and heart muscle tissue are generally believed to have very little turnover (Fuchs, 2009; Zhang et al., 2008; Bergmann et al., 2009), whereas other tissues such as epidermis and blood, have a rapid turnover in steady state (Watt, 2002; Orkin and Zon, 2008). Besides the variation observed between different stem cell systems, heterogeneity within the system itself must be considered as well. Stem cell populations, existing of kinetically and/or functionally distinct subpopulations have been described extensively across a wide range of taxa (plants: Yanpaisan et al., 1998; hydra: David and Campbell, 1972; Campbell and David, 1974; mammals: Clausen et al., 1986b; Cheshier et al., 1999; Collins et al., 2005; Quesenberry, 2006). For instance, emerging evidence indicates that both quiescent (out of cell cycle and in a lower metabolic state) and active stem cell subpopulations coexist in several mammalian tissues (Li and Clevers, 2010, and references therein). These subpopulations are often considered to be organized in a hierarchical structure, with the quiescent stem cells (described as 'true' stem cells) occupying the top (Greco and Guo, 2010). These 'true' stem cells are highly clonogenic (see below), and give rise to a population of potentially restricted, rapidly dividing precursor cells, the so-called transit amplifying cells (TACs) (Figure 1.1) (van der Kooy and Weiss, 2000; Passegué et al., 2005; Alison and Islam, 2009).

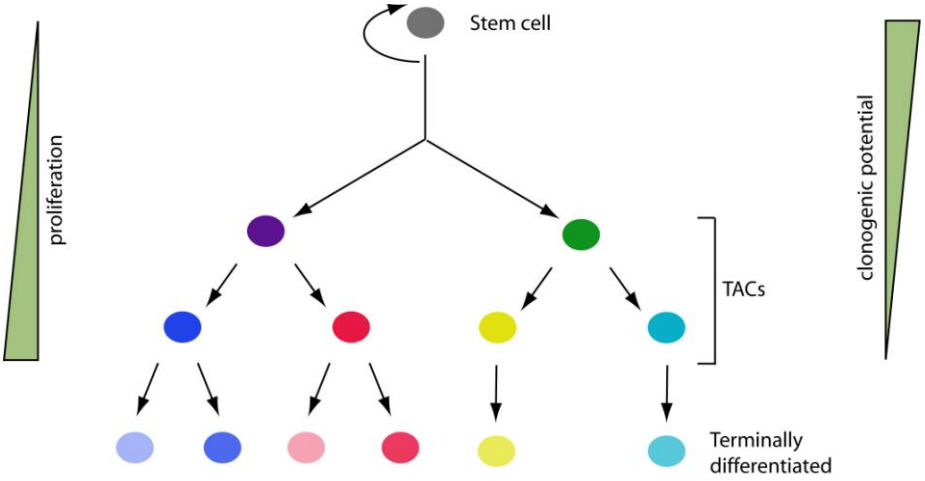

Figure 1.1:

Hypothetical example of a stem cell hierarchy, adapted from (Alison and Islam, 2009). In most renewing systems a cell hierarchy can be recognized, in which a limited number of self-renewing (flexed arrow) stem cells give rise to a series of transit amplifying cells (TACs) which, in turn, give rise to terminally differentiated cells. Usually, the cells at the top of the hierarchic structure demonstrate little proliferative activity and a high clonogenic potential. Descending in the hierarchy results in increased proliferative activity and decreased clonogenicity.

Such a hierarchical differentiation scheme makes sense from the perspective of organismal longevity. It permits the production of large numbers of differentiated cells from a single stem cell by combining subsequent steps in differentiation with proliferation (Momma et al., 2000). Indeed, under such conditions, there is a limited proliferative demand on the self-renewing stem cell at the top of the stem cell population (Sharpless and Depinho, 2007). The importance of cell cycle inactivity for preserving stem cell function is demonstrated in a number of genetic models in which induced proliferation leads to failure in the maintenance of long-term repopulating activity (Orford and Scadden, 2008, and references therein).

From the top to the base layers of the hierarchical structure, proliferation activity of its occupants increases, while clonogenic potential decreases. The varying clonogenic

potential of stem cells has classically been described by the following definitions (Jaenisch and Young, 2008):

Clonogenic potential ↑

Totipotent: ability to form all cell types of the body, including those that make up the extra-embryonic tissues (e.g. blastomeres in early fertilized eggs)

Pluripotent: ability to form all cell types of the body, except those that make up the extra-embryonic tissues (e.g. embryonic stem cells)

Multipotent: ability to develop into a number of cell types of a closely related family (e.g. hematopoietic stem cells)

Unipotent: ability to form one single cell type (e.g. spermatogonial stem cells)

Stem cells in adult organisms, so-called adult stem cells (ASCs) or somatic stem cells, are normally lineage restricted *in vivo* such that they typically generate only the cell types found in the tissues in which they reside (Anderson et al., 2001; Wagers et al., 2002).

To generate cells that constitute tissues and organs, obviously cell division is necessary. This process occurs through a series of stages that are collectively termed the cell cycle (Figure 1.2). The cell cycle is a highly ordered process that results in the duplication and transmission of genetic information from one cell generation to the next (Israels and Israels, 2001). This cycle comprises the first gap phase (G1-phase), a DNA-synthesis phase (S-phase), the second gap phase (G2-phase), and the mitosis phase (M-phase). At the G1-phase, a period of variable duration, the cellular content, excluding the chromosomes, is duplicated. During the S-phase, DNA-synthesis takes place which results in a doubling of the genome. The quality of this synthesis is checked and errors are repaired during the G2-phase. The actual cell division takes place at the M-phase. In addition, a fifth phase (G0-phase), is described in which quiescent cells reside that are not part of the cell cycle, but may rejoin the cycling population after having received suitable stimuli (Johnson and Walker, 1999). In any tissue there are also cells that can no longer divide, thus every cell population can be divided into a cycling and a non-cycling compartment (Hall and Levison, 1990).

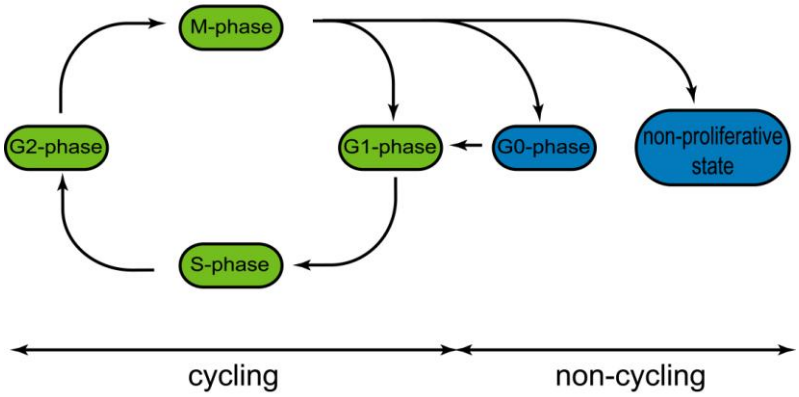

Figure 1.2:

The cell cycle is a highly ordered process, comprising four phases (green): the first gap phase (G1), the DNA-synthesis phase (S), the second gap phase (G2), and the mitotic segregation phase (M) during which cells actually divide. Additionally, in any tissue, non cycling cells are present (blue).Quiescent cells reside in the G0-phase, from which they may be activated to rejoin the cyclin population after having received suitable stimuli. Cells which have left the cell cycle permanently are in an non-proliferative state. Adapted from (Hall and Levison, 1990).

Although several questions remain, large advances have been made in our understanding of the eukaryotic cell cycle, with the help of a wide range of diverse strategies. Some examples of such strategies are analysis of ultrastructural changes and varying DNA-content, the use of antibodies against cell cycle related genes and proteins (e.g. phosphorylated histon-H3, PCNA*), and incorporation of nucleotide analogs during the DNA-synthesis phase (e.g. bromodeoxyuridine) (reviewed in Hall and Levison, 1990; Darzynkiewicz et al., 2011). Such studies have been conducted in a diversity of model organisms, which has greatly promoted the knowledge of the cell cycle and its regulation. Furthermore, extensive interplay between research conducted in a wide range of taxa, has demonstrated modifications of this biological process in response to the specific environmental challenges of each organism (Jensen et al., 2006). Therefore, model

organisms in which stem cells can be studied *in vivo* are particularly well suited to study how the cell cycle is regulated by both intrinsic signals and environmental cues (e.g. tissue damage, nutrient deprivation, irradiation).

1.1.4. Stem cell dynamics during regeneration

It is the regenerative capacity of stem cells that accounts for the expanding biomedical interest in these cells. However the mechanisms by which such cells contribute to tissue regeneration are not fully defined yet.

Tissue damage, leading to a sudden demand for increased proliferation, places a heavy burden on stem cell populations. Stem cells must be able to swiftly adjust their proliferation rate, in order to restore and, once restored, maintain a proper balance in the tissue they reside in (Fuchs, 2009). A valuable source to meet the need for increased proliferation, lies within cellular quiescence, which is considered to be a fundamental trait of many stem cell populations. Indeed, re-entrance of such 'dormant' cells into the cell cycle has been observed in diverse models upon tissue damage (Schultz and McCormick, 1994; Wilson et al., 2008; Li et al., 2010a). The mechanisms that regulate the transition of G0-arrested cells into the G1-phase of the cell cycle, although not fully understood yet, are beginning to unravel in several vertebrate stem cell systems (Yusuf and Fruman, 2003; Dhawan and Rando, 2005). One might imagine that re-activation of quiescent cells involves increased expression of genes promoting growth. However, there is growing evidence that quiescence is under active transcriptional control, and therefore relief from inhibitors stimulates re-entry into the cell cycle (Glynne et al., 2000; Yusuf and Fruman, 2003). Given the common biology of stem cells in different systems, it has been stated that such molecules and mechanisms are similar amongst diverse models (Dhawan and Rando, 2005).

Besides re-activation of quiescent stem cells, adjustment of the cell cycle transit time upon receiving regenerative cues has been demonstrated for stem cells as well. Although the minimal duration of the S- and M-phase are considered to be relatively fixed, considerable variance in the duration of both gap-phases has been described upon various changes in

the environment. For example, a link between feeding and a reduction of the time spent in G1 and G2, has been demonstrated in freshwater triclad flatworms (further in the text referred to as 'Planaria') and in Hydra, respectively (Kang and Sánchez Alvarado, 2009; David and Campbell, 1972). During regeneration, a shortening of the G1-phase has been described in vertebrate models (Ford and Young, 1963; Clausen et al., 1986a).

A third feature that has been demonstrated to account for the plasticity of tissues to recover from injury is *in vivo* dedifferentiation of terminally differentiated cells, which induces the cell to recapitulate earlier stages of development. Dedifferentiation is extensively described in plants (Fehér et al., 2003; Inzé and De Veylder, 2006) and is furthermore suggested to occur during regeneration in some vertebrates, such as newts (Tsai et al., 2002; Nye et al., 2003).

Regardless of the exact strategy – or several thereof – that induces adjustment of the cell dynamics, it is clear that regulatory mechanisms of cell cycle progression are inevitably linked to changes in the environment.

1.1.5. Models for stem cell research

Stem cells are widely present within the animal kingdom. Because they are considered highly conserved biological units of development and regeneration, it should be possible to gain insights on their biology through the study of simpler animals (Sánchez Alvarado, 2004; Laird et al., 2005; Bosch, 2009).

1.1.5.1. *In vitro* and *in vivo*

The potential of stem cells in regenerative medicine relies upon removing them from their natural habitat, propagating them in culture, and placing them into foreign tissue environment. Therefore, the need for *in vitro* stem cell research is obvious. Still, prior to effectively and safely using stem cells for therapeutic applications, it is essential to fully understand the mechanisms that regulate when and how to proliferate and, particularly, when to stop proliferating, in order to maintain appropriate numbers of cells. Since differences in stem cell kinetics *in vivo* and *in vitro* have been demonstrated manifold

(Schultz and McCormick, 1994; Morshead et al., 1998; Gabay et al., 2003; Joseph and Morrison, 2005; Iwashita et al., 2003), the microenvironment in which these cells reside is widely accepted as a controlling parameter in these processes (Fuchs, 2009). Nonetheless, relatively little is known on *in vivo* population dynamics of stem cells in steady-state, during growth, or during regeneration. In fact, models for the regulation of the population dynamics of metazoan stem cells have been worked out primarily *in vitro* (Sánchez Alvarado, 2007a). Given that *in vitro* culture systems are unable to emulate the microenvironment, additional *in vivo* stem cell research is indispensible in order to gain complete knowledge on stem cell behavior (Sánchez Alvarado, 2007a).

However, *in vivo* stem cell research is often challenging because of experimental difficulties caused by tissue depth and motion artefacts in vertebrates (Sánchez Alvarado et al., 2002; Tsai et al., 2002; Tanaka, 2003; Pellettieri and Sánchez Alvarado, 2007; Sharpless and Depinho, 2007; Austad, 2009). Flatworms have been described as promising models for stem cell research, as many of the limitations linked to *in vivo* research, are overcome in these organisms. Most importantly, they possess a large population of ASCs that are accessible for experimental manipulation (reviewed in Sánchez Alvarado, 2007a; Ladurner et al., 2008). The inherent flatness of flatworms, and the transparent nature of the body in some species (e.g. *Macrostomum lignano*), greatly facilitates *in vivo,* whole mount cell imaging.Furthermore, flatworms are known for their extraordinary plasticity in response to amputation and starvation, on account of their stem cells. This is in direct contrast to the rigidity displayed by frequently used invertebrate models such as *Caenorhabditis elegans* and *Drosophila melanogaster* (Sánchez Alvarado et al., 2002).

Although flatworm stem cells differ in some respects from mammalian stem cells (see general discussion: 6.2.) , they offer a unique opportunity to study pluripotent stem cells and their contribution to the regenerative process *in vivo* in an intact adult animal (Gentile et al., 2011). So far, these animals have been, and will continue to be a major source of insight into stem cell biology (Sánchez Alvarado et al., 2002; Pellettieri and Sánchez Alvarado, 2007; Gönczy, 2008; Austad, 2009; Gentile et al., 2011).

1.2. Flatworms as stem cell models

1.2.1. The Phylum Platyhelminthes

Flatworms (Plathylminthes) are one of the simplest animals that are bilaterally symmetrical, unsegmented and acoelomate as only mesenchymal cells separate the epidermis from the gut (Rieger et al., 1991). They possess a primitive cellular mesoderm (triploblastic) and an anterior concentration of neural tissue (cephalization). Flatworms belong to the Lophotrochozoa, which is a sister group of the Ecdysozoa, containing e.g. arthropods and nematodes. Together the Lophotrochozoa and Ecdysozoa are sister to the Deuterostomia, which include the vertebrates (Figure 1.3) (Edgecombe et al., 2011).

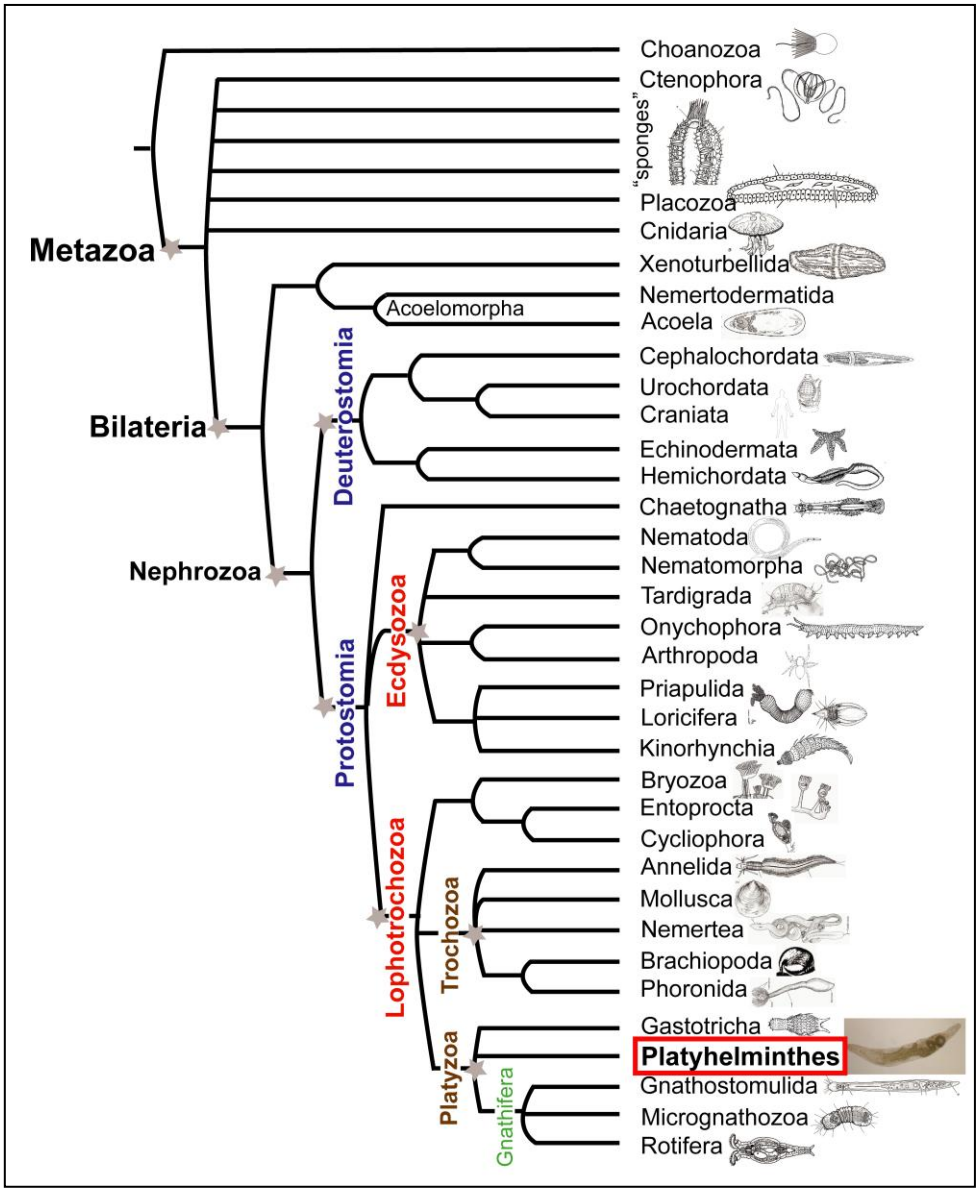

Figure 1.3: Summary of relationships within Metazoa. Nodes labelled with stars have received broad consensus. Modified from (Edgecombe et al., 2011; Orford and Scadden, 2008).

Flatworms, particularly planarians*, are best known for their adult pluripotent stem cell system (so-called neoblast-system) which governs their great regenerative potential (Newmark and Sánchez Alvarado, 2002; Reddien and Sánchez Alvarado, 2004; Saló, 2006). Nowadays, a handful of species have been adopted for laboratory studies, such as *Macrostomum lignano* (Macrostomorpha), *Schmidtea mediterranea, Dugesia japonica, Schmidtea polychroa,* and *Girardia tigrina* (all four belonging to the Tricladida) (Ladurner et al., 2008; Newmark and Sánchez Alvarado, 2002; Oviedo et al., 2008; Saló, 2006).

1.2.2. Stem cells in flatworms

Flatworm stem cells are historically referred to as neoblasts. The term neoblast was first coined by Harriet Randolph (1892) to describe the small, undifferentiated, embryonic-like cells found in the adult body plan of earthworms. The term was extended to planarian flatworms when similar cells were found in their body plan (Sánchez Alvarado, 2007a).

Neoblasts possess the capacity to self-renew and create progeny that can differentiate into various cell types, thereby fulfilling the definition of stem cells (Brøndsted, 1969; Sánchez Alvarado and Kang, 2005; Rieger et al., 1999; Ladurner et al., 2000). A unique feature of these cells is that they are the only cells that remain mitotically active during adulthood, which is demonstrated by the lack of mitotic figures in somatic cells (Morita and Best, 1984; Baguñà and Romero, 1981). Hence, the neoblasts system is solely responsible for cell renewal of all body cells, including the germ line, during homeostasis and regeneration (Brøndsted, 1969; Baguñà et al., 1994; Rieger et al., 1999). This is demonstrated by extensive light and electron microscopy data, and cell lineaging experiments, showing differentiation of neoblasts into any different cell type, including those of the germ line (references, see: Sato et al., 2006; Ladurner et al., 2008). Relatively recently, the neoblast pool is shown, by means of gene expression data, to be a heterogeneous population (Sato et al., 2006; Rossi et al., 2006; Handberg-Thorsager et al., 2008; Eisenhoffer et al., 2008). This heterogeneity is also confirmed by X-ray treatments and FACS analysis, demonstrating two groups of irradiation-sensitive cells, X1 and X2 (Reddien et al., 2005b; Hayashi et al., 2006; Higuchi et al., 2007; Salvetti et al., 2009). These groups diverge in both expression of

proliferation markers and in ultrastructural features. Hence, the term neoblasts does not refer to a single population of stem cells but to a compound of different subpopulations of stem cells each of which expresses particular molecular markers and, consequently, could have different biological properties (Salvetti et al., 2009). Only very recently, the study of Wagner and colleagues (2011) have delivered tangible evidence for the pluripotency of individual neoblasts.

Vast advances have been made in the molecular characterization of neoblasts. However, this information will be truly useful if more information on the behavior of neoblast populations under a variety of conditions is acquired (Sánchez Alvarado, 2007a). Yet, the study of cellular dynamics in flatworms is currently relatively understudied (Kang and Sánchez Alvarado, 2009).

1.2.3. *Macrostomum lignano* as a model for the *in vivo* study of stem cell dynamics

1.2.3.1. *Macrostomum lignano*

M. lignano is an emerging flatworm model for studying stem cell biology, regeneration, aging and sex allocation (Ladurner et al., 2008 and references therein; Mouton et al., 2009b; Mouton et al., 2009a; Pfister et al., 2008; Egger et al., 2009; De Mulder et al., 2010), complementary to the well studied planarians. It is a marine, free living flatworm and a member of the Macrostomida, the second-earliest diverging clade of the Platyhelminthes (Schockaert et al., 2008). *M. lignano* is a simultaneous hermaphrodite*, reproducing exclusively sexually (Figure 1.4.A) (Ladurner et al., 2005b).

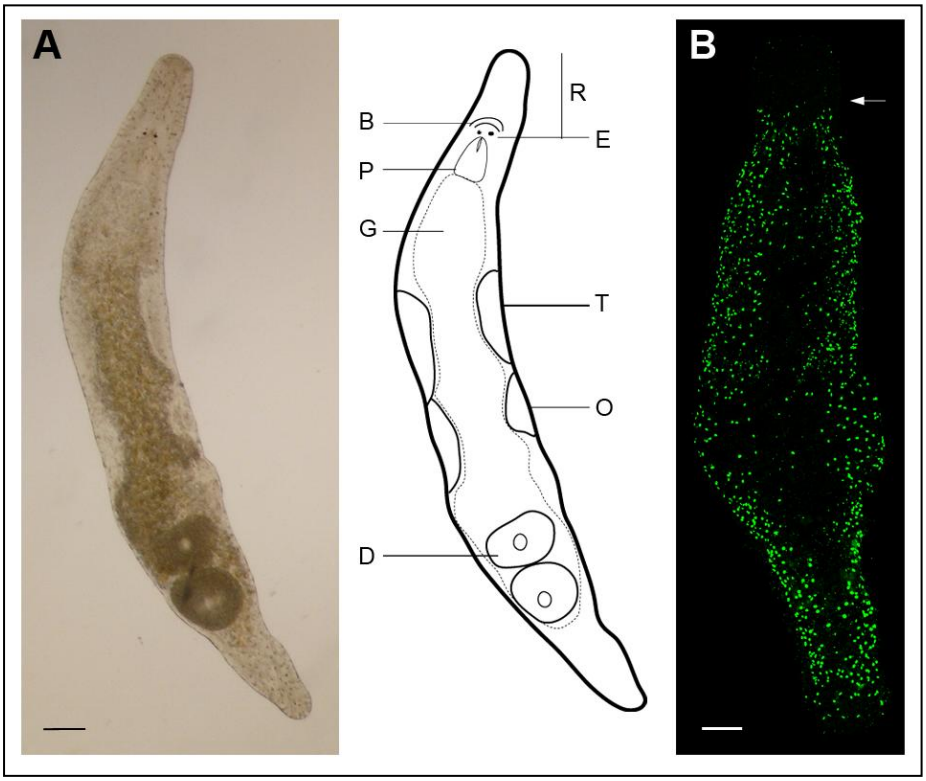

Figure 1.4:

Macrostomum lignano **(A)**: Light microscopic picture of an adult specimen (left panel). Schematic drawing (right panel). Abbreviations: R, rostrum; B, brain; E, eye; P, pharynx; G, gut; T, testis; O, ovary; D, developing egg. **(B)**: Distribution of S-phase cells, as shown by 30 min BrdU incorporation (confocal projection). During homeostasis, proliferating neoblasts are distributed in a bilateral pattern. Arrow indicates the level of the eyes. Anterior is on top. Scale bars: 50 µm. Adapted from (Verdoodt et al., 2012b).

Mass cultures of *M. lignano* can easily and cost-effectively be maintained under laboratory conditions, with an average of one egg per day per animal the whole year round. The feeding status of the individuals can be standardized by providing a constant source of the diatom *Nitzschia curvilineata* (SAG, Germany). This implies an important advantage for studying stem cell dynamics, given that under such conditions, neoblasts proliferation is asynchronized, meaning that a constant proliferation rate of neoblasts is maintained

(Ladurner et al., 2000). Planarian cultures on the other hand, are maintained by time-restricted moments of feeding, resulting in partial synchronization of neoblast proliferation, and thus fluctuations of stem cell dynamics depending on the feeding status of the animal (Kang and Sánchez Alvarado, 2009). Another major advantage of *M. lignano*, is the simple manner by which thymidine analogs can be applied. Such analogs (e.g. bromodeoxyuridine, BrdU) are an important tool for studying proliferation. In *M. lignano*, simply soaking the individual in the analog for a period as short as five minutes is sufficient for labelling (Ladurner et al., 2000). Hence, the exact start and duration of the pulse can be tightly controlled, and pulse, pulse-chase, and continuous labelling experiments can be performed meticulously. In planarians, on the other hand, successful labelling of adult specimens with thymidine analogs occurs through feeding or injection (Newmark and Sánchez Alvarado, 2000). Both of these manipulations affect cell proliferation and are slower in distributing the BrdU to all of the cells in the body, which impedes analysis of the resulting data (Wenemoser and Reddien, 2010).

M. lignano has a well documented regenerative capacity that is, although more limited when compared to planarians, remarkable given that all organs can regenerate if the brain and pharynx remain intact (Egger et al., 2006).

1.2.3.2. Neoblasts in *M. lignano*

Neoblasts in *M. lignano* comprise approximately 6.5% of all body cells (reviewed in Ladurner et al., 2008). This number corresponds to true neoblasts and cells that are already committed, yet have retained neoblast-like features (Bode et al., 2006). Using light microscopy, these cells are identified as small (5-10μm), round cells with a large nucleus and nucleolus and scanty cytoplasm (Ladurner et al., 2000). Based on these morphological characteristics, neoblasts can be distinguished from differentiated cells such as epidermal, gut, and muscle cells (Figured 1.5A-D). Ultrastructurally, heterogeneity has been observed among neoblasts. Electron microscopal observations revealed different stages of neoblasts (stage I to stage III), based on the organization of the chromatin and the level of specialization of the cytoplasm (Figures 1.5E,F) (Bode et al., 2006; Rieger et al., 1999). The

authors suggested that this heterogeneity could either reflect different stages of the cell cycle, or different subpopulations of neoblasts (possibly with different cell cycle characteristics). A strong argument for the second hypothesis, was the increasing level of specialization of the cytoplasm from stage I to stage III. The presence of chromatoid bodies* close to the nucleus is described in somatic and germ line specific neoblasts (Pfister et al., 2008; De Mulder et al., 2009).

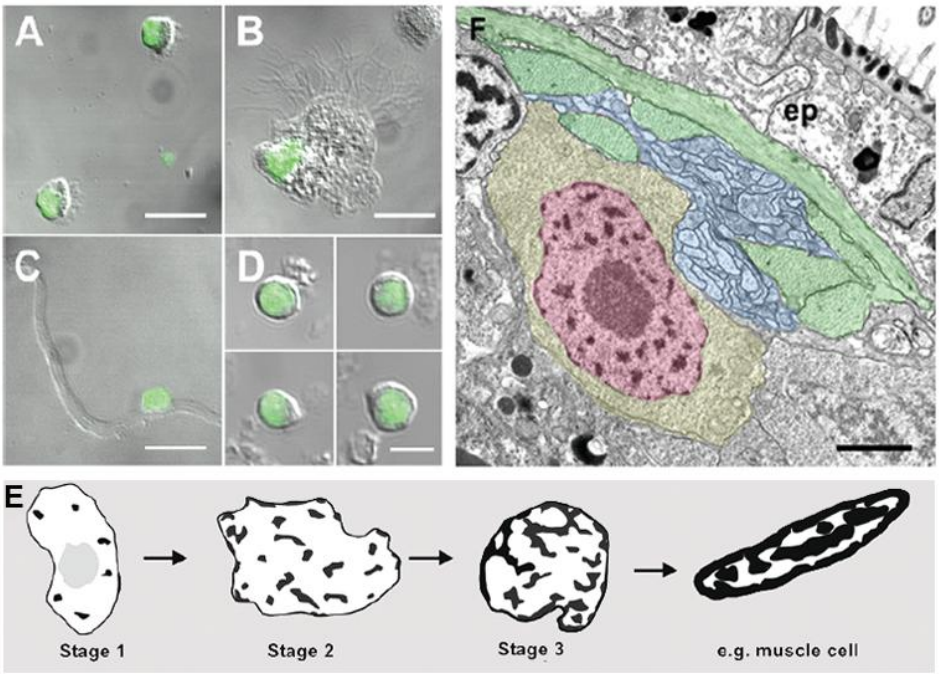

Figure 1.5

Morphology and identification of *M. lignano* neoblasts. (A–D) Cells of macerated BrdU labeled animals; BrdU labeled nuclei are stained green. (A) Epidermal cells, (B) gut cell, (C) muscle cell after continuous 14-day exposure to BrdU. (D) Neoblasts after a 30-min BrdU pulse. (E) Schematic drawing of neoblast nuclei with increasing complexity of chromatin structure. (F) Ultrastructure of a neoblast with nucleus (red) containing patchy clumps of condensed chromatin, surrounded by a thin rim of cytoplasm (yellow). The neoblast is in direct contact with the main lateral nerve cord (blue) located below the body wall musculature (green) and the epidermis (ep). Scale bars (A–D) 10 µm, (F) 2 µm. (Ladurner et al., 2008)

In *M. lignano*, neoblasts are predominantly distributed in a bilateral pattern (Figure 1.4.B). Neoblasts, outside the bilateral pattern are observed, medially, at the level of the pharynx and at the level of the tail. No neoblasts are observed in the rostrum, the region anterior to the eyes. Based on their location, neoblasts have been divided in three subpopulations: (1) mesodermal neoblasts, located in the parenchym* between the gut and the epidermis, (2) gonadal neoblasts, located in the testes and ovaries, and (3) gastrodermal neoblasts, located in the gut region (Ladurner et al., 2000).

1.2.3.3. Cellular dynamics of neoblasts during homeostasis

The thymidine analog BrdU (Figure 1.4B), which allows labelling of cells in S-phase, and the mitotic marker anti-posphorylated histone H3 (anti-phos-H3) have been used to study the kinetics of neoblasts in *M. lignano* (Nimeth et al., 2004; Nimeth et al., 2007).

M. lignano has a high rate of cell turnover*. Nimeth et al. (2002) have determined that in two weeks, nearly one third of all cells are being replaced, which comes down to approximately 21 cells/h. In this study, the presence of a relatively small number of apoptotic cells was demonstrated in *M. lignano*. Since the observed number was insufficient to explain the level of cell renewal, it was suggested that apoptosis independent mechanisms are involved (Ladurner et al., 2008).

Performing continuous BrdU pulses, differentiation of neoblasts into various cell types has been amply demonstrated (Ladurner et al., 2000; Nimeth et al., 2002; Bode et al., 2006). However, differentiation pathways remain an open question and cell lineages have not been fully established.

Migration of neoblasts, to all regions of the body has been demonstrated, via two main routes: medially and rostrally. As migrating cells were observed to enter proliferation-free regions in the body, they are most likely already determined (Ladurner et al., 2000). Moreover, migration into the rostrum, a region which is devoid of neoblasts, allowed estimating the migration rate of cells, which was determined to be approximately 6.7μm/h (Ladurner et al., 2000).

Cellular dynamics of neoblasts in *M. lignano* have, so far, mostly been studied by combined usage of BrdU and anti-phos-H3 (Nimeth et al., 2004; Nimeth et al., 2007). Although many questions remain to be answered, already some important insights have been generated. Based on the results of diverse experimental set-ups using BrdU and anti-phos-H3, the passage through the G2-phase of the cell cycle could be analyzed. The duration of this phase was observed to be rather short, given that the majority of mitotic cells (around 70%) were observed to be still in some stage of the S-phase (most likely the end stage), 4h prior to visualization of M-phase cells. Based on this result, it could be concluded that the majority of neoblasts need approximately 4h to traverse the phase between S- and M-phase, or the G2 phase. Furthermore a proportion of neoblasts (10-20%) seemed to pass through G2 in less than 2h. The observation of a small percentage of neoblasts (2%) that needed more than 48 hours to cycle through G2, indicated the presence of a subpopulation of G2 arrested cells in *M. lignano* (Nimeth et al., 2004). Furthermore, the presence of slow cycling, or cell cycle arrested neoblasts was also demonstrated by Bode and colleagues (2006). In their study, continuous BrdU-labelling experiments revealed the presence of unlabelled neoblasts after a continuous pulse of 14 days, indicating that a subset of neoblasts did not go through S-phase during this time interval. Additionaly, a subpopulation of neoblasts with a remarkably fast cell cycle has been observed by Nimeth et al. (2007). In this study, 20% of all cells that are in mitosis at a given moment had cycled through the whole S- and G2- phase in merely two hours.

Taken together, it is clear that the neoblast pool in *M. lignano* is not a homogeneous collection of stem cells. Instead, kinetic heterogeneity has been demonstrated, as well as topological and ultrastructural heterogeneity (see 2.3.2). Currently, the nature of heterogeneity is not fully understood for all separate levels, nor is the relation between these three levels of heterogeneity. Furthermore, concerning the specific parameters of the cell cycle, some important questions remain to be answered, such as the separate phase durations and the total cell cycle duration.

1.2.3.4. Cellular dynamics of neoblasts during regeneration

The neoblast system in *M. lignano*, demonstrates a remarkable plasticity during repair upon amputation. For example, amputation behind the pharynx results in a reduction of the neoblast pool by roughly 90%, yet, regenerates need merely two to three weeks to restore normal body size and replenish the neoblast population (Egger et al., 2006). The remaining somatic neoblasts were not only able to replenish the somatic stem cell population, but gonadal stem cells as well. Furthermore, repetitive amputation and regeneration has been demonstrated up to 29 times (Egger et al., 2006), suggesting a highly robust repair system.

Regeneration of the tail, after amputation at the level of the female gonoporus, has been studied extensively. The formation of a blastema, a bulge of undifferentiated neoblasts and differentiating cells, was observed 24 hours after amputation, but is probably present even sooner (Egger et al., 2009).

Using BrdU and anti-phos-H3, the kinetics of neoblasts have been studied during regeneration of the tail in *M. lignano* (Nimeth et al., 2007). An initial decrease of mitotic cells was observed during the first hours (2h-8h) after wounding in regions close to the wound as well as in regions far from the wound. Subsequently, after 24h and 48h, M-phase as well as S-phase numbers rose significantly, in the region close to the wound. In the region far from the wound, these numbers approached control values, indicating a local response. Interestingly, double labelling with BrdU and anti-phos-H3 demonstrated that, in *M. lignano*, the duration of G2 could not be reduced during regeneration, at least not during the first hours of regeneration. Elongation of G2-phase, on the other hand, could be observed during starvation (Nimeth et al., 2004). Based on these observations, it was concluded that the G2-phase can be prolonged in case of lack of food, but cannot be shortened during an emergency situation such as regeneration. Taken together a massive proliferative response is observed upon amputation of the tail plate, demonstrating adjusted kinetics in the neoblast pool. The exact nature of these adjustments, however, remains unknown. Furthermore no information is available on the proliferative response of

the neoblast pool upon anterior regeneration. Nonetheless, given that the region anterior to the eyes is devoid of proliferating cells, as opposed to the tail region, comparing the response of the neoblasts system in both situations promises to contribute to a more complete understanding of regeneration in *M. lignano*.

1.3. Aims of this study

The general aim of this thesis was to contribute to a better understanding of the population of adult stem cells in the flatworm *Macrostomum lignano*. Specifically, we have focused on the proliferative dynamics of this cell population during homeostasis, as well as regeneration. This was performed by pursuing different sub-aims:

1) Identifying a population of label-retaining cells (LRCs) and evaluating the cause for label-retention:

Label-retention is a common aspect of stem cell biology in many model systems. Our first aim was to evaluate whether a population of LRCs could be identified in *M. lignano*, by designing an elaborate pulse-chase scheme. Secondly, we sought to evaluate whether label-retention in neoblasts can be attributed to non-random segregation of DNA-strands during divisions of LRSc, or cellular quiescence (Chapter 2).

2) The effect of amputation on neoblast proliferation:

Our goal was to study the proliferation activity of neoblasts after amputation of the rostrum, a region devoid of neoblasts, and compare our results with available information on stem cell dynamics after amputation of the tail plate (Chapter 3).

3) Gaining information on the cell cycle dynamics of active and quiescent neoblasts:

On one hand our goal was to determine specific parameters of cycling cells, and compare them between homeostasis and regeneration (of the rostrum). On the other hand, we evaluated cycling activity of LRCs during homeostasis and regeneration To this end, two different experimental approaches were used.

- double immunohistochemical labelling (CldU and IdU) and colocalization analysis, in order to determine the duration of the S-phase (Chapter 4)

- flow cytometry-based methods to determine (1) cell cycle distribution, (2) cell cycle duration, and (3) cycling activity of LRCs (Chapter 5)

1.4. Outline of this study

This thesis is divided into 8 chapters.

Chapter 1 is a general introduction, illustrating the context in which this study is situated and the aims that were set.

Chapter 2-5 contain the results that were obtained, and their discussion. These chapters are designed according to requirements for manuscripts in A1-journals.

- Chapter 2, **Stem cells propagate their DNA by random segregation in the flatworm *Macrostomum lignano***, presents the study of label-retention and the mode of DNA-segregation in *M. lignano*.
- Chapter 3, **Proliferative response of the stem cell system during regeneration of the rostrum in Macrostomum lignano (Platyhelminthes)**, describes the morphology and the number of S-phase cells during regeneration of the rostrum.
- Chapter 4, **Measuring S-phase duration of adult stem cells in the flatworm *Macrostomum lignano* by double replication labelling and quantitative colocalization analysis,** summarizes the method that was established for colocalization analysis, and the determination of the S-phase during homeostasis and regeneration.
- Chapter 5, **Cell cycle parameters of adult stem cells in *Macrostomum lignano* (Platyhelminthes) during homeostasis and regeneration: the study of actively cycling and label-retaining stem cells using flow cytometry**, presents the flow cytometry-based methods that were established, and the therewith obtained results on cell cycle parameters in *M. lignano*.

Chapter 6 contains a general discussion, which integrates the content of Chapter 1-5.

Chapter 7 is a glossary, explaining terms that were marked with an asterisk in the text.

Chapter 8 holds an English and Dutch summary of this thesis.

1.5. References

Alison M.R. and Islam S. (2009). Attributes of adult stem cells. J Pathol *217*, 144-160.

Anderson D.J., Gage F.H., and Weissman I.L. (2001). Can stem cells cross lineage boundaries? Nat Med *7*, 393-395.

Austad S.N. (2009). Is there a role for new invertebrate models for aging research? J Gerontol A-Biol *64*, 192-194.

Baguñà J. and Romero R. (1981). Quantitative analysis of cell types during growth, degrowth and regeneration in the planarians *Dugesia mediterranea* and *Dugesia tigrina*. Hydrobiologia *84*, 181-194.

Baguñà J., Saló E., Romero R., Garciafernandez J., Bueno D., Munozmarmol A.M., Bayascasramirez J.R., and Casali A. (1994). Regeneration and pattern-formation in planarians - cells, molecules and genes. Zoolog Sci *11*, 781-795.

Bergmann O., Bhardwaj R.D., Bernard S., Zdunek S., Barnabe-Heider F., Walsh S., Zupicich J., Alkass K., Buchholz B.A., Druid H., Jovinge S., and Frisen J. (2009). Evidence for cardiomyocyte renewal in humans. Science *324*, 98-102.

Bode A., Salvenmoser W., Nimeth K., Mahlknecht M., Adamski Z., Rieger R.M., Peter R., and Ladurner P. (2006). Immunogold-labeled S-phase neoblasts, total neoblast number, their distribution, and evidence for arrested neoblasts in *Macrostomum lignano* (Platyhelminthes, Rhabditophora). Cell Tissue Res *325*, 577-587.

Bosch T.C.G. (2009). Hydra and the evolution of stem cells. Bioessays *31*, 478-486.

Brøndsted H.V. (1969). Planarian Regeneration. (Oxford, New York: Pergamon Press).

Cairns J. (1975). Mutation selection and natural history of cancer. Nature *255*, 197-200.

Campbell R.D. and David C.N. (1974). Cell cycle kinetics and development of *Hydra attenuata* .2. Interstitial cells. J Cell Sci *16*, 349-358.

Cheshier S.P., Morrison S.J., Liao X.S., and Weissman I.L. (1999). *In vivo* proliferation and cell cycle kinetics of long-term self-renewing hematopoietic stem cells. Proc Natl Acad Sci U S A *96*, 3120-3125.

Clausen O.P.F., Kirkhus B., and Schjolberg A.R. (1986a). Cell cycle progression kinetics of regenerating mouse epidermal cells: An *in vivo* study combining DNA flow cytometry, cell sorting, and [^{3}H] dThd autoradiography. J Invest Dermatol *86*, 402-405.

Clausen O.P.F., Kirkhus B., Thorud E., Schjolberg A., Moen E., and Cromarty A. (1986b). Evidence of mouse epidermal subpopulations with different cell cycle times. J Invest Dermatol *86*, 266-270.

Collins C.A., Olsen I., Zammit P.S., Heslop L., Petrie A., Partridge T.A., and Morgan J.E. (2005). Stem cell function, self-renewal, and behavioral heterogeneity of cells from the adult muscle satellite cell niche. Cell *122*, 289-301.

Darzynkiewicz Z., Traganos F., Zhao H., Halicka H.D., and Li J.W. (2011). Cytometry of DNA replication and RNA synthesis: Historical perspective and recent advances based on "Click Chemistry". Cytometry A *79A*, 328-337.

David C.N. and Campbell R.D. (1972). Cell cycle kinetics and development of *Hydra attenuata* .1. Epithelial cells. J Cell Sci *11*, 557-568.

De Mulder K., Kuales G., Pfister D., Egger B., Seppi T., Eichberger P., Borgonie G., and Ladurner P. (2010). Potential of *Macrostomum lignano* to recover from gamma-ray irradiation. Cell Tissue Res *339*, 527-542.

De Mulder K., Pfister D., Kuales G., Egger B., Salvenmoser W., Willems M., Steger J., Fauster K., Micura R., Borgonie G., and Ladurner P. (2009). Stem cells are differentially regulated during development, regeneration and homeostasis in flatworms. Dev Biol *334*, 198-212.

DeGregori J. (2011). Evolved tumor suppression: why are we so good at not getting cancer? Cancer Res *71*, 3739-3744.

Dhawan J. and Rando T.A. (2005). Stem cells in postnatal myogenesis: molecular mechanisms of satellite cell quiescence, activation and replenishment. Trends Cell Biol *15*, 666-673.

Edgecombe G.D., Giribet G., Dunn C.W., Hejnol A., Kristensen R.M., Neves R.C., Rouse G.W., Worsaae K., and Sorensen M.V. (2011). Higher-level metazoan relationships: recent progress and remaining questions. Org Divers Evol *11*, 151-172.

Egger B., Gschwentner R., Hess M.W., Nimeth K.T., Adamski Z., Willems M., Rieger R., and Salvenmoser W. (2009). The caudal regeneration blastema is an accumulation of rapidly proliferating stem cells in the flatworm *Macrostomum lignano*. BMC Dev Biol *9*.

Egger B., Ladurner P., Nimeth K., Gschwentner R., and Rieger R. (2006). The regeneration capacity of the flatworm *Macrostomum lignano* - on repeated regeneration, rejuvenation, and the minimal size needed for regeneration. Dev Genes Evol *216*, 565-577.

Eisenhoffer G.T., Kang H., and Sánchez Alvarado A. (2008). Molecular analysis of stem cells and their descendants during cell turnover and regeneration in the planarian *Schmidtea mediterranea*. Cell Stem Cell *3*, 327-339.

Fehér A., Pasternak T.P., and Dudits D. (2003). Transition of somatic plant cells to an embryogenic state. Plant Cell Tiss Org *74*, 201-228.

Ford J. and Young R. (1963). Cell proliferation and displacement in the adrenal cortex of young rats injected with tritiated thymidine. Anat Rec *146*, 125-137.

Fuchs E. (2009). The tortoise and the hair: Slow-cycling cells in the stem cell race. Cell *137*, 811-819.

Fuchs E., Tumbar T., and Guasch G. (2004). Socializing with the neighbors: Stem cells and their niche. Cell *116*, 769-778.

Gabay L., Lowell S., Rubin L.L., and Anderson D.J. (2003). Deregulation of dorsoventral patterning by FGF confers trilineage differentiation capacity on CNS stem cells *in vitro*. Neuron *40*, 485-499.

Gentile L., Cebria F., and Bartscherer K. (2011). The planarian flatworm: an *in vivo* model for stem cell biology and nervous system regeneration. Dis Model Mech *4*, 12-19.

Glynne R., Ghandour G., Rayner J., Mack D.H., and Goodnow C.C. (2000). B-lymphocyte quiescence, tolerance and activation as viewed by global gene expression profiling on microarrays. Immunol Rev *176*, 216-246.

Gönczy P. (2008). Mechanisms of asymmetric cell division: flies and worms pave the way. Nat Rev Mol Cell Biol *9*, 355-366.

Greco V. and Guo S. (2010). Compartmentalized organization: a common and required feature of stem cell niches? Development *137*, 1586-1594.

Hall P.A. and Levison D.A. (1990). Review - assessment of cell proliferation in histological material. J Clin Pathol *43*, 184-192.

Handberg-Thorsager M., Fernandez E., and Saló E. (2008). Stem cells and regeneration in planarians. Front Biosci *13*, 6374-6394.

Hayashi T., Asami M., Higuchi S., Shibata N., and Agata K. (2006). Isolation of planarian X-ray-sensitive stem cells by fluorescence-activated cell sorting. Dev Growth Differ *48*, 371-380.

Higuchi S., Hayashi T., Hori I., Shibata N., Sakamoto H., and Agata K. (2007). Characterization and categorization of fluorescence activated cell sorted planarian stem cells by ultrastructural analysis. Dev Growth Differ *49*, 571-581.

Houghton J., Morozov A., Smirnova I., and Wang T.C. (2007). Stem cells and cancer. Semin Cancer Biol *17*, 191-203.

Inzé D. and De Veylder L. (2006). Cell cycle regulation in plant development. Annu Rev Genet *40*, 77-105.

Israels E.D. and Israels L.G. (2001). The cell cycle. Stem Cells *19*, 88-91.

Ito K., Hirao A., Arai F., Matsuoka S., Takubo K., Hamaguchi I., Nomiyama K., Hosokawa K., Sakurada K., Nakagata N., Ikeda Y., Mak T.W., and Suda T. (2004). Regulation of oxidative stress by ATM is required for self-renewal of haematopoietic stem cells. Nature *431*, 997-1002.

Iwashita T., Kruger G.M., Pardal R., Kiel M.J., and Morrison S.J. (2003). Hirschsprung disease is linked to defects in neural crest stem cell function. Science *301*, 972-976.

Jaenisch R. and Young R. (2008). Stem cells, the molecular circuitry of pluripotency and nuclear reprogramming. Cell *132*, 567-582.

Jensen L.J., Jensen T.S., de Lichtenberg U., Brunak S., and Bork P. (2006). Co-evolution of transcriptional and post-translational cell-cycle regulation. Nature *443*, 594-597.

Johnson D.G. and Walker C.L. (1999). Cyclins and cell cycle checkpoints. Annu Rev Pharmacol Toxicol *39*, 295-312.

Joseph N.M. and Morrison S.J. (2005). Toward an understanding of the physiological function of mammalian stem cells. Dev Cell *9*, 173-183.

Kang H. and Sánchez Alvarado A. (2009). Flow cytometry methods for the study of cell cycle parameters of planarian stem cells. Dev Dyn *238*, 1111-1117.

Kobayashi C.I. and Suda T. (2012). Regulation of reactive oxygen species in stem cells and cancer stem cells. J Cell Physiol *227*, 421-430.

Ladurner P., Egger B., De Mulder K., Pfister D., Kuales G., Salvenmoser W., and Schärer L. (2008). The stem cell system of the basal flatworm *Macrostomum lignano*. In Stem cells: from Hydra to man, Th.C.G.Bosch, ed. (Berlin - Heidelberg - New York: Springer), pp. 75-94.

Ladurner P., Rieger R., and Baguñà J. (2000). Spatial distribution and differentiation potential of stem cells in hatchlings and adults in the marine platyhelminth *Macrostomum* sp.: A bromodeoxyuridine analysis. Dev Biol *226*, 231-241.

Ladurner P., Schärer L., Salvenmoser W., and Rieger R.M. (2005). A new model organism among the lower Bilateria and the use of digital microscopy in taxonomy of meiobenthic Platyhelminthes: *Macrostomum lignano*, n. sp. (Rhabditophora, Macrostomorpha). J Zool Syst Evol Res *43*, 114-126.

Laird D.J., De Tomaso A.W., and Weissman I.L. (2005). Stem cells are units of natural selection in a colonial ascidian. Cell *123*, 1351-1360.

Lansdorp P.M. (2007). Immortal strands? Give me a break. Cell *129*, 1244-1247.

Li F.S., Lu L.L., and Lu J.J. (2010). Identification and location of label retaining cells in mouse liver. J Gastroenterol *45*, 113-121.

Li L.H. and Clevers H. (2010). Coexistence of quiescent and active adult stem cells in Mammals. Science *327*, 542-545.

Momma S., Johansson C.B., and Frisen J. (2000). Get to know your stem cells. Curr Opin Neurobiol *10*, 45-49.

Morita M. and Best J.B. (1984). Electron microscopic studies of planarian regeneration. III. Degeneration and differentiation of muscles. J Exp Zool *229*, 413-424.

Morrison S.J. and Spradling A.C. (2008). Stem cells and niches: Mechanisms that promote stem cell maintenance throughout life. Cell *132*, 598-611.

Morshead C.M., Craig C.G., and van der K.D. (1998). *In vivo* clonal analyses reveal the properties of endogenous neural stem cell proliferation in the adult mammalian forebrain. Development *125*, 2251-2261.

Mouton S., Willems M., Back P., Braeckman B.P., and Borgonie G. (2009a). Demographic analysis reveals gradual senescence in the flatworm *Macrostomum lignano*. Front Zool *6*.

Mouton S., Willems M., Braeckman B.P., Egger B., Ladurner P., Schärer L., and Borgonie G. (2009b). The free-living flatworm *Macrostomum lignano*: A new model organism for ageing research. Exp Gerontol *44*, 243-249.

Newmark P.A. and Sánchez Alvarado A. (2000). Bromodeoxyuridine specifically labels the regenerative stem cells of planarians. Dev Biol *220*, 142-153.

Newmark P.A. and Sánchez Alvarado A. (2002). Not your father's planarian: A classic model enters the era of functional genomics. Nat Rev Genet *3*, 210-219.

Nimeth K., Ladurner P., Gschwentner R., Salvenmoser W., and Rieger R. (2002). Cell renewal and apoptosis in *Macrostomum* sp. [Lignano]. Cell Biol Int *26*, 801-815.

Nimeth K.T., Egger B., Rieger R., Salvenmoser W., Peter R., and Gschwentner R. (2007). Regeneration in *Macrostomum lignano* (Platyhelminthes): cellular dynamics in the neoblast stem cell system. Cell Tissue Res *327*, 637-646.

Nimeth K.T., Mahlknecht M., Mezzanato A., Peter R., Rieger R., and Ladurner P. (2004). Stem cell dynamics during growth, feeding, and starvation in the basal flatworm *Macrostomum* sp. (Platyhelminthes). Dev Dyn *230*, 91-99.

Nussbaum J., Minami E., Laflamme M.A., Virag J.A.I., Ware C.B., Masino A., Muskheli V., Pabon L., Reinecke H., and Murry C.E. (2007). Transplantation of undifferentiated murine embryonic stem cells in the heart: teratoma formation and immune response. Faseb J *21*, 1345-1357.

Nye H.L.D., Cameron J.A., Chernoff E.A.G., and Stocum D.L. (2003). Regeneration of the urodele limb: A review. Dev Dyn *226*, 280-294.

Orford K.W. and Scadden D.T. (2008). Deconstructing stem cell self-renewal: genetic insights into cell-cycle regulation. Nat Rev Genet *9*, 115-128.

Orkin S.H. and Zon L.I. (2008). Hematopoiesis: An evolving paradigm for stem cell biology. Cell *132*, 631-644.

Oviedo N.J., Pearson B.J., Levin M., and Sánchez Alvarado A. (2008). Planarian PTEN homologs regulate stem cells and regeneration through TOR signaling. Dis Model Mech *1*, 131-143.

Park Y. and Gerson S.L. (2005). DNA repair defects in stem cell function and aging. Annu Rev Med *56*, 495-508.

Passegué E., Wagers A.J., Giuriato S., Anderson W.C., and Weissman I.L. (2005). Global analysis of proliferation and cell cycle gene expression in the regulation of hematopoietic stem and progenitor cell fates. J Exp Med *202*, 1599-1611.

Pellettieri J. and Sánchez Alvarado A. (2007). Cell turnover and adult tissue homeostasis: From humans to planarians. Annu Rev Genet *41*, 83-105.

Pfister D., De Mulder K., Hartenstein V., Kuales G., Borgonie G., Marx F., Morris J., and Ladurner P. (2008). Flatworm stem cells and the germ line: Developmental and evolutionary implications of macvasa expression in *Macrostomum lignano*. Dev Biol *319*, 146-159.

Quesenberry P.J. (2006). The continuum model of marrow stem cell regulation. Curr Opin Hematol *13*, 216-221.

Rando T.A. (2007). The immortal strand hypothesis: Segregation and reconstruction. Cell *129*, 1239-1243.

Randolph H. (1892). The regeneration of the tail in lumbriculus. J Morphol *7*, 317-344.

Reddien P.W., Oviedo N.J., Jennings J.R., Jenkin J.C., and Sánchez Alvarado A. (2005). SMEDWI-2 is a PIWI-like protein that regulates planarian stem cells. Science *310*, 1327-1330.

Reddien P.W. and Sánchez Alvarado A. (2004). Fundamentals of planarian regeneration. Annu Rev Cell Dev Biol *20*, 725-757.

Rieger R.M., Legniti A., Ladurner P., Reiter D., Asch E., Salvenmoser W., Schurmann W., and Peter R. (1999). Ultrastructure of neoblasts in microturbellaria: significance for understanding stem cells in free-living Platyhelminthes. Inver Rep Dev *35*, 127-140.

Rieger R.M., Tyler S., Smith III J., and Rieger G.E. (1991). Platyhelminthes: Turbellaria. In Platyhelminthes and Nemertinea, F.W.Harrison and B.J.Bogotisch, eds. (New York: Wiley-Liss), pp. 7-140.

Rossi D.J., Bryder D., Zahn J.M., Ahlenius H., Sonu R., Wagers A.J., and Weissman I.L. (2005). Cell intrinsic alterations underlie hematopoietic stem cell aging. Proc Natl Acad Sci U S A *102*, 9194-9199.

Rossi D.J., Jamieson C.H.M., and Weissman I.L. (2008). Stems cells and the pathways to aging and cancer. Cell *132*, 681-696.

Rossi L., Salvetti A., Lena A., Batistoni R., Deri P., Pugliesi C., Loreti E., and Gremigni V. (2006). DjPiwi-1, a member of the PAZ-Piwi gene family, defines a subpopulation of planarian stem cells. Dev Genes Evol *216*, 335-346.

Saló E. (2006). The power of regeneration and the stem-cell kingdom: freshwater planarians (Platyhelminthes). Bioessays *28*, 546-559.

Salvetti A., Rossi L., Bonuccelli L., Lena A., Pugliesi C., Rainaldi G., Evangelista M., and Gremigni V. (2009). Adult stem cell plasticity: Neoblast repopulation in non-lethally irradiated planarians. Dev Biol *328*, 305-314.

Sánchez Alvarado A. (2004). Regeneration and the need for simpler model organisms. Philos Trans R Soc Lon Ser B-Biol Sci *359*, 759-763.

Sánchez Alvarado A. (2007). Stem cells and the planarian *Schmidtea mediterranea*. Comptes Rendus Biologies *330*, 498-503.

Sánchez Alvarado A. and Kang H. (2005). Multicellularity, stem cells, and the neoblasts of the planarian *Schmidtea mediterranea*. Exp Cell Res *306*, 299-308.

Sánchez Alvarado A., Newmark P.A., Robb S.M.C., and Juste R. (2002). The Schmidtea mediterranea database as a molecular resource for studying platyhelminthes, stem cells and regeneration. Development *129*, 5659-5665.

Sato K., Shibata N., Orii H., Amikura R., Sakurai T., Agata K., Kobayashi S., and Watanabe K. (2006). Identification and origin of the germline stem cells as revealed by the expression of nanos-related gene in planarians. Dev Growth Differ *48*, 615-628.

Schockaert E.R., Hooge M., Sluys R., Schilling S., Tyler S., and Artois T. (2008). Global diversity of free living flatworms (Platyhelminthes, Turbellaria) in freshwater animal diversity assessment. E.V.Balian, H.Segers, and K.Martens, eds. Springer Netherlands), pp. 41-48.

Schultz E. and McCormick K. (1994). Skeletal muscle satellite cells. Ergeb Physiol *123*, 213-257.

Sharpless N.E. and Depinho R.A. (2007). How stem cells age and why this makes us grow old. Nat Rev Mol Cell Biol *8*, 703-713.

Tanaka E.M. (2003). Cell differentiation and cell fate during urodele tail and limb regeneration. Curr Opin Genet Dev *13*, 497-501.

Tannenbaum E., Sherley J.L., and Shakhnovich E.I. (2005). Evolutionary dynamics of adult stem cells: Comparison of random and immortal-strand segregation mechanisms. Phys Rev E *71*, 041914.

Tsai R.Y.L., Kittappa R., and McKay R.D.G. (2002). Plasticity, niches, and the use of stem cells. Dev Cell *2*, 707-712.

van der Kooy D. and Weiss a.S. (2000). Why Stem Cells? Science *287*, 1439-1441.

Verdoodt F., Willems M., Mouton S., De Mulder K., Bert W., Houthoofd W., Smith III J., and Ladurner P. (2012). Stem cells propagate their DNA by random segregation in the flatworm *Macrostomum lignano*. Plos One *7*, e30227.

Wagers A.J., Sherwood R.I., Christensen J.L., and Weissman I.L. (2002). Little evidence for developmental plasticity of adult hematopoietic stem cells. Science *297*, 2256-2259.

Watt F.M. (2002). The stem cell compartment in human interfollicular epidermis. J Dermatol Sci *28*, 173-180.

Wenemoser D. and Reddien P.W. (2010). Planarian regeneration involves distinct stem cell responses to wounds and tissue absence. Dev Biol *344*, 979-991.

Wilson A., Laurenti E., Oser G., van der Wath R.C., Blanco-Bose W., Jaworski M., Offner S., Dunant C.F., Eshkind L., Bockamp E., Lio P., MacDonald H.R., and Trumpp A. (2008). Hematopoietic stem cells reversibly switch from dormancy to self-renewal during homeostasis and repair. Cell *135*, 1118-1129.

Yanpaisan W., King N.J.C., and Doran P.M. (1998). Analysis of cell cycle activity and population dynamics in heterogeneous plant cell suspensions using flow cytometry. Biotechnol Bioeng *58*, 515-528.

Yusuf I. and Fruman D.A. (2003). Regulation of quiescence in lymphocytes. Trends Immunol *24*, 380-386.

Zhang R.L., Zhang Z.G., Roberts C., LeTourneau Y., Lu M., Zhang L., Wang Y., and Chopp M. (2008). Lengthening the G(1) phase of neural progenitor cells is concurrent with an increase of symmetric neuron generating division after stroke. J Cereb Blood Flow Metab *28*, 602-611.

2. Stem cells propagate their DNA by random segregation in the flatworm *Macrostomum lignano*

Modified from:

Verdoodt F, Willems M, Mouton S, De Mulder K, Bert W, Houthoofd W, Smith III J, and Ladurner P (2012) Stem cells propagate their DNA by random segregation in the flatworm Macrostomum lignano. Plos One 7(1):e30227

2.1. Abstract

Adult stem cells are proposed to have acquired special features to prevent an accumulation of DNA-replication errors. Two such mechanisms, frequently suggested to serve this goal are cellular quiescence, and non-random segregation of DNA strands during stem cell division, a theory designated as the immortal strand hypothesis. To date, it has been difficult to test the *in vivo* relevance of both mechanisms in stem cell systems. It has been shown that in the flatworm *Macrostomum lignano* pluripotent stem cells (neoblasts) are present in adult animals. We sought to address by which means *M. lignano* neoblasts protect themselves against the accumulation of genomic errors, by studying the exact mode of DNA-segregation during their division.

In this study, we demonstrated four lines of *in vivo* evidence in favor of cellular quiescence. Firstly, performing BrdU pulse-chase experiments, we localized 'Label-Retaining Cells' (LRCs). Secondly, EDU pulse-chase combined with Vasa labeling demonstrated the presence of neoblasts among the LRCs, while the majority of LRCs were differentiated cells.We showed that stem cells lose their label at a slow rate, indicating cellular quiescence. Thirdly, CldU/IdU- double labeling studies confirmed that label-retaining stem cells showed low proliferative activity. Finally, the use of the actin inhibitor, cytochalasin D, unequivocally demonstrated random segregation of DNA-strands in LRCs.

Altogether, our data unambiguously demonstrated that the majority of neoblasts in *M. lignano* distribute their DNA randomly during cell division, and that label-retention is a direct result of cellular quiescence, rather than a sign of co-segregation of labeled strands.

2.2. Introduction

Adult stem cells (ASCs) have a long-term and dual responsibility to both self-renew and produce differentiated progeny, thereby playing a crucial role during the entire lifetime of an organism (Morrison et al., 1997; Morrison and Spradling, 2008). Given the constant demand for proliferation and the error-prone nature of DNA replication, these cells possess a high risk for malignant transformation (Sharpless and Depinho, 2007). As a consequence, it has long been postulated that ASCs might have acquired specialized features to protect their genome (Tannenbaum et al., 2005; Cairns, 2006). A highly efficient DNA-repair system is commonly described as a stem cell trait, which would serve this purpose (Morrison and Spradling, 2008).

Additionally, a putative mechanism by which ASCs might limit accumulating erroneous genetic information, was originally proposed by Cairns (1975) as the immortal strand hypothesis. According to this hypothesis, stem cells segregate their DNA strands non-randomly upon asymmetric self-renewing cell divisions. Those sister chromatids containing the original template DNA strands are selectively retained in one daughter cell, destined to be the renewed stem cell. The newly synthesized strands, which might have acquired mutations during replication, are passed on to the tissue committed cell. A common strategy to verify this hypothesis, relies on pulse-chase studies with nucleotide tracers, such as tritiated thymidine, bromodeoxyuridine (BrdU), or chlorodeoxyuridine (CldU). Labeling the original 'immortal' DNA strands when they are synthesized during development or regeneration, should result in 'Label-Retaining Cells' (LRCs), considering that these labeled strands are co-segregated during cell divisions (Figure 2.1A, top panel).

Alternatively, retention of label in stem cells can likewise be explained as a result of cellular quiescence. Restricting the number of stem cell divisions seems an equally valuable mechanism for preservation of genome integrity and furthermore prevents stem cell exhaustion (Orford and Scadden, 2008; Fuchs, 2009; Wilson et al., 2008; Arai and Suda, 2007; Alison and Islam, 2009; Li and Clevers, 2010). Low or absent proliferative activity,

after cells were labeled with nucleotide tracers, reduces the chance of label-dilution and allows quiescent ASCs to be identified as 'Label-Retaining Cells' (LRCs) (Figure 2.1B, top right panel). Conversely, in more rapidly cycling progeny cells the label is gradually diluted (Figure 2.1B, top left panel). Performing a double labeling protocol using a second nucleotide tracer serves as a promising tool to assess information on the proliferative activity of LRCs (Figure 2.1A, B, bottom panel).

Figure 2.1

Possible interpretation of label-retention studies, using a double labeling approach. **(A):** Cairns' theory, known as the immortal strand hypothesis, postulates that adult stem cells (ASCs) segregate their DNA-strands non-randomly and permanently retain original template DNA. Using a thymidine derivate such as CldU, these template DNA strands can be labeled at the moment they are synthesized during development, which results in two daughter cells in which complementary DNA-strands are composed of 1 labeled template strand next to an unlabeled normal DNA strand. Because of co-segregation of the labeled template DNA-strands, from the second division after establishment of labeled immortal strands on, the label is passed on to only one daughter cell. Therefore, cells are able to retain label indefinitely during adulthood and are referred to as label-retaining cells (LRCs). By performing a second pulse with another thymidine analog such as IdU, LRCs can become double labeled. **(B):** If DNA is segregated randomly, labeled DNA-strands which are created during a first pulse period with CldU, are distributed over both daughter cells, instead of only one. By consequence, in a regularly cycling cell, the label is diluted under the detection threshold after a certain number of cell cycles in CldU-free medium (left panel). Thus, initially-labeled cells do not retain the label and a second pulse-period with IdU will not result in double labeled cells. However, if cells remain quiescent after they incorporated CldU, the chance of dilution of the label is reduced due to low or even absent cell proliferation (right panel). This results in LRCs. Creating double labeled LRCs after a second pulse with a thymidine derivate (IdU), is therefore possible, yet unlikely because of low cell cycle activity. Abbreviations: LRC, label-retaining cell; CldU, 5-chloro-2'-deoxyuridine; IdU, 5-iodo-2'-deoxyuridine.

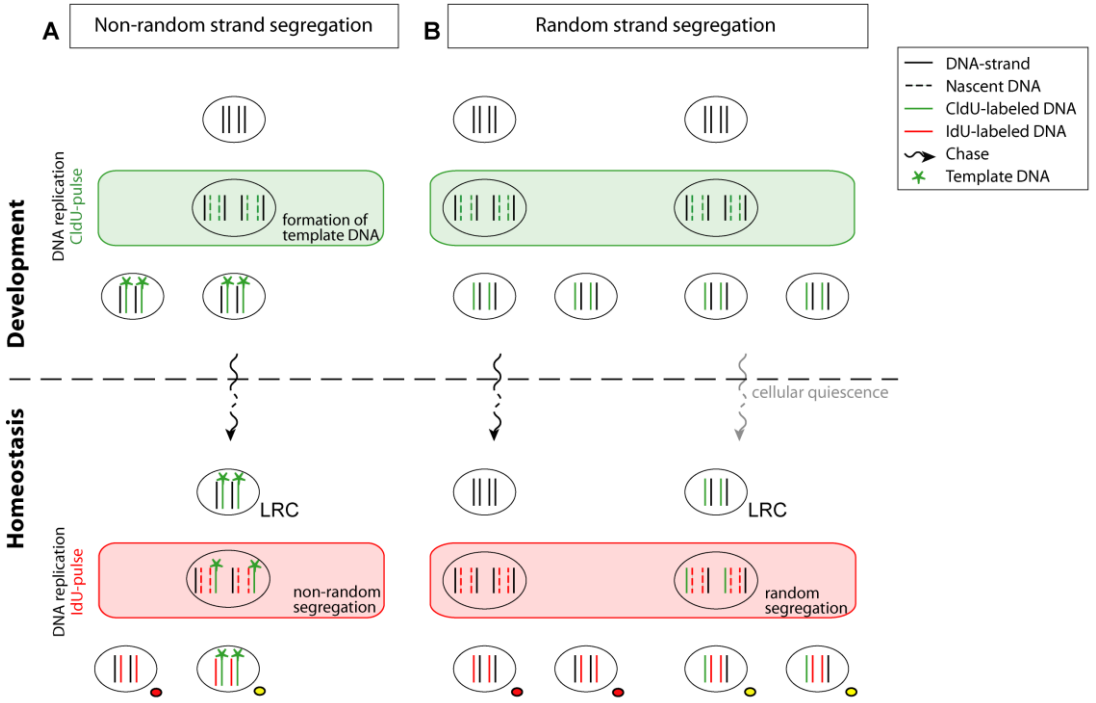
A
Non-random strand segregation
B
Random strand segregation
DNA-strand
Nascent DNA
CldU-labeled DNA
IdU-labeled DNA
Chase
Template DNA
Development
DNA replication
CldU-pulse
formation of template DNA
cellular quiescence
Homeostasis
LRC
LRC
DNA replication
IdU-pulse
non-random segregation
random segregation

Elucidating the label-retention theory remains a matter of intense debate, fueled by publications confirming the theory of cellular quiescence on one hand (Wilson et al., 2008; Cotsarelis et al., 1990; Wei et al., 1995; Braun et al., 2003; Waghmare et al., 2008; Sotiropoulou et al., 2008), versus those supporting non-random segregation of DNA strands on the other hand (Potten et al., 1978; Potten et al., 2002; Karpowicz et al., 2005; Smith, 2005; Shinin et al., 2006; Karpowicz et al., 2009). It has been shown that culture environments can alter the patterning of cells in ways that modify their fates and proliferative potential (Blanpain et al., 2004; Joseph and Morrison, 2005). Therefore, the use of model organisms in which stem cells can be studied *in vivo* has attracted substantial attention (Fuchs et al., 2004; Spradling et al., 2001; Yamashita et al., 2005; Watt and Hogan, 2000; Kuroki and Murakami, 1989; Tsai et al., 2002). However, the *in vivo* data on this topic is mainly gathered in systems in which the analysis of stem cell behavior is hindered by the rare incidence of stem cells, relative inaccessibility of these cells for experimental manipulation *in vivo*, and lack of specific stem cell markers (Lansdorp, 2007).

Over the last decennia, flatworms have been put forward as valuable model organisms to unravel the complex biology of stem cells (Sánchez Alvarado, 2004; Agata, 2003; Handberg-Thorsager et al., 2008; Rossi et al., 2008; Ladurner et al., 2008). These simple, triploblastic metazoans exhibit a powerful stem cell system that is maintained through adult life and which lies at the root of their exceptional developmental plasticity and regeneration capacity (Newmark and Sánchez Alvarado, 2002). The flatworm stem cell population is comprised of pluripotent stem cells, referred to as neoblasts, which remain mitotically active during adulthood, unlike all differentiated cells in the organism (Dubois, 1948; Steph and Gilgenkrantz, 1961; Lange and Gilbert, 1968; Lange, 1968; Baguñà, 1981; Wagner et al., 2011). Among flatworms, *Macrostomum lignano* (Figure 2.2A) has been recently described as a highly advantageous model for *in vivo* stem cell research (Ladurner et al., 2008; Ladurner et al., 2000; Nimeth et al., 2004; Pfister et al., 2007; Pfister et al., 2008; Egger et al., 2009; De Mulder et al., 2009; Mouton et al., 2009b). Advantages are the ease

of culturing (Ladurner et al., 2000; Mouton et al., 2009b), the short embryonic and post-embryonic development (5 and 14 days, respectively), and the limited number of cells (25 000 in total) which facilitates cell quantification (for references see Ladurner et al., 2008). Furthermore, neoblasts are well characterized and present in large numbers (6.5% of the total cell number) (Bode et al., 2006). They can easily be distinguished from non-stem cells, based on morphological traits, and by using an antibody against neoblast-specific Macvasa proteins (Ladurner et al., 2000; Pfister et al., 2008). Immunohistochemical staining of S-phase neoblasts with the thymidine analog bromodeoxyuridine (BrdU), and mitotic neoblasts with an anti-phospho histone H3 mitosis marker (anti-phos-H3), have revealed a bilateral distribution of these cells (Ladurner et al., 2000; Nimeth et al., 2004) (Figure 2.2B). Pulse and pulse-chase studies with thymidine analogs such as BrdU can easily be performed by soaking the animals in the analog-containing medium during the pulse period. Moreover, an *in vivo* double labeling technique using two different thymidine derivates, iododeoxyuridine (IdU) and chlorodeoxyuridine (CldU), can be applied (Ladurner et al., 2008). To our knowledge, this technique has been performed only once before to test the segregation mode of DNA-strands *in vivo* (Kiel et al., 2007). Altogether, these advantages enable *in vivo* analysis of the exact mode of DNA segregation in ASCs in the flatworm *M. lignano*.

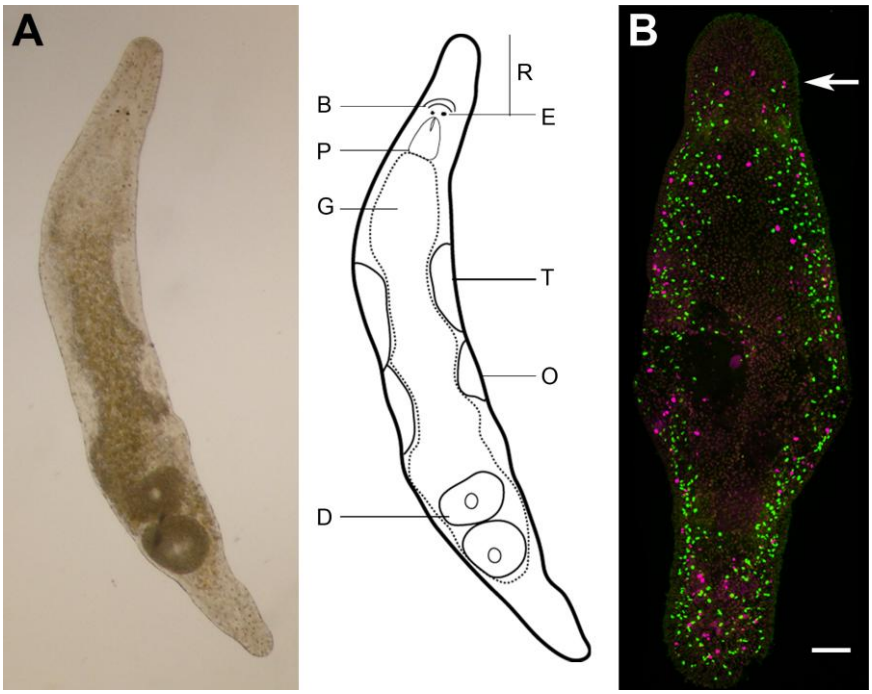

Figure 2.2

Macrostomum lignano (Platyhelminthes). **(A)**: Light microscopic picture of an adult specimen, dorsal view (left panel). Schematic drawing (right panel). Abbreviations: R, rostrum; B, brain; E, eye; P, pharynx; G, gut; T, testis; O, ovary; D, developing egg. **(B)**: Confocal projection of a double BrdU/phospho histone H3 immunostaining (green S-phase cells, red mitoses converted to magenta) after a 30-min BrdU pulse (no chase) in an adult animal. During homeostasis, proliferating neoblasts are distributed in a bilateral pattern. S-phase, nor mitotic cells are visible anterior to the eyes. Arrow indicates the level of the eyes. Anterior is on top. Scale bars: 50 µm.

We aimed to elucidate if label-retaining stem cells exist in *M. lignano*. Performing long-term pulse-chase studies, four different *in vivo* approaches were used. First, a single BrdU pulse-chase experiment was performed to demonstrate the existence of LRCs. Second, among this population of LRCs, Macvasa-positive (Macvasa^{+}) neoblasts were identified. Third, double labeling of the LRCs with chlorodeoxyuridine (CldU) and iododeoxyuridine (IdU) gave information on the proliferative activity. Finally, the actin inhibitor cytochalasin D was used to directly analyze the segregation of labeled DNA strands at the single-cell level. Altogether, our results demonstrate that in *M. lignano* random segregation of DNA strands is predominant, and that label-retention is a direct result of cellular quiescence.

2.3. Methods

2.3.1. Animal Culture

Cultures of *M. lignano* were reared in standard culture medium (f/2) (Guillard and Ryther, 1962) as described previously (Mouton et al., 2009b; Rieger et al., 1988). To obtain animals of a standardized age, adult worms were put together for 24 hours, after which the eggs were collected. Animals that were pulsed with a thymidine analog, were protected from light.

2.3.2. BrdU pulse labeling and immunocytochemistry in whole-mount organisms and macerated cell suspensions

A 24-hour incubation period in the thymidine analog 5-bromo-2'-deoxyuridine (BrdU - Sigma) was given to 11 standardized age groups of embryos (at day 1, 2, 3, 4, or 5 of development) and hatchlings (at day 6, 7, 8, 9, 10, or 11 of development). Together, the initial five age groups cover the embryonic development of *M. lignano*, while the following groups cover the first six days of post-embryonic development. Both embryos and hatchlings were pulsed, simply by soaking them in f/2 containing BrdU (500 µM). Animals

were then kept in standard culture medium, in the presence of food (*ad libitum*), for two or six months in the absence of BrdU. Subsequently, BrdU positive cells were localized using the protocol described below.

The procedure for visualization of the incorporated BrdU in whole mount animals was modified from a previous publication (modified from Ladurner et al., 2000). Specimens were relaxed in $MgCl_2$ (1:1 $MgCl_2.6H_2O$ (7.14%):f/2, 5 min – $MgCl_2.6H_2O$ (7.14%), 5 min), fixed in 4% paraformaldehyde (PFA, 30 min), and rinsed in PBS-T (phosphate-buffered saline + 0.1% Triton X-100, 3 x 10 min). Animals were then treated with Protease XIV (0.2 mg/ml in PBS-T, 37°C, under visual control) and DNA was denatured with 2N HCl (1 h, 37°C). Rinsing with PBS-T (6 x 10 min) and blocking in BSA-T (PBS-T + 1% bovine serum albumin, 30 min) were followed by overnight incubation in the primary antibody, rat-anti-BrdU (1:800 in BSA-T, 4°C - AbD Serotec). Subsequently, animals were washed in PBS-T (3 x 10 min) and incubated in the secondary antibody, FITC-conjugated donkey-anti-rat (1:600 in BSA-T, 1 h – Rockland). Finally animals were rinsed in PBS (3 x 10 min) and mounted in Vectashield (Vector Laboratories).

Simultaneous visualization of S- phase and mitotic neoblasts, using anti-BrdU and anti-phos-H3, was performed as described by Nimeth *et al*. (Nimeth et al., 2004), with the exceptions that both the Protease XIV and HCl treatment was performed as described above. Rhodamine-conjugated goat-anti-rabbit (1:150 in BSA-T, 1 h – Millipore) was used as a secondary antibody for the mitosis marker.

In macerated cell suspensions, the incorporated BrdU was visualized as described before (Ladurner et al., 2000), though some modifications were made. Twenty animals were incubated in 100µl of maceration solution (glacial acetic acid:glycerol:distilled water 1:1:13 - 9% sucrose, 10 min), after which calcium/magnesium-free medium (CMF, 100µl) was added. Thirty minutes after addition, animals were gently pipetted until they fell apart into single cells. Cells were then pelleted (130 x g, 20 min), supernatant was removed, and the pellet was resuspended in PBS (200 µl). The cell suspension was spread onto poly-L-lysine coated slides. The staining of BrdU, was performed directly on these slides in a humid chamber, and was identical to the protocol for whole-mount preparations, with the

exclusion of the Protease XIV step. Prior to the mounting of slides with Vectashield, DNA was stained using DAPI (1 µg/ml in PBS, 1 h). The morphology of single cells was studied, following the methods described earlier (Ladurner et al., 2000; Nimeth et al., 2004). Neoblasts were identified as small, rounded cells (5-10 µm) with a large nucleus and scanty cytoplasm.

2.3.3. Double labeling with CldU and IdU and immuno-cytochemistry of whole mounts

Standardized age groups of embryos and hatchlings were pulsed with the thymidine analog 5-chloro-2'-deoxyuridine (CldU; 500 µM in f/2, 24 h - Sigma) following the same protocol as described for BrdU-labeling. Animals were then chased for six months in the presence of food (*ad libitum*) in CldU-free standard culture medium, after which they were pulsed with 5-iodo-2'-deoxyuridine (IdU; 50 µM in f/2 – Sigma) continuously for 7 days. The following steps were identical to the single BrdU-labeling in whole-mount animals (starting from $MgCl_2$-relaxation until incubation in BSA-T). Animals were then incubated in the first primary antibody, mouse-anti-IdU (1:800 in BSA-T, overnight, 4°C - Becton-Dickinson); washed in PBS-T (3 x 10 min); incubated in stringency buffer (0.5 M NaCl + 36 mM Tris HCl + 0.5% Tween 20, 15 min) for removal of nonspecifically-bound primary antibody; and washed again in PBS-T (3 x 10 min). Subsequently, specimens were incubated in the first secondary antibody, Alexa Fluor 568-conjugated goat-anti-mouse (1:900 in BSA-T, 1 h - Invitrogen); the second primary antibody, rat-anti-CldU (1:800 in BSA-T, overnight, 4°C - AbD Serotec); and the second secondary antibody, FITC-conjugated donkey-anti-rat (1:600 in BSA-T, 1 h - Rockland). Incubation-periods in antibodies were separated by washing steps in PBS-T (3 x 10 min). Finally, animals were rinsed in PBS (3 x 10 min) and mounted in Vectashield.

2.3.4. EdU-pulse labeling, immunocytochemistry in macerated cell suspensions and the use of cytochalasin D

Embryos and hatchlings, standardized by age, were soaked in the thymidine analog 5-ethynyl-2'-deoxyuridine (EdU; 20µM in f/2 - Invitrogen) during development, respectively from day 1 until day 5 continuously, and from day 6 until day 11 continuously. Animals were then chased in the presence of food (*ad libitum*) for two months in EdU-free medium, followed by a seven-day incubation period in the actin-binding protein cytochalasin D (5µM in f/2 - Sigma). Subsequently, they were macerated, following the protocol described earlier and cells were spread onto poly-L-lysine coated slides, washed in PBS (3 x 10 min), blocked with BSA-T-1% (PBS + 1% Triton X-100 + 1% BSA, overnight, 4°C) and incubated in Click-iT® EdU reaction cocktail (concentrations according to manufacturer's instructions - Invitrogen). Afterwards, slides were washed thoroughly in BSA-T-1% (1 h), DNA was stained with DAPI (1µg/ml in PBS, 1 h) and cells were mounted using Vectashield (Vector Laboratories).

2.3.5. EdU-pulse labeling, immunocytochemistry in whole mounts and the use of Macvasa antibody

An EdU-pulse was performed as described above, in embryos (day 1-5, continuously) and hatchlings (day 6-11, continuously), after which a three-month chase was performed in the presence of food in EdU-free medium. Subsequently, animals were relaxed, fixed, and rinsed with PBS-T, as described above. Blocking was performed with BSA-T (2 h), followed by incubation in Click-iT® EdU reaction cocktail (concentrations according to manufacturer's instructions – Invitrogen). Next, Macvasa^{+} cells were visualized as described by Pfister *et al.* (2008), using primary rabbit-anti-Macvasa and secondary TRITC-conjugated goat-anti-rabbit. Finally, animals were rinsed in PBS (3 x 10 min) and mounted in Vectashield.

2.3.6. Imaging and quantification of LRCs in whole-mounts

Epifluorescence and phase-contrast microscopy was performed on a Zeiss Axiovert 200M inverted microscope, followed by image processing using AxioVision 4.7.2. software (Zeiss) and Photoshop CS2. A Nikon Eclipse C1si confocal microscope was used for generating confocal images of whole mount animals. An argon laser (488nm) in combination with a narrow band-pass filter (BP 515/30), and a helium-neon laser (543nm) in combination with a narrow band-pass filter (BP 593/40) were used for visualization of the FITC-fluorochromes (CldU) and the Alexa Fluor 568-fluorochromes (IdU), respectively. Images where processed, using Nikon EZ-C1 3.40 software and Adobe Photoshop CS2.

Quantification of $BrdU^+$ LRCs was performed on confocal images, using the free software program Image J (Abramoff et al., 2004). Images were prepared by performing automatic thresholding, after which cells were quantified automatically, using the 'Analyze Particles' plug-in in Image J. In order to exclude labelled differentiated cells from the cell counts, exclusion parameters were activated based on size and shape of the labelled particles (Size pixel ^2: 10-100; Circularity: 0.80-1.00). Based on their location in regions which are known to lack neoblasts in *M. lignano* (Ladurner et al., 2000), labelled cells in the rostrum (anterior to the eyes) and at the median axis were not considered to be stem cells and were therefore excluded from counts. Given that the data are based on a relatively low sample size, non-parametric Mann-Whitney U ($BrdU^+$ LRC's) and Kruskal-Wallis ($CldU^+$ /IdU^+ LRC's) tests were implemented.

2.4. Results

2.4.1. Establishment of LRCs in *M. lignano*

To evaluate whether LRCs were present in *M. lignano*, animals were pulsed with BrdU during development, allowing nascent neoblasts to incorporate the thymidine analog into their DNA. For BrdU-incorporation, five groups of embryos and six groups of hatchlings, standardized by age, were pulsed at successive 24-hour time intervals during both embryonic (days 1-5) and postembryonic (days 6-11) development (Figure 2.3A). This wide developmental window was chosen to ascertain that the potential founder label-retaining neoblasts were covered by the pulse period. In order to pinpoint a specific time interval during which these neoblasts originate, BrdU-incubation was limited to intervals of 24 hours. Following the BrdU pulse, specimens were chased in the presence of food, for two and six months in BrdU-free medium. Subsequently, after both chase periods, 10 randomly chosen animals of every pulse-group (days 1-11) were sacrificed, BrdU was visualized, and animals were examined for the presence of LRC's.

After two months of chase, the presence of cells that had retained the BrdU label was confirmed in all studied animals that were pulsed during embryonic and post-empbryonic development (total n=110). LRCs were distributed all over the body (Figure 2.3B, left panel). A high density of $BrdU^+$ cells was observed in a bilateral pattern, which is in accordance with the distribution of neoblasts in *M. lignano* (Figure 2.2B) (Ladurner et al., 2000). Outside this bilateral pattern, two separate clusters of labelled cells were found; one at the level of the brain, and another at the level of the mouth and pharynx. To test whether LRCs could be established during homeostasis as well, adult individuals were pulsed with BrdU and then chased for two months. Similarly, this resulted in the presence of LRCs in all studied individuals (data not shown).

After a six-month chase-period, 95% of a total of 110 randomly chosen animals could be labelled (n=104), and LRCs were present in all of them. These labelled cells were scattered

throughout the body (Figure 2.3B, right panel). An accumulation of labelled cells, similar to those after two months chase, at the brain region, the mouth-pharynx region, or both was visible in 75% of the animals.

For every pulse-group, both at two and six months chase, the number of LRCs was quantified in five animals (Figure 2.3C), as described in the Methods section. The number of LRCs was significantly lower in all pulse-groups at six months chase when compared to the same groups after two months chase (for all pulse-groups, $p<0.05$). Thus, a considerable amount of LRCs have lost their label over time, meaning that these cells are not able to retain label indefinitely, or labelled cells were replaced by the progeny of unlabelled neoblasts during tissue homeostasis. The number of LRCs after two months chase seemed to vary, with a mean value of 31 LRCs per animal (± 9, n=55). After 6 months chase, the mean number of LRCs for all pulse groups combined was 13 per animal (± 6, n=55).

These LRCs might represent differentiated progeny of labelled stem cells, in which case the label is retained due to the post-mitotic state of differentiated cells in flatworms. In order to verify whether LRCs, or a fraction thereof, could be identified as neoblasts, two month chased animals were macerated into single cells and BrdU was visualized. By analyzing the morphology of BrdU-positive cells, the existence of label-retaining neoblasts was confirmed (Figure $2.3D_{1,2}$). In addition, several differentiated labelled cells were found, including cells displaying the morphology of nerve cells (Figure $2.3D_3$) and epidermis cells (not shown).

Figure 2.3

LRCs can be established during both embryonic and post-embryonic development, and lose their label at a slow rate. **(A)**: Scheme of the experimental set-up. Animals were pulsed with BrdU (24h) at successive 24-hour time frames of embryonic and post-embryonic development, followed by chase times of 2 and 6 months in BrdU-free medium. Subsequently BrdU was visualized and the presence of LRCs was analyzed. **(B)**: Visualization of LRCs (green) in whole mount animals (confocal projections of BrdU immunostaining). Left panel, from left to right: animal pulsed at day 3 (ED), animal pulsed at day 6 (PED); both animals were chased for 2 months. Right panel, from left to right: animal pulsed at day 4 (ED), animal pulsed at day 6 (PED); both animals were chased for 6 months. Abbreviations: b., cluster of $BrdU^+$ cells at the level of the brain; ph., cluster of $BrdU^+$ cells at the mouth-pharynx region. Anterior is on top. **(C):** Graph representing the quantification of LRCs (mean number + Standard deviation, n=5), chased for 2 and 6 months. LRCs were present in all animals of all pulse groups, both after two and six months. In animals, chased for 6 months, a significant lower number of LRCs was present, compared to animals that were pulsed for 2 months. Abbreviations: BrdU, 5-bromo-2'-deoxyuridine; ED, embryonic development; PED, post-embryonic development. **(D):** Visualization of LRCs in macerated cell suspensions. Superimposition of interference contrast and fluorescence images of BrdU immunostaining (left), interference contrast images (middle) and fluorescent images (right). Animals were pulsed during embryonic and post-embryonic development, and chased for 2 months. Pictures show labeled neoblasts with a large nucleus surrounded by a small rim of cytoplasm (D1, D2), and a labeled nerve cell (D3). Scale bars: B, 50µm; D, 5µm.

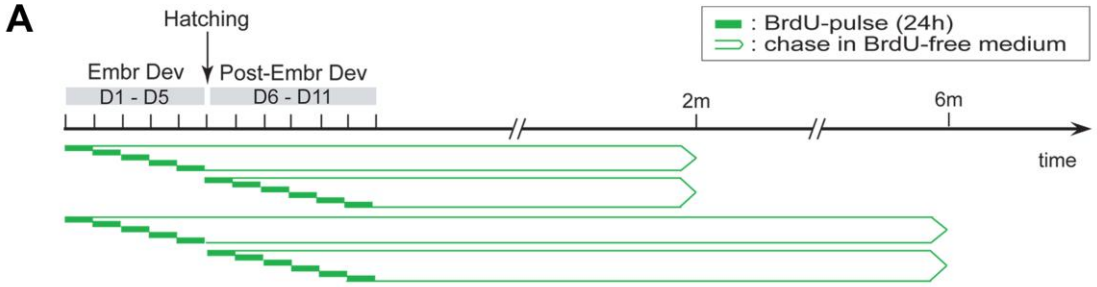
A
Hatching
Embr Dev
D1 - D5
Post-Embr Dev
D6 - D11
: BrdU-pulse (24h)
: chase in BrdU-free medium
2m
6m
time

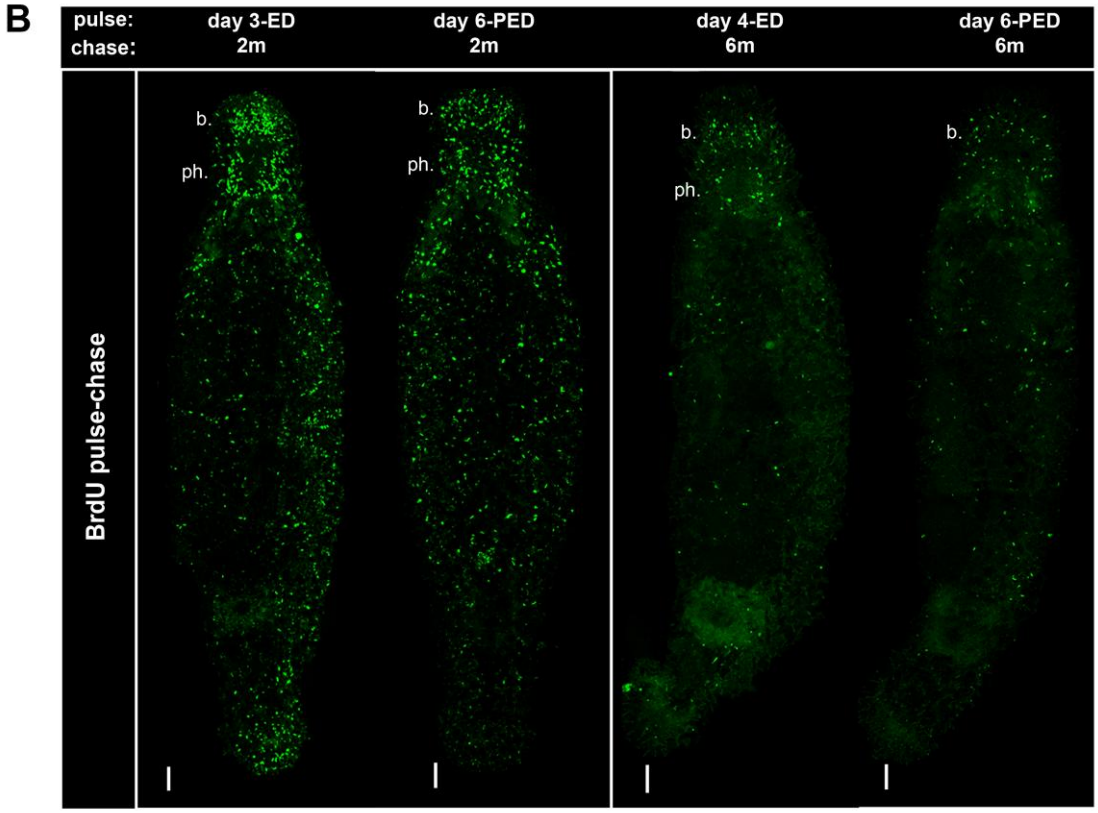
B
pulse:
chase:
day 3-ED
2m
day 6-PED
2m
day 4-ED
6m
day 6-PED
6m
BrdU pulse-chase
b.
ph.

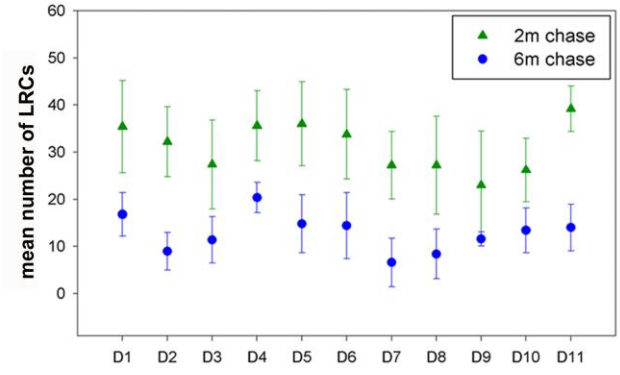
C
mean number of LRCs
2m chase
6m chase
D1
D2
D3
D4
D5
D6
D7
D8
D9
D10
D11

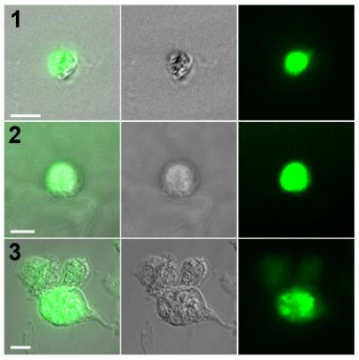
D
1
2
3

2.4.2. Label-retaining stem cells are positive for the neoblast marker Macvasa

An additional experiment was performed to test whether neoblasts could be identified within the population of LRCs. For this purpose, a polyclonal antibody against a homolog of the highly conserved Vasa protein of *M. lignano* (Macvasa) was used. Unlike in other metazoans, where Vasa is almost exclusively detected in germ line cells, Macvasa in *M. lignano* is also present in a subset of somatic stem cells in a characteristic pattern - a ring of Macvasa-labelled spots of nuage surrounding the nucleus (Pfister et al., 2008). Consequently, Macvasa can be used as a neoblast marker in this flatworm. In this experiment, LRCs were established using EdU, since HCl-denaturation is unnecessary for the visualization of this thymidine analog, which enabled simultaneous labelling of Macvasa proteins. The specificity of EdU-labelling was observed comparable to BrdU (see supplementary Figure 2.S1, supplementary Method 2.S1).

In the first pulse group, individuals were pulsed continuously with the thymidine analog EdU for five days during embryonic development (day 1 until day 5). A second group of individuals was pulsed continuously with EdU during the first six days of post-embryonic development (day 6 until day 11). Individuals were then chased for three months, in the presence of food (Figure 2.4A), after which EdU-positive (EdU^+) and $Macvasa^+$ cells were visualized.

$Macvasa^+$ LRCs were identified in all individuals pulsed during embryonic (day 1 – day 5) as well as in individuals pulsed during post-embryonic development (day 6 – day 11) (Figure 2.4B). Macvasa protein in double labelled cells, was visible in spots of nuage around the EdU-labelled nucleus, as observed previously (Pfister et al., 2008). $Macvasa^+$ LRCs were located at the lateral sides of the animal, the area described to contain somatic neoblasts (Ladurner et al., 2000). Double positive cells were never observed in the testes, nor ovaries.

In conclusion, these results directly confirm the existence of neoblasts among the population of LRCs, which are distributed among other somatic neoblasts.

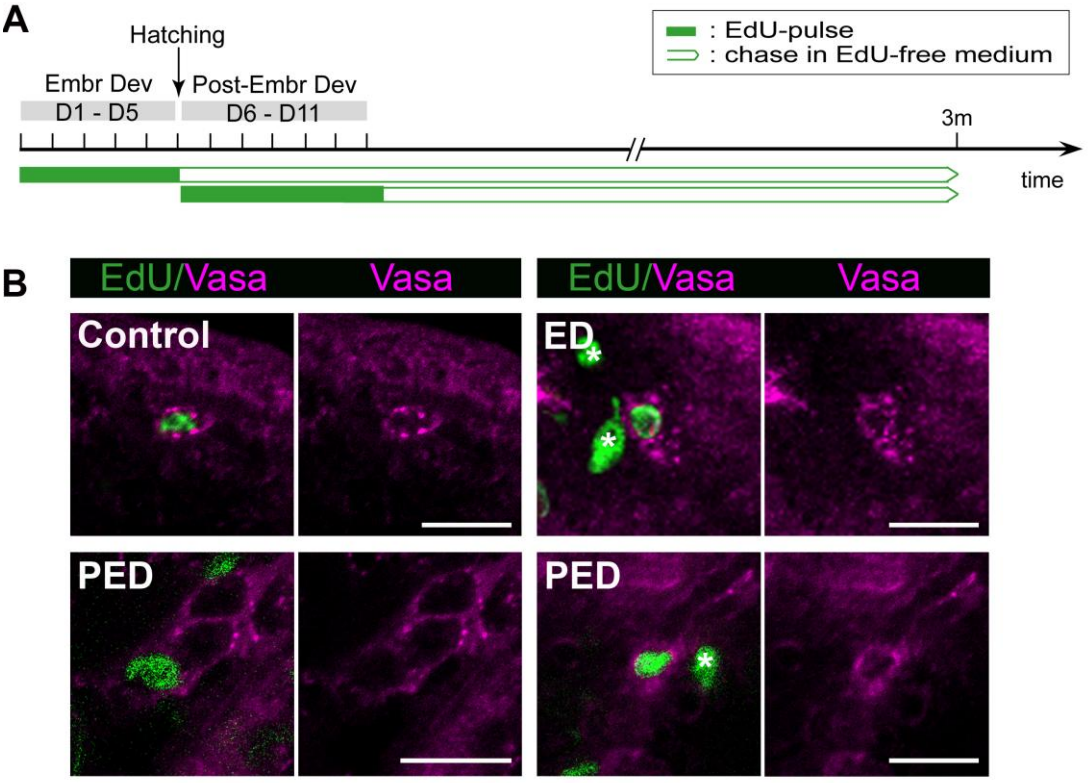

Figure 2.4

Identification of neoblasts among the population of LRCs, using an antibody against neoblast-specific Macvasa proteins. **(A):** Scheme of the experimental set-up. Animals were pulsed continuously with EdU during embryonic development (day1-day5) and during post-embryonic development (day6-day11), followed by a chase time of 3 months in EdU-free medium. Subsequently, EdU was visualized in combination with Macvasa. **(B):** Visualization of label-retaining neoblasts in whole-mount animals (confocal image). LRCs (EdU) are green. The TRITC-signal of the Macvasa proteins, was converted to magenta. $EdU^+/Macvasa^+$ cell in a control animal (no chase) displays Macvasa proteins in a ring of nuage around the nucleus (upper left panel). $EdU^+/Macvasa^+$ cell in an animal pulsed during ED (upper right panel). $EdU^+/Macvasa^+$ cells in an animal pulsed during PED (lower left and right panel). LRCs that are Macvasa-negative (asterisks) are visible in individuals pulsed during ED and PED (right panels). Abbreviations: EdU, 5-ethynyl-2'-deoxyuridine ; Vasa, Macvasa; ED, embryonic development ; PED, post-embryonic development. Scale bars: 10µm.

2.4.3. Label-retaining stem cells manifest low proliferative activity

To further analyze the proliferative activity of label-retaining stem cells, a CldU/IdU double labelling method was applied to label the S-phase of stem cells after a six months chase time. In these experiments, CldU was administered continuously for 24 hours to different groups of embryos and hatchlings at successive time frames of embryonic (days 1-5) and post-embryonic (days 6-11) development, followed by a chase time of six months in CldU-free culture medium. Following the chase period, a second pulse with IdU was performed for seven days continuously to embrace all LRCs that proliferated during this week (Figure 2.5A). Immediately afterwards, animals were immunostained for CldU and IdU. Consequently, every $CldU^+$ LRC going through S-phase during the second pulse period with IdU incorporates this thymidine analog as well and therefore becomes double labelled.

The presence of proliferating LRCs ($CldU^+/IdU^+$ cells) was confirmed in representatives of every pulse group (day 1-11) (Figure 2.5B). Since neoblasts are the only somatic cells that are actively dividing in *M. lignano*, this directly proves that each 24-hour pulse period resulted in neoblasts that were able to retain their label for six months. Hence, no specific time-frame could be pinpointed for the establishment of proliferating label-retaining stem cells. The distribution of all $CldU^+/IdU^+$ cells was in accordance with the normal distribution of neoblasts (Ladurner et al., 2000), except for two cells that were located in the rostrum. These two cells were probably differentiated and migrated during the seven day administration of the second pulse.

A quantitative study of double labelled cells was performed in animals that were pulsed during embryonic development (days 1-5) and chased for six months. Overall, the number of $CldU^+$ /IdU^+ cells was very low, with an observed maximum of three double labelled cells per worm (8% of all animals observed, n=38). In most animals (58%) zero double labelled cells were quantified, and 24% and 11% of all observed animals had one and two $CldU^+$ /IdU^+ cells, respectively. When analyzed for each of the five pulse groups, the mean numbers of double positive cells per worm did not significantly differ between the groups

($p>0.8$). This low number of double labelled cells indicated little proliferative activity among the label-retaining stem cells.

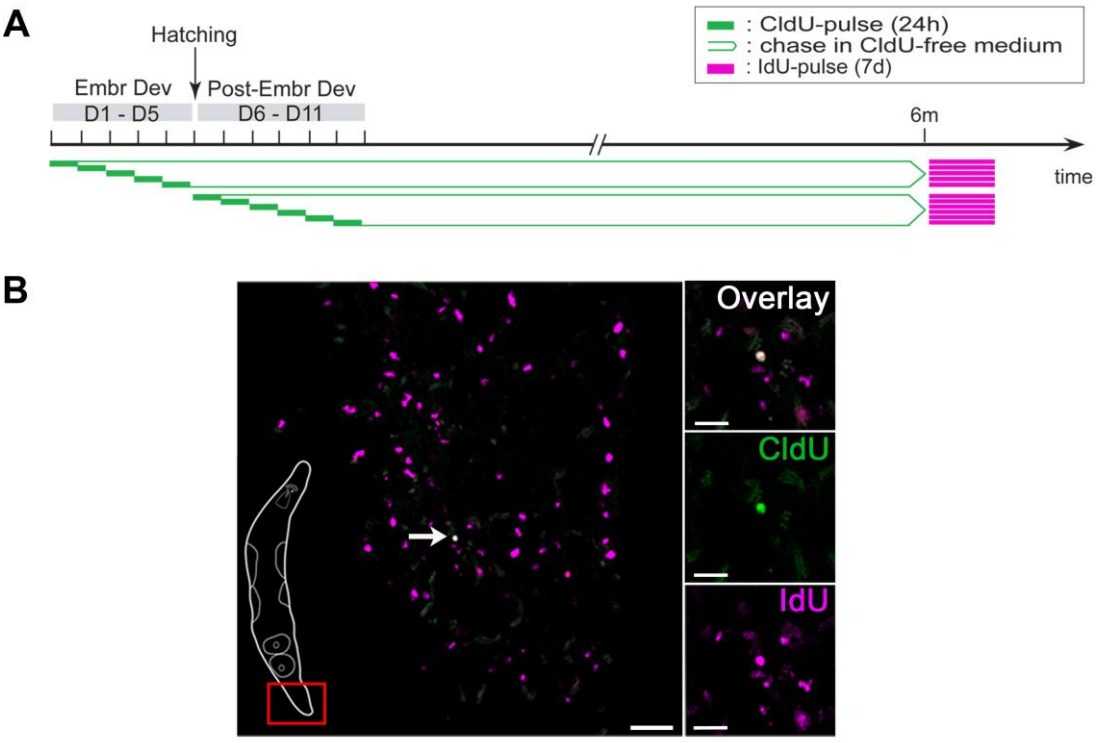

Figure 2.5

Analysis of the proliferative activity of LRCs in *M. lignano*, performing a double labeling technique with the proliferation markers CldU and IdU. **(A)**: Scheme of the experimental set-up. Animals were pulsed with CldU (24h) at successive 24-hour time frames during embryonic and post-embryonic development, followed by a chase time of six months in CldU-free medium. Subsequently animals were pulsed for 7 days continuously with IdU, after which both markers were visualized and the presence of double labeled cells was analyzed. **(B)**: Double labeled LRC located in the tail region (left inset), in a whole mount animal (confocal plane) that was pulsed with CldU (green) on day 1 of embryonic development, chased for six months, and pulsed again with IdU (red, converted to magenta). Every LRC (labeled during the first pulse) that proliferates during the second pulse will become overlabeled with IdU, and is $CldU^+/IdU^+$ (white, indicated with arrow). LRCs that do not proliferate during the second pulse are $CldU^+$ (green) and cells which are proliferating during the second, but not the first pulse, are IdU^+ (magenta). Abbreviations: CldU, 5-chloro-2'-deoxyuridine; IdU, 5-Iodo-2'-deoxyuridine. Scale bars: C, 50µm; C inset, 20µm.

2.4.4. The use of cytochalasin D indicates random segregation of DNA strands

In order to directly test the segregation pattern of DNA strands *in vivo*, cytochalasin D was used. This actin binding protein blocks cytokinesis, while karyokinesis is unaffected, thereby maintaining one cell with two daughter nuclei.

In order to incorporate EdU in all cells, embryos were pulsed continuously during the whole embryogenesis (day 1 until day 5). In a second pulse-group, hatchlings were continuously treated with EdU from day 6 until day 11. Animals were then chased in the presence of food for two months and subsequently incubated in cytochalasin D for one week (Figure 2.6A). Immediately afterwards, animals were macerated into single cells and stained for EdU. As a consequence, each label-retaining stem cell that proliferated during this one week incubation-period was blocked, resulting in a binucleate cell. This made it possible to analyze the distribution of labelled strands in the daughter nuclei.

All EdU^+ binucleate cells that were observed displayed an equivalent EdU-signal in both daughter nuclei (Figure 2.6B). No cells were found that contained a labelled nucleus next to an unlabelled one, or otherwise displayed evidence of unequal fluorescence distribution.

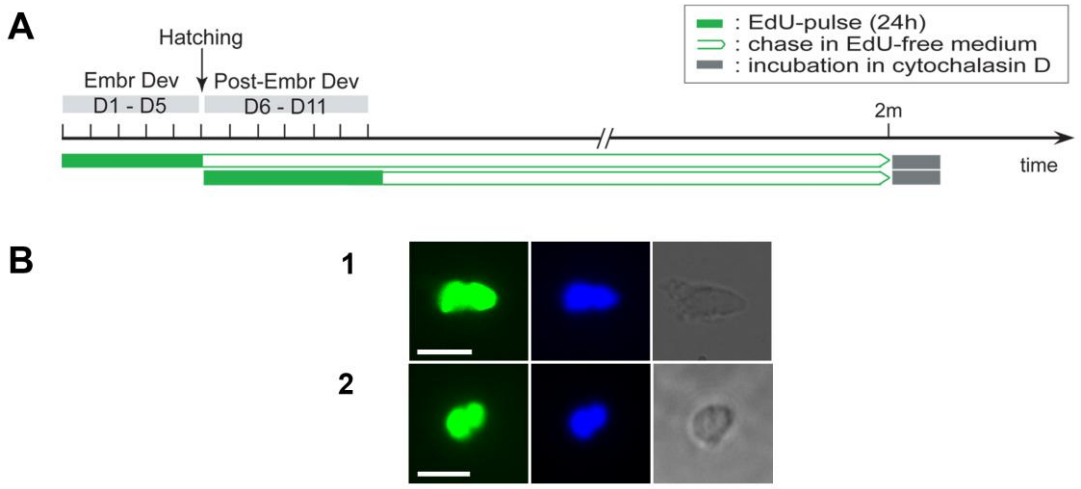

Figure 2.6

Analysis of the distribution of labeled DNA-strands among daughter nuclei of label-retaining cells (LRCs) on single cell level, using the actin-binding protein cytochalasin D. Cytochalasin D is an actin-binding protein that inhibits cytokinesis, while karyokinesis remains unaffected. Thereby, binucleate cells are created, which enables analysis of the distribution of DNA-strands among daughter nuclei on single cell level. **(A)**: Scheme of the experimental set-up. Animals were pulsed continuously with EdU during embryonic development (day1-day5) and during post-embryonic development (day6-day11), followed by a chase time of 2 months in EdU-free medium. Subsequently animals were soaked in cytochalasin D for 7 days, EdU was visualized and DNA was stained with DAPI. **(B)**: Visualization of binucleate LRCs in macerated cell suspensions. Fluorescence images of EdU (left), DAPI (middle), and interference contrast images (right) of binucleate LRCs, pulsed during embryonic (B1) and post-embryonic (B2, B3) development. Binucleate EdU^+ cells display equivalent EdU-signal in both daughter nuclei. Abbreviations: EdU, 5-ethynyl-2'-deoxyuridine. Scale bars: 5µm.

2.5. Discussion

In *M. lignano* four different *in vivo* approaches were used to analyze the exact segregation mode of DNA-strands during stem cell division. None of these approaches produced evidence for non-random segregation of DNA-strands, and were therefore inconsistent with the immortal strand hypothesis. In contrast, our long-term label-retention analyses are rather a confirmation of the existence of a population of relatively quiescent stem cells. BrdU pulse-chase experiments were performed to test whether LRCs can be established in *M. lignano*. In order to enable pinpointing the origin of LRCs to a specific developmental window, an elaborate pulse scheme was designed. The data demonstrated that LRCs could be established in all specimen pulsed during 11 different time periods of development. A similar pulse-chase experiment in adult worms also resulted in LRCs. Thus, our study demonstrates that LRCs can be established in *M. lignano*, not only during the complete duration of embryonic development (day1 - day 5), but also during post-embryonic development (day 6 - day 11) and even during adulthood. Of possible concern was that label-retention is caused by an artifactual withdrawal from the cell cycle, caused by a possible deleterious effect of the incorporated thymidine analog. However, our double labelling experiment contradicts this hypothesis, since label-retaining neoblasts are observed to proliferate. Previously, a continuous BrdU pulse (50 µM) from hatching to maturity in *M. lignano*, has been observed to result in viable labelled sperm (Schärer et al., 2007b). Furthermore, other reports on the use of BrdU in *M. lignano* (with continuous pulse durations up to 14d) have demonstrated no major effect on the dynamics of proliferating cells, since pulsing was not observed to affect morphology, animal behavior, cell cycle dynamics of fast cycling cells, differentiation of $BrdU^+$ cells, and sperm production and differentiation (Ladurner et al., 2000; Nimeth et al., 2004; Bode et al., 2006; Schärer et al., 2007b; Schärer et al., 2004). Based on the results presented in this study and in previous studies, we can conclude that the effect of analog incorporation is minimal and that label-retention is not caused by a cell cycle arrest. Another possible caveat of label-

retention studies is that the label is retained due to the post-mitotic state of differentiated cells. Working with *M. lignano*, however, enables identification of stem cells, based on their morphology (Ladurner et al., 2000), expression of *Macvasa* (Pfister et al., 2007), and their ability to incorporate a thymidine analog, as the only proliferating somatic cells (Ladurner et al., 2000). In this study, the presence of label-retaining neoblasts among the LRCs was proven in three ways: (1) labelled neoblasts were identified morphologically, (2) Macvasa proteins were demonstrated in a subset of LRCs, and (3) a small number of LRCs were observed to incorporate IdU in our double labelling experiment. These double labelled cells were found in all pulse groups, meaning that every pulse that was performed resulted in stem cells which retained label for extended periods of time. Thus, if label-retention would be a result of non-random segregation of labelled DNA-strands and 'immortal' strands do exist in *M. lignano*, our observations indicate that they would be synthesized continuously during embryonic and post-embryonic development, as well as during homeostasis. Serially creating new 'immortal' strands is totally incompatible with the purpose of the immortal strand hypothesis. On the other hand, the results of our analysis for the establishment of LRCs are compatible with the existence of a population of relatively quiescent stem cells. The inability to pinpoint the origin of LRCs to a specific developmental window, has previously been observed to be compatible with the existence of quiescent stem cell in mice (Sotiropoulou et al., 2008).

Quantitative analysis of LRCs after two and six months chase demonstrates a significant decline in the number of LRCs. Still, neoblasts are observed to be able to retain label for as long as six months, a period equivalent to the median life span of *M. lignano* (Mouton et al., 2009a). Thus, the label of LRCs is lost at an extremely slow rate, indicating little cell proliferation, a sign for cellular quiescence. To directly test the proliferative activity of LRCs during homeostasis, *in vivo* CldU/IdU double labelling experiments were performed. The extremely low numbers of double labelled LRCs demonstrate little proliferation. Both our single and double labelling experiment, therefore, deliver strong arguments for the existence of a population of quiescent stem cells in *M. lignano*. The combined outcome of our single and double labelling experiment after prolonged chase times, and the

implications thereof, are explained in Figure 2.7A. These experiments have demonstrated the establishment of a population of LRCs, consisting of labelled neoblasts on one hand, and differentiated progeny of labelled neoblasts on the other hand. By pulsing with CldU during embryonic or post-embryonic development, cells become labelled in S-phase (Figure 2.7A, left panel). During successive development and growth, these CldU-labelled cells proliferate and create labelled progeny. The labelled progeny then migrates and differentiates to participate in homeostasis. As a result of proliferation, migration and differentiation CldU-labelled cells are distributed throughout the whole animal with some clustering at the brain and pharynx (Figure 2.7A, middle panel). CldU labelled stem cells that go through S-phase during a second, 7d-pulse period with IdU incorporate the second label. Due to cell renewal, autophagy and apoptosis, the amount of differentiated cells, and the amount of neoblasts that have retained label decreases with increasing chase time duration (Figure 2.7A, right panel). In summary, this mode of cell turn over leads to the conclusion that random segregation of DNA-strands is the preliminary mechanism during neoblast divisions. Based on the results obtained from our label-retention study, a hypothetical graph is presented elucicating the persistance of labelled cells during the life span of *M. lignano* (Figure 2.7B).

Figure 2.7

LRCs in *M. lignano*: their establishment, persistence and disappearance. A): Explanatory scheme of the results of a double labeling technique, using CldU and IdU. See text for details. (B): Explanatory graph representing the curve of the number of LRCs during the lifespan of *M. lignano*. Two starting points correspond to hypothetical pulses, one in hatchlings and one in adults. After performing a single pulse in hatchlings (dotted line curve) or adults (full line curve), a certain number of cells incorporate the thymidine analog and become labeled. Due to proliferation and differentiation this initial population of labeled cells expands. Their progeny either retains neoblast identity (blue) or loses mitotic activity to eventually become differentiated cells (green). After an initial period of expansion, the number of CldU-labeled cells decreases as a result of cell replacement from unlabeled progeny (green curve) and dilution of the CldU in proliferating neoblasts (blue curve). After six months, a small proportion of differentiated cells and neoblasts have retained the CldU-label, respectively due to long-term functionality and cellular quiescence.

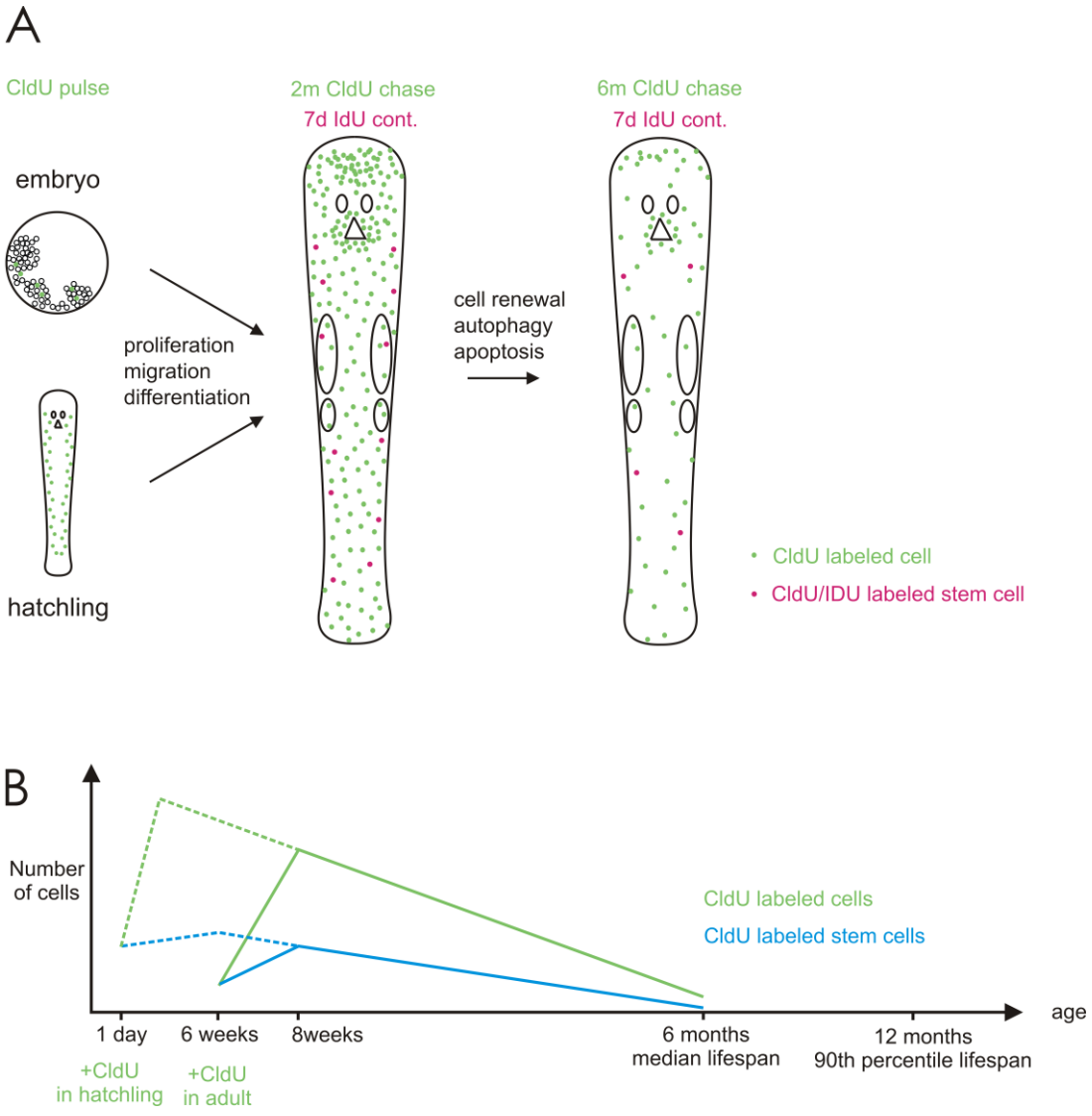
A
CldU pulse
2m CldU chase
7d IdU cont.
6m CldU chase
7d IdU cont.
embryo
proliferation
migration
differentiation
cell renewal
autophagy
apoptosis
hatchling
CldU labeled cell
CldU/IDU labeled stem cell
B
Number
of cells
CldU labeled cells
CldU labeled stem cells
age
1 day
6 weeks
8weeks
6 months
median lifespan
12 months
90th percentile lifespan
+CldU
in hatchling
+CldU
in adult

Finally, the actin-binding protein cytochalasin D was used to inhibit cytokinesis, thereby allowing analysis of the actual distribution of labelled DNA-strands among daughter cells of LRCs. This technique was performed for the first time *in vivo*. All binucleate cells observed, demonstrated equal distribution of labelled DNA-strands among daughter nuclei, indicating random segregation of DNA-strands in LRCs. However, it should be noted that if non-random segregation does occur, unequal distribution of fluorescence would not be visible until the second cell division after pulsing. Nonetheless, not one binucleate cell was found displaying non-random segregation of DNA-strands. Given the long chase time, and the fact that the number of LRCs was observed to decline with increasing chase time, it is unlikely that all binucleate cells divided only once after they were labelled during embryonic or post-embryonic development. In conclusion, this experiment corroborated the random distribution of DNA-strands in LRCs. The presence of a small population of quiescent neoblasts has been demonstrated previously in *M. lignano*. However, to date evidence was only produced for a short quiescent period of one week (Bode et al., 2006). In irradiation studies on *M. lignano,* quiescent neoblasts that were activated upon radiation, were suggested to be responsible for recovery of the animals (De Mulder et al., 2010). Our results, though, clearly demonstrate cellular quiescence on a considerably larger scale, since the foundation of a population of quiescent neoblasts appears to be already laid during the earliest stages of development. Moreover, these stem cells are shown to remain in this relatively quiescent state for a period as long as the median life-span in *M. lignano*.

In literature, adult stem cells are often suggested to exit the cell cycle upon reaching adulthood and form a dormant population of reserve cells. Additionally, developmental quiescence has been observed in a number of organisms. For example, in mice, the presence of quiescent or slow-cycling stem cells during the later stages of development has been observed in multiple tissues (Ahn and Joyner, 2005; Nowak et al., 2008). It is not clear however, whether these cells remain in this dormant state during adulthood. Similarly, in lower organisms, cell cycle arrest has been described for vulval precursor cells during

development in *C. elegans*. Still, these cells already resume proliferation during a later stage of development (Clayton et al., 2008). Thus, our observation of such an early onset of stem cell quiescence that persists for such a long time during adulthood, sheds light on a remarkable feature of neoblasts in *M. lignano* and opens venues for additional research.

Our study demonstrates that the neoblasts in *M. lignano* can be divided in at least two distinct subpopulations. The coexistence of quiescent and active neoblasts can serve to accomplish the two defining tasks of stem cell compartments, respectively maintaining a reserve for long-term repopulation, and creating progeny to cope with the high demand for proliferation. To date, it is not known whether these two populations are divided even further into a hierarchy of neoblast subpopulations with gradual limited differentiation potential. Such an organization of the stem cell pool has been postulated to greatly decrease the maximum number of cell divisions stem cells must undergo (Morrison and Spradling, 2008), hence reducing the risk of accumulating genomic errors. Furthermore, based on the high tolerance against radiation, neoblasts in *M. lignano* have been suggested to exhibit a highly efficient DNA repair system (De Mulder et al., 2010). In its natural environment *M. lignano* is exposed to harsh environmental conditions such as e. g desiccation, very high or low salinity and temperatures. These stress conditions can damage DNA integrity. Therefore, *M. lignano* might have evolved competent DNA repair mechanisms that are indirectly highly beneficial for the stem cell system.

As previously mentioned, the immortal strand hypothesis is almost impossible to reject (Rando, 2007; Lansdorp, 2007). Although this study produced evidence for quiescent stem cells and failed to detect non-random segregation of DNA-strands, it cannot be ruled out that only a proportion of the chromosomes are unequally distributed among daughter cells, as was reported by Armakolas and Klar (2006). In the same way, it can never be excluded that some rare cells in the neoblasts population display non-random segregation of DNA-strands. However, the biological relevance of such a system can be questioned if it is only present in a very limited number of cells.

In this long-term *in vivo* study, the exact mode of DNA-segregation during stem cell division was tested in the flatworm *M. lignano*. Altogether, our data suggest random segregation of

DNA-strands and that label-retention is a direct result of cellular quiescence. We therefore conclude that the *M. lignano* stem cell system is protected by the presence of a population of quiescent neoblasts , probably together with a high capacity of DNA repair. Our findings contribute to a better understanding of how stem cell systems are organized in flatworms and higher organisms, including humans.

2.6. Supplementary Material

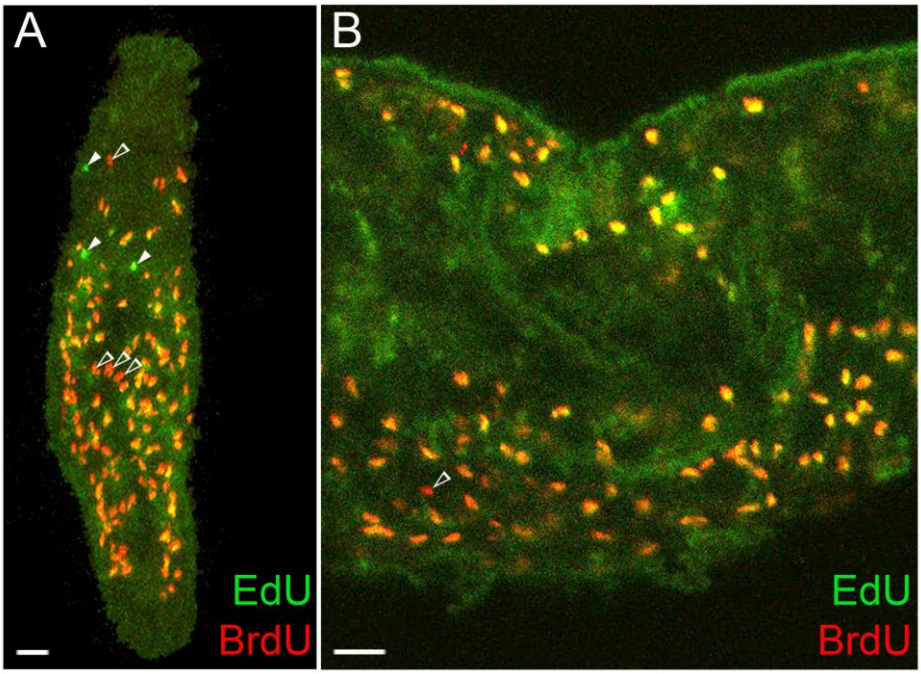

Figure 2.S1

BrdU/EdU double labeling. To test the specificity by which EdU labels cells in S-phase, an EdU/BrdU double labeling was performed. Due to unequal binding kinetics of both analogs, however, a simultaneous pulse could not be performed. Instead, hatchlings and adults were pulsed with EdU (40min), immediately followed by a pulse with BrdU (40min). Subsequently both EdU and BrdU were visualized. **(A, B):** Visualization of EdU (green) and BrdU (red) in whole mount animals (epifluorescence). Labeled cells are $EdU^{+}/BrdU^{+}$, with the exception of a small number of $EdU^{+}/BrdU^{-}$ cells (arrowhead) and $EdU^{-}/BrdU^{+}$ cells (open arrowhead). These single labeled cells most likely represent cells that have left S-phase during the first pulse, and cells that have entered S-phase during the second pulse. **(A):** hatchling, complete animal. **(B):** adult, area of the gut. Abbreviations: EdU, 5-ethynyl-2'-deoxyuridine; BrdU, 5-bromo-2'-deoxyuridine. Scale Bars: 20µm

Supplementary method 2.S1

Animals were successively pulsed with EdU (40 min - Invitrogen) and BrdU (40 min – Sigma). Subsequently, animals were relaxed for 15 min with 7.14% $MgCl_2$ and then fixed in paraformaldehyde (4% in PBS, 30 min). Next, specimens were washed with PBS-T, treated with Protease XIV and incubated in 2N HCl, as described for detection of BrdU. EdU detection with the Click-iT EdU Alexa Fluor (Invitrogen) was performed according to the manufacturer´s instructions. After washings steps in PBS-T (5 x 5 min), specimen were incubated with rabbit-anti-BrdU (1:1000 in BSA-T, overnight, 4°C - Roche). After washing with PBS-T (3 x 10 min), specimens were incubated in TRITC-conjugated swine-anti-rabbit (1:250 in BSA-T, 1 h, at room temperature - DAKO). Finally, specimen were washed with PBS-T (3 x 10 min) and mounted in Vectashield mounting medium (Vector Laboratories).

Acknowledgements

The authors want to thank Marjolein Couvreur for help with cultures of *M. lignano,* and Dr. Bernhard Egger for help with the IdU/CldU double labelling protocol.

2.7. References

Abramoff M.D., Magelhaes P.J., and Ram S.J. (2004). Image processing with Image J. Biophotonics Int *11*, 36-42.

Agata K. (2003). Regeneration and gene regulation in planarians. Curr Opin Genet Dev *13*, 492-496.

Ahn S. and Joyner A.L. (2005). In vivo analysis of quiescent adult neural stem cells responding to Sonic hedgehog. Nature *437*, 894-897.

Alison M.R. and Islam S. (2009). Attributes of adult stem cells. J Pathol *217*, 144-160.

Arai F. and Suda T. (2007). Maintenance of quiescent hematopoietic stem cells in the osteoblastic niche. Hemat Stem Cell Vi *1106*, 41-53.

Armakolas A. and Klar A.J.S. (2006). Cell type regulates selective segregation of mouse chromosome 7 DNA strands in mitosis. Science *311*, 1146-1149.

Baguñà J. (1981). Planarian neoblasts. Nature *290*, 14-15.

Blanpain C., Lowry W.E., Geoghegan A., Polak L., and Fuchs E. (2004). Self-renewal, multipotency, and the existence of two cell populations within an epithelial stem cell niche. Cell *118*, 635-648.

Bode A., Salvenmoser W., Nimeth K., Mahlknecht M., Adamski Z., Rieger R.M., Peter R., and Ladurner P. (2006). Immunogold-labeled S-phase neoblasts, total neoblast number, their distribution, and evidence for arrested neoblasts in *Macrostomum lignano* (Platyhelminthes, Rhabditophora). Cell Tissue Res *325*, 577-587.

Braun K.M., Niemann C., Jensen U.B., Sundberg J.P., Silva-Vargas V., and Watt F.M. (2003). Manipulation of stem cell proliferation and lineage commitment: visualisation of label-retaining cells in wholemounts of mouse epidermis. Development *130*, 5241-5255.

Cairns J. (1975). Mutation selection and natural history of cancer. Nature *255*, 197-200.

Cairns J. (2006). Cancer and the immortal strand hypothesis. Genetics *174*, 1069-1072.

Clayton J.E., van den Heuvel S.J.L., and Saito R.M. (2008). Transcriptional control of cell-cycle quiescence during C. elegans development. Dev Biol *313*, 603-613.

Cotsarelis G., Sun T.T., and Lavker R.M. (1990). Label-retaining cells reside in the bulge area of pilosebaceous unit - implications for follicular stem-cells, hair cycle, and skin carcinogenesis. Cell *61*, 1329-1337.

De Mulder K., Kuales G., Pfister D., Egger B., Seppi T., Eichberger P., Borgonie G., and Ladurner P. (2010). Potential of *Macrostomum lignano* to recover from gamma-ray irradiation. Cell Tissue Res *339*, 527-542.

De Mulder K., Pfister D., Kuales G., Egger B., Salvenmoser W., Willems M., Steger J., Fauster K., Micura R., Borgonie G., and Ladurner P. (2009). Stem cells are differentially regulated during development, regeneration and homeostasis in flatworms. Dev Biol *334*, 198-212.

Dubois F. (1948). Sur une nouvell méthode permettant de mettre en évidence la migration des cellules de régénération chez les planaires. C R Seances Soc Biol Fil *142*, 699-700.

Egger B., Gschwentner R., Hess M.W., Nimeth K.T., Adamski Z., Willems M., Rieger R., and Salvenmoser W. (2009). The caudal regeneration blastema is an accumulation of rapidly proliferating stem cells in the flatworm *Macrostomum lignano*. BMC Dev Biol *9*.

Fuchs E. (2009). The tortoise and the hair: Slow-cycling cells in the stem cell race. Cell *137*, 811-819.

Fuchs E., Tumbar T., and Guasch G. (2004). Socializing with the neighbors: Stem cells and their niche. Cell *116*, 769-778.

Guillard R. and Ryther J. (1962). Studies of marine planktonic diatoms. I. *Cyclotella nana* Hustedt, and *Detonula confervacea* (Cleve) Gran. Can J Microbiol *8*, 229-239.

Handberg-Thorsager M., Fernandez E., and Saló E. (2008). Stem cells and regeneration in planarians. Front Biosci *13*, 6374-6394.

Joseph N.M. and Morrison S.J. (2005). Toward an understanding of the physiological function of mammalian stem cells. Dev Cell *9*, 173-183.

Karpowicz P., Morshead C., Kam A., Jervis E., Ramuns J., Cheng V., and van der Kooy D. (2005). Support for the immortal strand hypothesis: neural stem cells partition DNA asymmetrically *in vitro*. J Cell Biol *170*, 721-732.

Karpowicz P., Pellikka M., Chea E., Godt D., Tepass U., and van der Kooy D. (2009). The germline stem cells of *Drosophila melanogaster* partition DNA non-randomly. Eur J Cell Biol *88*, 397-408.

Kiel M.J., He S.H., Ashkenazi R., Gentry S.N., Teta M., Kushner J.A., Jackson T.L., and Morrison S.J. (2007). Haematopoietic stem cells do not asymmetrically segregate chromosomes or retain BrdU. Nature *449*, 238-242.

Kuroki T. and Murakami Y. (1989). Random segregation of DNA strands in epidermal basal cells. Jpn J Cancer Res *80*, 637-642.

Ladurner P., Egger B., De Mulder K., Pfister D., Kuales G., Salvenmoser W., and Schärer L. (2008). The stem cell system of the basal flatworm *Macrostomum lignano*. In Stem cells: from Hydra to man, Th.C.G.Bosch, ed. (Berlin - Heidelberg - New York: Springer), pp. 75-94.

Ladurner P., Rieger R., and Baguñà J. (2000). Spatial distribution and differentiation potential of stem cells in hatchlings and adults in the marine platyhelminth *Macrostomum* sp.: A bromodeoxyuridine analysis. Dev Biol *226*, 231-241.

Lange C.S. (1968). A possible explanation in cellular terms of the physiological ageing of the planarians. Exp Gerontol *3*, 219-230.

Lange C.S. and Gilbert C.W. (1968). Studies on cellular basis of radiation lethality 3. Measurement of stem cell repopulation probability. Int J Radiat Biol Rel S Phys Chem Med *14*, 373-388.

Lansdorp P.M. (2007). Immortal strands? Give me a break. Cell *129*, 1244-1247.

Li L.H. and Clevers H. (2010). Coexistence of quiescent and active adult stem cells in Mammals. Science *327*, 542-545.

Morrison S.J., Shah N.M., and Anderson D.J. (1997). Regulatory mechanisms in stem cell biology. Cell *88*, 287-298.

Morrison S.J. and Spradling A.C. (2008). Stem cells and niches: Mechanisms that promote stem cell maintenance throughout life. Cell *132*, 598-611.

Mouton S., Willems M., Back P., Braeckman B.P., and Borgonie G. (2009a). Demographic analysis reveals gradual senescence in the flatworm *Macrostomum lignano*. Front Zool *6*.

Mouton S., Willems M., Braeckman B.P., Egger B., Ladurner P., Schärer L., and Borgonie G. (2009b). The free-living flatworm *Macrostomum lignano*: A new model organism for ageing research. Exp Gerontol *44*, 243-249.

Newmark P.A. and Sánchez Alvarado A. (2002). Not your father's planarian: A classic model enters the era of functional genomics. Nat Rev Genet *3*, 210-219.

Nimeth K.T., Mahlknecht M., Mezzanato A., Peter R., Rieger R., and Ladurner P. (2004). Stem cell dynamics during growth, feeding, and starvation in the basal flatworm *Macrostomum* sp. (Platyhelminthes). Dev Dyn *230*, 91-99.

Nowak J.A., Polak L., Pasolli H.A., and Fuchs E. (2008). Hair follicle stem cells are specified and function in early skin morphogenesis. Cell Stem Cell *3*, 33-43.

Orford K.W. and Scadden D.T. (2008). Deconstructing stem cell self-renewal: genetic insights into cell-cycle regulation. Nat Rev Genet *9*, 115-128.

Pfister D., De Mulder K., Hartenstein V., Kuales G., Borgonie G., Marx F., Morris J., and Ladurner P. (2008). Flatworm stem cells and the germ line: Developmental and evolutionary implications of macvasa expression in *Macrostomum lignano*. Dev Biol *319*, 146-159.

Pfister D., De Mulder K., Philipp I., Kuales G., Hrouda M., Eichberger P., Borgonie G., Hartenstein V., and Ladurner P. (2007). The exceptional stem cell system of *Macrostomum lignano*: Screening for gene expression and studying cell proliferation by hydroxyurea treatment and irradiation. Front Zool *4*.

Potten C.S., Booth D., Cragg N.J., O'Shea J.A., Tudor G.L., and Booth C. (2002). Cell kinetic studies in murine ventral tongue epithelium: cell cycle progression studies using double labelling techniques. Cell Prolif *35*, 16-21.

Potten C.S., Hume W.J., Reid P., and Cairns J. (1978). Segregation of DNA in epithelial stem cells. Cell *15*, 899-906.

Rando T.A. (2007). The immortal strand hypothesis: Segregation and reconstruction. Cell *129*, 1239-1243.

Rieger R., Gehlen M., Hazpruhnar G., Homlund M., Legnitit A., Salvenmoser W., and Tyler S. (1988). Laboratory cultures of marine Macrostomida (Turbellaria). Fortschr Zool *36*, 525.

Rossi D.J., Jamieson C.H.M., and Weissman I.L. (2008). Stems cells and the pathways to aging and cancer. Cell *132*, 681-696.

Sánchez Alvarado A. (2004). Regeneration and the need for simpler model organisms. Philos Trans R Soc Lon Ser B-Biol Sci *359*, 759-763.

Schärer L., Ladurner P., and Rieger R.M. (2004). Bigger testes do work more: experimental evidence that testis size reflects testicular cell proliferation activity in the marine invertebrate, the free-living flatworm *Macrostomum* sp. Behav Ecol Sociobiol *56*, 420-425.

Schärer L., Zaubzer J., Salvenmoser W., Seifarth C., and Ladurner P. (2007). Tracking sperm of a donor in a recipient: an immunocytochemical approach. Animal Biology *57*, 121-136.

Sharpless N.E. and Depinho R.A. (2007). How stem cells age and why this makes us grow old. Nat Rev Mol Cell Biol *8*, 703-713.

Shinin V., Gayraud-Morel B., Gomes D., and Tajbakhsh S. (2006). Asymmetric division and cosegregation of template DNA strands in adult muscle satellite cells. Nat Cell Biol *8*, 677-687.

Smith G.H. (2005). Label-retaining epithelial cells in mouse mammary gland divide asymmetrically and retain their template DNA strands. Development *132*, 681-687.

Sotiropoulou P.A., Candi A., and Blanpain C. (2008). The majority of multipotent epidermal stem cells do not protect their genome by asymmetrical chromosome segregation. Stem Cells *26*, 2964-2973.

Spradling A., Drummond-Barbosa D., and Kai T. (2001). Stem cells find their niche. Nature *414*, 98-104.

Steph F. and Gilgenkrantz F. (1961). Transplantation et regeneration chez la planaire *Dendrocoelum lacteum*. J Embryol Exp Morphol *9*, 642-649.

Tannenbaum E., Sherley J.L., and Shakhnovich E.I. (2005). Evolutionary dynamics of adult stem cells: Comparison of random and immortal-strand segregation mechanisms. Phys Rev E *71*, 041914.

Tsai R.Y.L., Kittappa R., and McKay R.D.G. (2002). Plasticity, niches, and the use of stem cells. Dev Cell *2*, 707-712.

Waghmare S.K., Bansal R., Lee J., Zhang Y.V., McDermitt D.J., and Tumbar T. (2008). Quantitative proliferation dynamics and random chromosome segregation of hair follicle stem cells. EMBO J *27*, 1309-1320.

Wagner D.E., Wang I.E., and Reddien P.W. (2011). Clonogenic neoblasts are pluripotent adult stem cells that underlie planarian regeneration. Science *332*, 811-816.

Watt F.M. and Hogan B.L.M. (2000). Out of Eden: Stem cells and their niches. Science *287*, 1427-1430.

Wei Z.G., Cotsarelis G., Sun T.T., and Lavker R.M. (1995). Label-retaining cells are preferentially located in fornical epithelium - implications on conjunctival epithelial homeostasis. Invest Ophthalmol Vis Sci *36*, 236-246.

Wilson A., Laurenti E., Oser G., van der Wath R.C., Blanco-Bose W., Jaworski M., Offner S., Dunant C.F., Eshkind L., Bockamp E., Lio P., MacDonald H.R., and Trumpp A. (2008). Hematopoietic stem cells reversibly switch from dormancy to self-renewal during homeostasis and repair. Cell *135*, 1118-1129.

Yamashita Y.M., Fuller M.T., and Jones D.L. (2005). Signaling in stem cell niches: lessons from the *Drosophila* germline. J Cell Sci *118*, 665-672.

3. Proliferative response of the stem cell system during regeneration of the rostrum in Macrostomum lignano (Platyhelminthes)

Modified from:

Verdoodt F, Bert W, Couvreur M, De Mulder K, and Willems M (2012) Proliferative response of the stem cell system during regeneration of the rostrum in Macrostomum lignano (Platyhelminthes). Cell Tissue Res 347(2):397-406

3.1. Abstract

Macrostomum lignano (Platyhelminthes) possesses pluripotent stem cells, also called neoblasts, which power its extraordinary regeneration capacity. We have examined the cellular dynamics of neoblasts during regeneration of the rostrum in *M. lignano*. First, using live squeeze observations, the growth curve of the rostrum was determined. Second, neoblasts were labelled with bromodeoxyuridine (BrdU) and anti-phospho histone H3 mitosis marker (anti-phos-H3) to analyze their proliferative response to amputation. During the regeneration process, both S- and M-phase cells were present anterior to the eyes, a region which is devoid of proliferating cells during homeostasis. Furthermore, BrdU pulse experiments revealed a biphasic S-phase pattern, different from the pattern known to occur during regeneration of the tail plate in *M. lignano*. During a first systemic phase, S-phase numbers significantly increased, both in the region adjacent to the wound (the anterior segment) and the region far from the wound (the posterior segment). During the second, spatially restricted phase, S-phase numbers in the anterior segment rose to a peak at three to five days post-amputation (p-a), while in the posterior segment, S-phase activity approached control values again. A blastema, characterized as a build-up of S- and M-phase cells, was formed one day p-a.

Altogether, our data present new insights into the cellular response of the neoblast system upon amputation, clearly demonstrating important differences from the situation known to occur during regeneration of the tail plate. Furthermore, the presence of proliferating cells in the region anterior to the eyes shows a clear alteration in stem cell regulation during regeneration.

3.2. Introduction

Flatworms are famous for their extraordinary ability to regenerate lost body parts. During this process, adult stem cells—the so-called neoblasts—have been shown to play an indispensable role. The majority of the regeneration research within flatworms has focused on triclads (Brøndsted, 1969; Saló and Baguñà, 2002; Agata, 2003; Reuter and Kreshchenko, 2004; Reddien and Sánchez Alvarado, 2004; Saló, 2006). However, within macrostomids, *Macrostomum lignano* (Ladurner et al., 2005b) is becoming a complementary model organism for studying adult stem cells and regeneration *in vivo*. This is mostly due to their small size, which allows for straightforward quantitative analysis, and the ability to label S-phase cells with the thymidine analogue 5-bromo-2'-deoxyuridine (BrdU), by simply soaking (Ladurner et al., 2000). In contrast, successful BrdU-labelling in triclads requires feeding or injection, which were both reported to inflict changes on the proliferative status of neoblasts (Newmark and Sánchez Alvarado, 2000).

M. lignano can regenerate all organ systems as long as brain and pharynx are present (Egger et al., 2006). To date, detailed reports are mainly available on regeneration of the tail plate in this flatworm. One study on the dynamics of the stem cell pool has demonstrated massive neoblast proliferation upon amputation, though restricted to neoblasts located near the wound region (Nimeth et al., 2007). The caudal blastema, an accumulation of proliferating cells that is visible 24 hours after amputation, was described in great detail (Egger et al., 2009), as was the restoration of the muscle system (Salvenmoser et al., 2001). Despite the attention paid to tail plate regeneration in *M. lignano*, no more information on regeneration of the rostrum is currently available, other than live observations showing that it can occur successfully given that the brain remains intact (Egger et al., 2006). The reaction of the neoblast system on amputation of the rostrum in *M. lignano* remains unknown. Nonetheless, given that this region is devoid of neoblasts in control worms, it is a compelling region in that it allows precise analysis of neoblast migration. To our knowledge, within the macrostomids, the stem cell response

during regeneration of the rostrum was described only once, in *Microstomum lineare* (Palmberg, 1986). However, contrary to *M. lignano*, this species reproduces asexually and does have proliferative cells in the rostrum during homeostasis. Remarkably, on a morphological level, *M. lineare* showed no sign of blastema formation (Palmberg, 1986), though it must be noted that detailed spatial and temporal analyses of the stem cell dynamics were not undertaken in this study.

In the current study, the regeneration of the rostrum in *M. lignano* was analyzed, performing amputation anterior to the brain. Firstly, live squeeze observations were used to describe the regeneration process morphologically and determine its time course. Secondly, immunolabelling techniques were performed with BrdU and anti-phospho-histone H3 mitosis marker (anti-phos-H3) to study the cellular dynamics of the neoblast pool following amputation. For accurate analysis of the results, a distinction is made between neoblasts located in a region near the wound and those in a region far from the wound (the anterior and posterior segment, respectively). Quantitative analysis demonstrates a biphasic S-phase pattern, consisting of an initial systemic phase, followed by a secondary spatially restricted phase. One day p-a, a regeneration blastema was formed in the rostrum, in which a build-up of S-phase and mitotic cells was apparent.

3.3. Materials & Methods

3.3.1. Cultures

M. lignano cultures were grown in f/2-medium (Guillard and Ryther, 1962) and fed ad libitum with the diatom *Nitzschia curvilineata*, as described by Mouton et al (2009b). Amputations were performed with a fine steel surgical blade (SM62, Swann-Morton) under a stereo microscope, while worms were relaxed in a small droplet of 1:1 $MgCl_2.6H_2O$ (7.14%) and ASW (artificial sea water). Immediately thereafter, specimens were washed in

f/2 medium. Unless otherwise stated, regenerates were then transferred to culture dishes filled with f/2 medium and diatoms and left to regenerate.

3.3.2. *In vivo* observations

For determination of the growth curve of the rostrum, a time series was made, observing the same individuals at successive time points post-amputation (p-a) (0, 2, 4, 6, 8, 10, and 12 days). Animals were anaesthetized in a 2:1 mixture of $MgCl_2.6H_2O$ (7.14%) and ASW, and live squeeze preparations were made using a standardized spacer (35 µm), as specified by Schärer and Ladurner (2003).

To study the regeneration process of anatomical structures in the rostrum, animals were observed at several time points p-a (0, 1, 2, 4, 8, and 12 hours; 1, 2, 4, 6, 8, and 10 days). Live squeeze preparations were made without a spacer, using a drop (20µl) of a 2:1 mixture of $MgCl_2.6H_2O$ (7.14%) and ASW. Specimens were observed with interference contrast microscopy (Olympus BX51), and images were made with an Olympus C-5060 camera. For the growth curve of the rostrum, measurements of the length of the rostrum and mouth opening were performed, using the free software program Image J (Abramoff et al., 2004), and statistical analysis was performed, using repeated measurements Anova (Statistica 7).

3.3.3. Staining of muscle F-actin and serotonergic nerve cells

Muscle F-actin filaments were stained according to the protocol described by Salvenmoser et al. (2001), using TRITC-conjugated Phalloidin (1:200, Sigma). Staining of the serotonergic nervous system was performed by relaxing the animals, first in a 1:1 mixture of $MgCl_2.6H_2O$ (7.14%) and ASW (5min), then in $MgCl_2.6H_2O$ (7.14%) (undiluted, 5min), followed by fixation in paraformaldehyde (PFA, 4% in PBS, 60min). Subsequently, animals were rinsed with phosphate-buffered saline (PBS, 3 x 5min) and blocked in bovine serum albumin, containing triton (BSA-T, 0.1% Triton X-100, 60min). Animals were then incubated in primary rabbit-anti-5HT (1:400 in BSA-T, 48h, 4°C, Sigma), rinsed with PBS-T (0.1% Triton X-100, 5 x 5min), and incubated in secondary TRITC-conjugated goat-anti-rabbit (1:100 in

BSA-T, 2h, room temperature, Millipore). Finally, animals were rinsed with PBS (5 x 10min) and slides were mounted using Vectashield (Vector Laboratories).

3.3.4. Scanning electron microscopy

Specimens were relaxed (as described for staining of the nervous system), fixed in glutaraldehyde (2.5% in sodium cacodylate buffer – 0.2M, pH 7,4, 2d, 4°C), and rinsed with sodium cacodylate buffer (0.2M, 4 x 5min). Fixed specimens were then dehydrated in graded ethanol solutions (30%, 50%, 75%, 90%, 95%, and 99% ethanol - 1 x 20min each; and 100% ethanol - 3 x 15min). Subsequently, animals were rinsed with liquid CO_2 (5 x), critical-point dried (Balzers Union, CPD020), mounted onto stubs with carbon tabs and coated with gold (JFC1200 Finecoater, Jeol). Finally, they were examined with a Jeol JSM-840 scanning electron microscope.

3.3.5. BrdU pulse, BrdU pulse-chase, and anti-phos-H3 labelling

During pulse periods, the thymidine analogue 5'-bromo-2'-deoxyuridine (BrdU, Sigma) is incorporated into the nuclei of cells in S-phase. Organisms were labelled with BrdU (5mM in ASW), soaking them for 30min. For BrdU pulse experiments, groups of animals were pulsed at different time points p-a (2, 4, 8, 12, and 24 hours; 2, 3, 4, 5, 6, 7, 8, 9, and 10 days), after which the incorporated BrdU was visualized. For BrdU pulse-chase experiments, animals were pulsed immediately following amputation, washed with f/2 (3 x 5min) and chased in f/2 for 0, 2, 4, 8, or 12 hours; 1 or 2 days (in the dark). BrdU was visualized after completion of the chase-period.

For visualization of the BrdU, animals were relaxed and fixed, as described for staining of the serotonergic nervous system, followed by several rinses with PBS (3 x 5min) and incubation in PBS-T (60min). Specimens were treated with Protease XIV (0.2mg/ml in PBS-T, 37°C, under visual control, Sigma), exposed to 0.1M HCl (10min, on ice) and 2M HCl (1h, 37°C), washed several times with PBS (3 x 10min), and blocked in BSA-T (30min). Incorporated BrdU was localized using a monoclonal mouse-anti-BrdU antibody (1:600 in

BSA-T, overnight, 4°C, Sigma). After being washed with PBS (3 x 10min), a secondary FITC-conjugated goat-anti-mouse antibody (1:200 in BSA-T, 1h, DAKO) was used.

To test the presence of mitotic cells in the rostrum of 1-day regenerates, the mitotic marker anti-phospho-histone H3 (anti-phos-H3) was used. Specimens were treated as described for the visualization of BrdU, starting from relaxation until the blocking treatment in BSA-T. Subsequently animals were incubated in primary anti-phos-H3 antibody (1:300 in BSA-T, overnight, 4°C, Upstate Biotechnology), rinsed in PBS (3 x 10min), and incubated in secondary TRITC-conjugated swine-anti-rabbit (1:150 in BSA-T, 1h, DAKO). Finally, animals were washed with PBS (3 x 10min) and slides were mounted using Vectashield (Vector Laboratories).

Immunohistochemical stainings were analyzed using a Nikon Eclipse C1si laser scanning microscope. An argon laser (488 nm) in combination with a narrow band-pass filter (BP 515/30), and a helium-neon laser (543 nm) in combination with a narrow band-pass filter (BP 593/40) were used for visualization of the FITC- (BrdU), and TRITC-fluorochromes (anti-phos-H3), respectively. Images were processed using Nikon EZ-C1 3.40 and Photoshop CS2 software.

3.3.6. Quantitative analysis of cellular dynamics

In control animals and in regenerating specimens, the number of S-phase cells was determined in the region anterior to the testes and the region posterior to the ovaries, respectively referred to as the anterior and posterior segment. Additionally, S-phase activity in the rostrum was analyzed quantitatively, by performing quantification of labelled cells in the rostral segment, the region marked by the anterior border of the eyes and the anterior tip of the rostrum. These quantification areas have the advantage of being able to be defined precisely for each animal by marking the border of the gonads or eyes. Quantification of BrdU-labelled cells was performed on confocal images using the cell-counter plug-in for Image J (Abramoff et al., 2004). Prior to the analysis of the cellular dynamics data, residual plots indicated homoscedastic error distributions, and formal testing did not reject the normality assumption of the error terms. However, these data

are based on a relatively low sample size, and small samples almost always pass a normality test. Hence, a non-parametric test, although having lower power efficiency, is more appropriate. Congruent with our independent-samples design, differences between observations were tested using a Mann-Whitney U Test (Statistica 7).

3.4. Results

3.4.1. Growth curve of the rostrum and morphological study of the regeneration process

The anterior margin of the brain, located in front of the eyes, was used as a reference point for amputation (Figure 3.1a). The duration of the regeneration process, when cut anterior to the brain, was determined by a morphological marker. A time series of individuals was made, measuring the ratio of the length of the rostrum to that of the mouth opening, before amputation and at different time points p-a (0, 2, 4, 6, 8, 10 and 12 days, n=4). This ratio was constant in control animals (Figure 3.1b). Following amputation, the value increased gradually as more newly formed tissue is present in time. Six days p-a, this ratio again approached the value of control animals (p=0.9).

Using *in vivo* squeeze preparations, the rostrum was studied in control animals (Figure 3.1c, c', and c") and regenerates (Figure 3.1d-f) after amputation at the designated level. A fast wound-closing mechanism was observed following amputation of the rostrum. After only 1h p-a, for the most part, the wound area was covered with a layer of flattened epidermal cells (Figure 3.1d). At this early stage however, the wound was still fragile and easily broke open when observed in animals anaesthetized with $MgCl_2$ *in vivo* squeeze preparations. Scanning electron microscopic (SEM) images confirmed that, 1h p-a, epidermal cells cover the wound almost completely, leaving only a small opening (Supplementary Figure 3.S1b). However, as the wound was observed to still be fragile, it cannot be excluded that this opening was a result of anaesthetizing the animals, prior to fixation. In addition to epidermal cells covering the wound area, reduction of the size of

the wound was observed. Staining of muscle F-actin, 1h p-a, confirmed contraction of muscle fibers at the wound site (Supplementary Figure 3.S2b). One day p-a, the presence of cilia of sensory receptors was visible at the anterior tip (Fig 1e, e'). Eight days p-a, the presence of morphologically visible structures —such as rhammites, rhabdites, and cilia of sensory receptors— resembled those in control animals. The formation of an extension of un-pigmented blastema cells at the level of the wound —as previously described during regeneration of the tail plate— could not be observed during live observation in one- (Figure 3.1e, e') or two- (Figure 3.1f, f') day regenerates, or at any other time-step of the regeneration process. A blastema extension was either absent or was not distinguishable due to the un-pigmented nature of neighboring differentiated cells in the rostrum.

Figure 2.1:

The regeneration process in Macrostomum lignano following amputation of the rostrum. **a** Schematic drawing of adult *M. lignano.* Amputation level (red dotted line) just anterior tot the brain. The rostrum (two-sided arrow) is described as the area in front of the eyes. Abbreviations: *ro* rostrum, *b* brain, *e* eye, *m* mouth, *ph* pharynx, *g* gut, *t* testis, and *o* ovary. **b** Graph representing the growth curve of the rostrum during the regeneration process (n=4). Y-values represent the ratio of the length of the rostrum to the length of the mouth (± standard deviation), which is observed to be constant in control animals. The X-axis represents time points after amputation (in days). Six days p-a, the ratio approaches the constant value again. Significant differences with the control value are indicated with an asterisk. c-f Light microscopic images of the rostrum area in *M. lignano*. c Control animal, showing epidermal layer (*ep*), and cilia of sensory receptors (*s*). Rhammite gland necks run through the brain into the rostrum (arrowheads). c' Detail of *s* in a control animal. c'' Detail of *ep*. d 1h p-a. The wound surface is covered by flattened epidermal cells (open arrowheads). Preparing the slides causes some epidermal cells to detach (x), which shows the fragility of the wound. e 1d p-a. Rhammite gland necks and *S* are visible. e' Detail of *s*. f 2d p-a. rhammite gland necks are visible. f' Detail of the anterior tip of the rostrum, showing rhammite gland necks. Anterior is on top. Bars c, d, e, f: 50µm. Bars c', e', f': 25µm. Bar c'': 10µm.

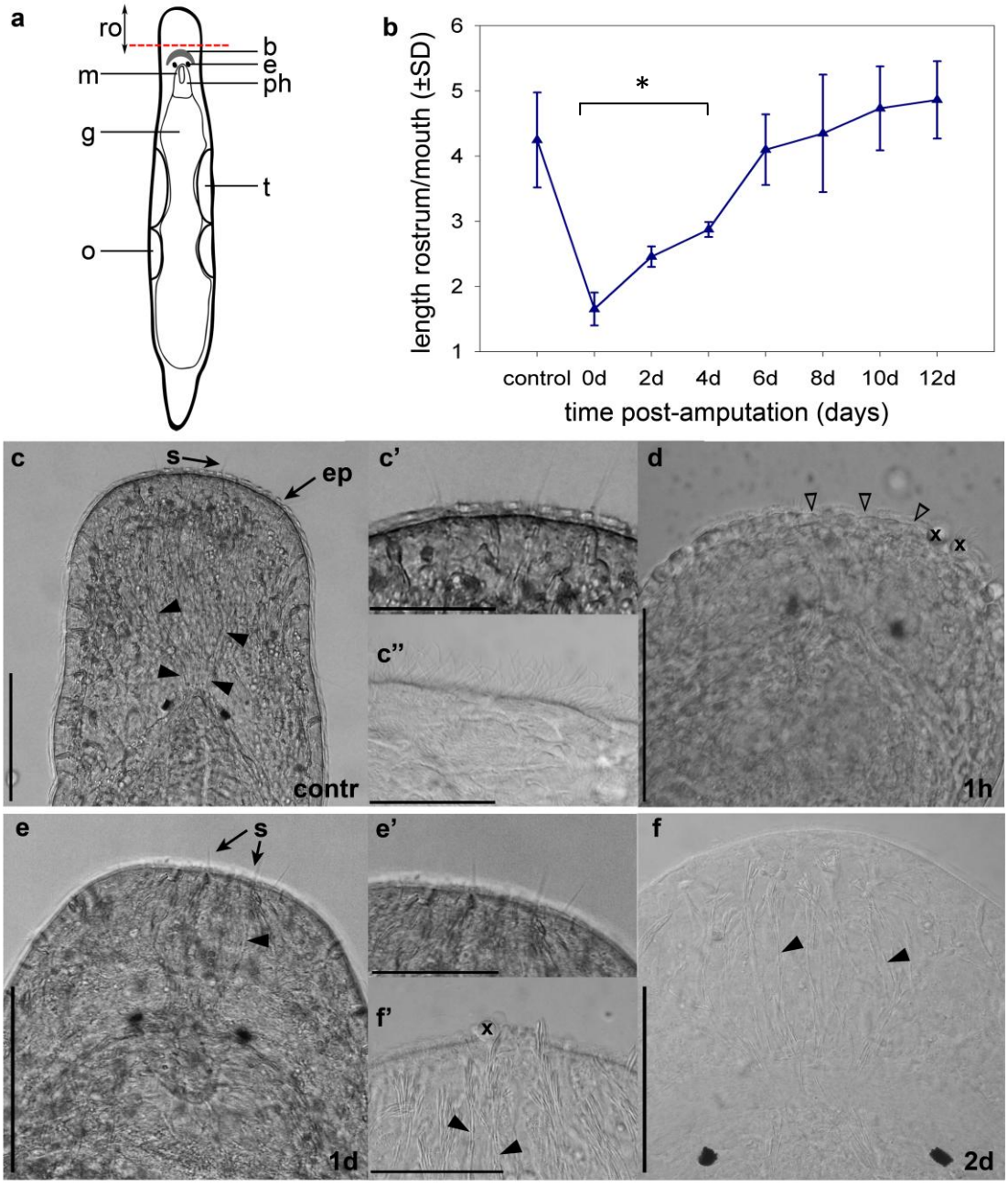
a
ro
b
e
m
ph
g
t
o
b
length rostrum/mouth (±SD)
6
5
4
3
2
1
*
control 0d 2d 4d 6d 8d 10d 12d
time post-amputation (days)
c
s
ep
contr
c'
c''
d
x
x
1h
e
s
1d
e'
f'
x
f
2d

3.4.2. Stem cell dynamics during regeneration of the rostrum

BrdU pulse experiments were performed to study the response of the neoblast pool as a reaction to amputation of the rostrum. To test whether loss of tissue causes a systemic response or a response that is spatially restricted, S-phase neoblasts were quantified in the region adjacent to the wound, as well as those in the region far from the wound.

For analysis of proliferation dynamics of the neoblasts near the wound, BrdU-labelled S-phase cells were quantified in the region marked by the wound itself and by the anterior border of the testes, the anterior segment (Figure 3.2a). Quantification of the number of S-phase cells was performed on control animals and on regenerates at different stages of the regeneration process (2, 4, 8, and 12 hours; 1, 2, 3, 4, 5, 6, 7, 8, 9, and 10 days) (Figure 3.2b). In control animals, 80 (±11, n=5) S-phase cells were present in the anterior segment. After amputation, a fast response was observed. Two hours p-a, the number of S-phase cells had increased significantly (114±12, n=7; Mann-Whitney U, p=0.04), and already at four hours p-a, this number exceeded a 50% increase (127±15, n=7; Mann-Whitney U, p=0.004). Subsequently, S-phase numbers further rose until 2d p-a (156±34, n=5), eventually resulting in an S-phase peak at three (193±38, n=7), four (192±36, n=7), and five days p-a (180±24, n=7). The number of S-phase cells had decreased significantly at six days p-a (128±39, n=9; Mann-Whitney U, p=0.02) and approached control values again at nine days p-a (119±42, n=9; Mann-Whitney U, p=0.05).

To test whether this S-phase response is systemic, S-phase cells were quantified in the posterior segment, the region marked by the posterior border of the ovaries and the tail of the animal (Figure 3.2a). Quantification was performed in control animals, and in regenerates at time points corresponding to the initial fast increase (2h, and 4h p-a) and the S-phase peak (3d, 4d and 5d p-a) as observed in the anterior segment (Figure 3.2c). Control animals were observed to have 169 (±38, n=8) S-phase cells in the posterior segment. In two-hour regenerates, this number had increased merely slightly (195±17, n=6; Mann-Whitney U, p=0.1). However, at four hours p-a, a significant increase was observed (212±35; Mann-Whitney U, n=8, p=0.028), demonstrating an initial systemic S-

phase response to amputation of the rostrum. In three- (163 ±23, n=6), four- (187±18, n=6), and five-day regenerates (172±26, n=5) the number of S-phase cells was not significantly different from control animals (Mann-Whitney U; p=0.95, p=0.2, and p=0.7, respectively). Thus, while S-phase numbers are significantly increased in the anterior region, the number of S-phase cells in the region far from the wound was comparable to controls. In conclusion, a biphasic S-phase response to amputation of the rostrum was observed, consisting of an initial systemic response and a secondary spatially restricted response.

Figure 3.2:

Dynamics of S-phase cells during regeneration of the rostrum in *M. lignano* (BrdU pulse)

a Schematic drawing of adult *M. lignano.* Light and dark grey area represent, respectively, the anterior and posterior segment in which S-phase cells were quantified. Amputation level (red dotted line) is anterior to the brain. **b, c** Graphs representing quantification data of S-phase cells during regeneration, respectively, in the anterior and posterior segment. Y-values represent the mean number of S-phase cells (± standard deviation). X-axes represent time p-a. (n=5-9) **b** An early onset increase of S-phase numbers is already observed 2h p-a. S-phase activity further increased, until reaching a peak at 3d–5d p-a. **c** A significant increase in S-phase cells is observed, 4h p-a. 3d, 4d, and 5d p-a, S-phase numbers approach control values. **d** BrdU-labelling after a 30-minute BrdU pulse. Confocal projection of a control animal. S-phase neoblasts are distributed in a bilateral pattern. No S-phase cells are present anterior to the level of the eyes (arrow). **e, f** Quantitative analysis of migration of S-phase cells into the rostrum. **e** Schematic drawing of adult *M. lignano.* Grey area represents the rostral segment in which S-phase cells were quantified. Amputation level (red dotted line) is anterior to the brain. **f** Graph representing quantification data of S-phase cells in the rostral segment during the regeneration process (n=5-7). Y-values represent the mean number of S-phase cells (± standard deviation). X-axis represents time p-a. **g-l** BrdU-labelling after a 30-minute BrdU pulse. Confocal projections of the rostrum area. **g** 4h p-a. The number of S-phase cells at the level of the eyes has increased. **h** 12h p-a. S-phase cells are present at the level of the wound, underneath the epidermis (open arrowhead). **i** 1d p-a, 2 individuals. A blastema is visible at the anterior tip of the rostrum, characterized by a build-up of S-phase cells which however varies in density (left panel versus right panel). (n=4) **j** 2d p-a, 2 individuals. S-phase activity in the blastema has decreased (left panel). S-phase activity in the blastema remains high (right panel). **k** 6d p-a. The S-phase cells that are located most anteriorly, are at the level of the eyes. **l** Confocal projection of the rostrum area after anti-phos-H3 labelling. 1d p-a. Mitotic cells are present in the blastema. Arrows indicate the level of the eyes. Anterior is on top. Bars: 50µm.

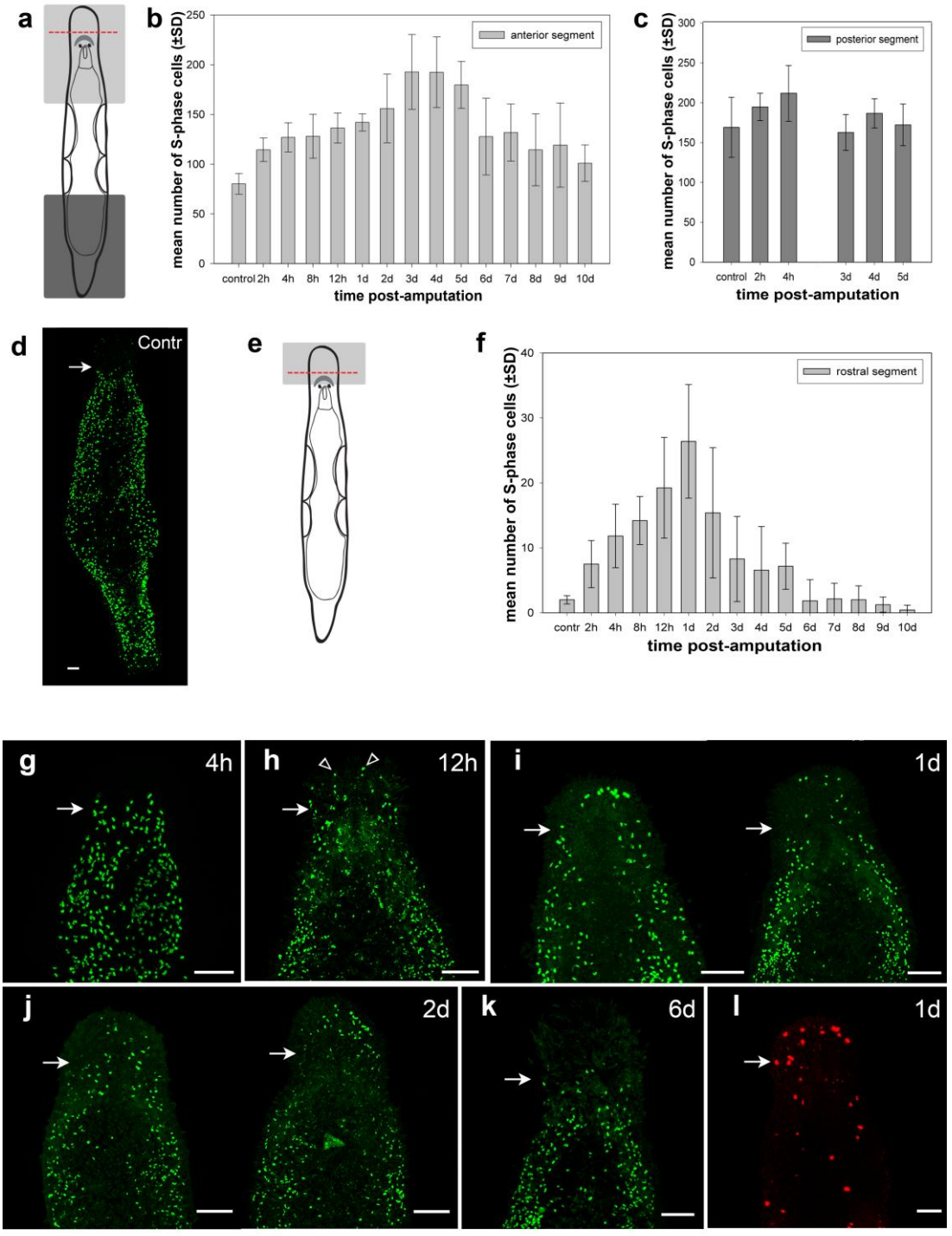
a
b
mean number of S-phase cells (±SD)
anterior segment
control 2h 4h 8h 12h 1d 2d 3d 4d 5d 6d 7d 8d 9d 10d
time post-amputation
c
posterior segment
control 2h 4h 3d 4d 5d
d
Contr
e
f
rostral segment
contr 2h 4h 8h 12h 1d 2d 3d 4d 5d 6d 7d 8d 9d 10d
g
4h
h
12h
i
1d
j
2d
k
6d
l
1d

3.4.3. Spatial Distribution of S-phase and Mitotic cells

In control animals, the most anterior position of S-phase neoblasts is at the level of the eyes (Figure 3.2d). S-phase cells were never observed more than 20µm (n=5) anterior to the upper border of the eyes. During regeneration of the rostrum, S-phase cells were observed in the rostrum. To analyze S-phase activity in the rostrum, labelled cells were quantified in the rostral segment (Figure 3.2e) at different time steps during the regeneration process (Figure 3.2f). In control animals, on average two (±1, n=5) S-phase cells were present. This number rapidly increased during the regeneration process, until it reached a maximum of 26 (±9, n=5; Mann-Whitney U, p=0.004) cells at 1d p-a. In three-day regenerates, this number had decreased significantly, compared to 1d p-a (8±7, n=7; Mann-Whitney U, p=0.01) and at six days p-a, the number approached control values (2±3, n=7; Mann-Whitney U, p=0.84).

Additionally, the presence of S-phase cells in the rostrum was analyzed qualitatively (Figure 3.2g-k; for additional images, see Supplementary Figure 3.S3). Four hours after amputation, the number of S-phase cells at the level of the eyes was increased in comparison to non-regenerating animals (Fig 2g). S-phase cells were visible for the first time at the level of the wound, underneath the epidermal cell layer, in animals that were left to regenerate for 12 hours (Figure 3.2h). One day p-a, cells going through S-phase accumulated, forming a regeneration blastema in the region below the wound. Although in all individuals, S-phase cells were present in this region, their density was observed to vary (Figure 3.2i, compare left panel to right panel). Two days p-a, S-phase activity in the blastema had decreased in most of the observed animals (Figure 3.2j, left panel). In 20% of the individuals, S-phase activity was still highly upregulated in the blastema (Figure 3.2j, right panel). In six-day regenerates, no S-phase activity was observed in the region below the wound. Instead, the S-phase cells which were located most anteriorly, were located within a distance of 20µm from the level of the eyes, comparable to control animals (Figure 3.2k). In two specimens, however (total n=10), a single S-phase cell was observed that was still located at a distance between 50µm and 100µm from the level of the eyes.

Our results demonstrate the temporary presence of cells in S-phase in the rostrum region. The S-phase activity in this region reached a maximum, one day p-a. In order to unambiguously prove the existence of actual cell division in this region, one-day regenerates were analyzed using anti-phos-H3. In all animals (n=4), mitotic cells were observed in the region anterior to the eyes and at the anterior tip of the rostrum, the region of the blastema (Figure 3.2l).

3.4.4. BrdU pulse-chase experiments to study cell cycle parameters and migration of cells

By means of BrdU pulse-chase experiments, cell cycle parameters and migration patterns of BrdU-labelled ($BrdU^+$) cells can be assessed. Animals were amputated at the level anterior to the brain, after which they received a 30min BrdU pulse, followed by a chase time during which $BrdU^+$ cells can divide and migrate. Thus, at the time of visualization of the BrdU, labelled cells are not necessarily S-phase cells anymore. BrdU was visualized in different groups of animals after a chase of 0, 2, 4, 8, and 12 hours, and after 1 and 2 days. As a consequence, a cohort of cells that were in S-phase, or started S-phase during the 30-minute time interval p-a, was followed in time during the regeneration process.

First, quantification of the number of $BrdU^+$ cells was performed in all groups (Figure 3.3a), allowing analysis of cell cycle parameters of these cells. A 30-minute BrdU pulse in control animals resulted in 83 (±10, n=4) $BrdU^+$ cells in the anterior segment (see Fig 2a). In BrdU pulsed regenerates that were not chased (0h), 106 (±18, n=7) labelled cells were visible. This significant (28%; Mann-Whitney U, p=0.014) increase represents an extra activation of cells due to amputation. In 2h chased animals, 114±13 (n=8; Mann-Whitney U, p=0.9) $BrdU^+$ cells were quantified. Between two, and four hours p-a, this number increased significantly to 143 (±16, n=9; Mann-Whitney U, p=0.003) $BrdU^+$ cells, which corresponds to a 35%-increase of the initial cohort of cells. This increase was caused by the division of labelled cells. In 8h-regenerates, 148 (±10, n=5) S-phase cells were quantified. This indicates that, during the time interval between four and eight hours of chase, only 4%

(p=0.6) of the $BrdU^+$ cells divided, assuming that no cells go through apoptosis. Subsequently, $BrdU^+$ cells further increased rapidly up to a doubling of cell numbers after a 2d-chase (209±20, n=7), every measured time point being significantly higher than the previous one (Mann-Whitney U, $p<0.05$).

Second, the spatial distribution of $BrdU^+$ cells was assessed, in order to investigate patterns of migration during the first two days of the regeneration process. After a 30-minute pulse and a two-hour chase, pairs of labelled cells could be observed (Figure 3.3b, inset). Longer chase times resulted in the observation of cells that migrated to the rostrum via a route that passes at the lateral sides of the regenerating rostrum (Figure 3.3c). Staining of the serotonergic nervous system demonstrated that, prior to the time-step when migration of neoblasts was visible (4h chase), severed nerve fibers were observed to run all the way to the anterior tip of the growing rostrum (Supplementary Figure 3.S4). After a 12-hour chase period, $BrdU^+$ cells were observed to have migrated medially in the rostrum, and labelled cells were present at the level of the wound, underneath the epidermal cell layer (Figure 3.3d). Starting from the level of the eyes, they migrated over an average distance of 116.4µm. Based on these data, the minimal, average migration rate of neoblasts during regeneration of the rostrum was estimated at 9.7µm/h. After a chase of one day, the amount of $BrdU^+$ cells that had migrated to the median axis of the rostrum was increased, and after a two-day chase, a tight accumulation of labelled cells was observed (Figure 3.3e).

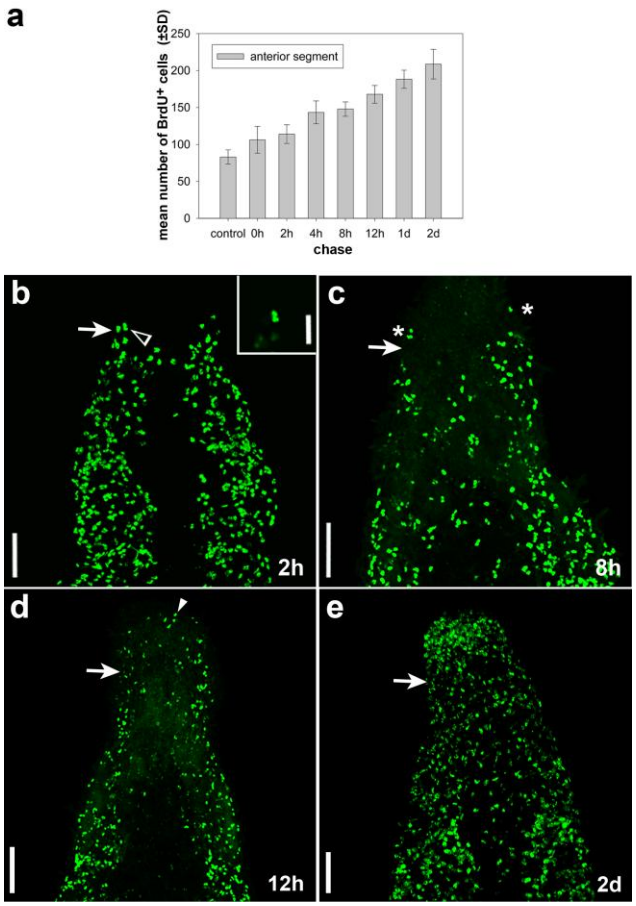

Figure 3.3

Animals received a 30-minute BrdU pulse immediately after amputation and were then chased. **a** Graph representing the quantification of $BrdU^+$ cells in the anterior segment. Y-values represent the mean number of $BrdU^+$ cells (± standard deviation) in the anterior segment. The X-axis represents the chase time duration. 0h chase demonstrates a significant increase, which represents an extra activation of cells upon amputation. $BrdU^+$ cells further increase up to a 100% increase after a 2d chase, due to cell division of labelled cells. **b-e** Confocal projections of the rostrum area after BrdU pulse-chase labelling. **b** 2h chase. Migration of $BrdU^+$ cells is not yet visible. A pair of labelled cells is visible (open arrowhead). Inset: Single confocal stack, showing the pair of labelled cells. **c** 8h chase. Cells, migrating in the direction of the wound area, at the lateral sides of the rostrum (asterisks). **d** 12h chase. $BrdU^+$ cells have migrated towards the midline of the rostrum (antero-posteriorly), and have reached the anterior tip of the rostrum (arrowhead). **e** 2d-chase. An accumulation of $BrdU^+$ cells is visible at the anterior tip of the organism. Arrows indicate the level of the eyes. Anterior is on top. Bars: 45μm, Bar inset: 20μm.

3.5. Discussion

3.5.1. Wound healing and blastema formation

Following amputation of the rostrum, a fast wound-closing mechanism was observed. Besides contraction of the musculature at the level of the wound, already one hour p-a, the wound was almost completely covered by a thin layer of flattened epidermal cells. The same mechanism was observed earlier for tail plate regeneration in *M. lignano* (Salvenmoser et al., 2001; Nimeth et al., 2007; Egger et al., 2009), and regeneration in triclads, so-called planarians (Baguñà et al., 1994; Alvarado and Newmark, 1998) and polychaetes (Paulus and Muller, 2006).

Our BrdU pulse and histon-H3 experiments in one-day regenerates, demonstrated the presence of a blastema, which was built up of cells in S- and M-phase. The fact that a clearly distinguishable blastema extension did not show up in our light microscopic analysis is most likely due to the un-pigmented nature of the rostrum area, hampering discernment of such an accumulation of un-pigmented cells.

3.5.2. Biphasic S-phase pattern

S-phase activity shows a biphasic pattern in response to amputation of the rostrum. During the first phase, S-phase numbers were observed to increase significantly, both in the region adjacent to the wound and the region far from the wound (the anterior and posterior segment, respectively). This systemic phase was followed by a second phase that was spatially restricted to the anterior segment.

The exact stimulus that leads to each of the two phases is not known. In triclads, similar findings have been reported when quantifying mitotic cells. In these organisms, amputation was shown to initially result in a systemic mitotic peak, followed by a local, second peak (Baguñà, 1976b; Saló and Baguñà, 1984; Wenemoser and Reddien, 2010). The first peak was shown to be caused by the stimulus of injury itself, while the second peak was uniquely caused by tissue absence (Wenemoser and Reddien, 2010).

Interestingly, amputation of the tail plate in *M. lignano* was observed to only cause a local proliferative response (Nimeth et al., 2007), resulting in a peak, temporally corresponding to the S-phase peak in our study. Increased S-phase activity was not observed in regions far from the wound.

Equally remarkable, amputation of the rostrum was observed to cause an early onset increase in S-phase numbers, while regeneration of the tail plate demonstrated an initial decrease of this number (Nimeth et al., 2007). The decrease which was observed during tail plate regeneration, coincided with wound closure (Salvenmoser et al., 2001), and was suggested by the authors as a mechanism to prevent the additional loss of regenerative cells through the wound opening. The apparent different reaction during regeneration of the rostrum, might be linked to the distribution of neoblasts during homeostasis. When amputating the tail plate, neoblasts are present within the vicinity of the wound. Therefore it seems beneficial to delay expansion of these valuable cells until the wound is safely closed. Amputation of the rostrum, on the other hand, does not imply danger of losing regenerative cells, since, at the time of amputation, the most anterior neoblasts are positioned at the level of the eyes. Proliferative cells were observed to need twelve hours to reach the wound, which by that time is already closed. Given this fact, there would be no reason to stall proliferation.

3.5.3. Migration and proliferation in the rostrum

Our BrdU-experiments demonstrate a migration of neoblasts to the rostrum, with an average migration speed of 9.7µm/h. This shows that, compared to a migration speed of 6.5µm/h during homeostasis (Ladurner et al., 2000), regeneration can induce an accelerated migration speed. These results correspond to previous observations of an accelerated migration in regenerating triclads (Saló and Baguñà, 1985).

Interestingly, for the first time, our study demonstrates transient neoblast proliferation in the region anterior to the eyes. Hitherto, proliferation in this region had never been observed, not in juveniles, adults, nor starved adults (Ladurner et al., 2000; Nimeth et al., 2004; Nimeth et al., 2007). Hence, during development, homeostasis, and starvation, stem

cells which maintain proliferative activity, are inhibited to migrate into the rostrum, and this region is solely maintained by the migration of post-mitotic cells. During regeneration, however, our study clearly shows that neoblasts are able to migrate into the rostrum and then go through S- and M-phase. It is not clear whether regeneration induces a stimulus that promotes migration prior to proliferation, or lifts a stimulus which inhibits migration of proliferative cells during homeostasis.

Comparison of S-phase activity in the rostral segment and the overlapping anterior segment demonstrates non-coinciding maxima in S-phase numbers, respectively at one day p-a, and at three to five days p-a. Hence, for chase times longer than one day, S-phase activity is mostly located in the region posterior to the eyes. Given that the growth curve of the rostrum indicates a considerable lengthening of the rostrum after one day p-a, at least a proportion of the S-phase cells in the lower part of the anterior segment are likely to migrate anteriorly and contribute to the regeneration of the rostrum. This shows that the progeny of cells, proliferating at the wound site, is not sufficient to fully restore the rostrum.

3.5.6. Cell cycle characteristics

Both our BrdU pulse and BrdU pulse-chase experiments clearly demonstrate an immediate effect of amputation on the dynamics of the stem cells. The 30min BrdU pulse/0h chase experiment demonstrated that amputation causes a significant extra activation (28%) of cells entering S-phase. In conclusion, within half an hour, a population of neoblasts is activated to contribute to the regeneration of missing tissues. Whether the cell cycle of these cells is accelerated or whether they belong to a population of arrested reserve cells is unclear. However, reports on tail plate regeneration in *M. lignano* have demonstrated that neoblasts do not reduce the duration of the cell cycle, at least not during the first four hours p-a. Therefore, a reduction of the cell cycle duration is unlikely to account for this population of cells. Activation of arrested reserve cells, on the other hand, seems a valuable alternative explanation, given that the presence of non-cycling neoblasts has been demonstrated in *M. lignano* (Bode et al., 2006). Their exact position within the cell cycle

remains to be elucidated, though. Given the short time interval (30 minutes) during which arrested cells are to enter S-phase in this study, re-activation of quiescent cells in G0-phase is most likely. Previously, irradiation in *M. lignano* was suggested to induce quiescent neoblasts to re-enter the cell cycle (De Mulder et al., 2010). In the same way, re-activation of G0 cells upon wounding has been described for haematopoietic stem cells (Wilson et al., 2008). Additionally, it is possible that activation of a pool of G2-arrested neoblasts accounts for the increased S-phase activity, observed here. The presence of a population of G2-arrested neoblasts, allowing for a fast mitotic response after wounding, has been suggested before in *M. lignano* (Nimeth et al., 2004; Bode et al., 2006; Egger et al., 2009) and in triclads (Saló and Baguñà, 1984). However, for G2-arrested cells to contribute also to the increased S-phase numbers observed in our experiments, these cells would have to finish G2-, M- and G1-phases within 30 minutes. This seems highly unlikely, but it cannot be ruled out until the dynamics of the cell cycle is completely understood in *M. lignano*.

In two-hour chased animals, the appearance of labelled cell pairs, which likely result from the division of a labelled cell, indicates that cells that were in S-phase during the pulse period, complete mitosis within two hours. The significant increase of labelled cells after four hours chase indicates that 34% of cells that were in S-phase during the 30-minute p-a period, need four hours to pass from S- to M-phase.

3.5.7. Conclusion

The cellular dynamics of the neoblast pool were analyzed after amputation of the rostrum, and were observed to differ from earlier descriptions of the situation during regeneration of the tail plate in *M. lignano*. Therefore, this study has provided essential information which contributes to a better and more complete understanding of the biology of neoblasts in this model organism.

Acknowledgements

We want to thank Bernhard Egger for advice concerning the BrdU-labellings and for useful comments and discussions. Carl Vangestel is acknowledged for advice on statistical methods. Furthermore, the authors thank the anonymous reviewers for their insightful comments and suggestions, which have led to a significant improvement of the manuscript. FV and MW received funding from the Institute for the Promotion of Innovation through Science and Technology in Flanders (IWT-Vlaanderen).

3.6. Supplementary Material

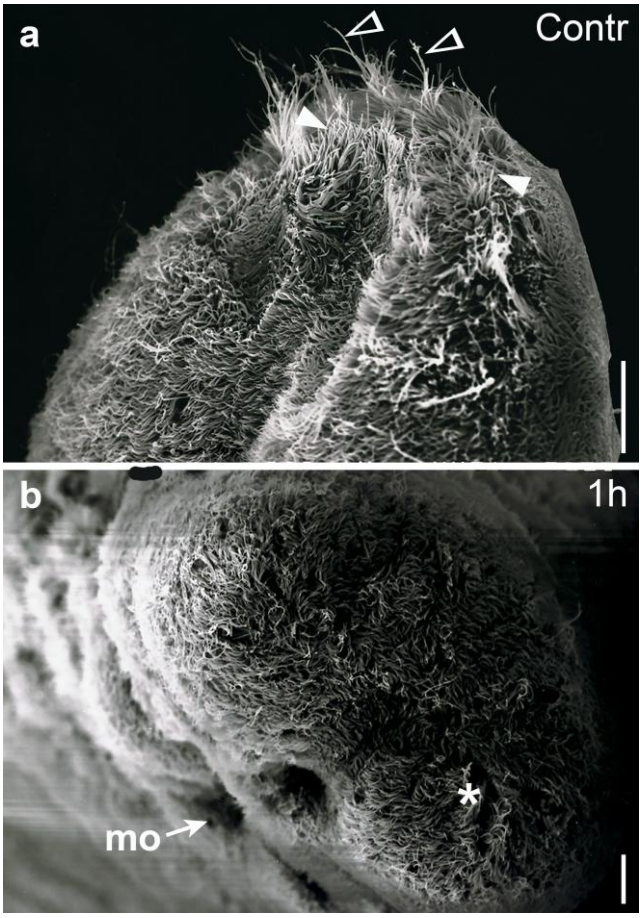

Supplementary Figure 3.S1

a-b Scanning electron microscopic images of the rostrum region in *M. lignano*. **a** Control animal. Lateral view on the rostrum area. Ciliae of epidermal cells (arrowheads) and longer ciliae of sensory nerves (open arrowheads) are visible. Anterior is on top, ventral side is on the left. **b** 1h p-a. View on the anterior tip of the regenerating rostrum. The wound area is almost completely covered with a layer of epidermal cells, leaving only a small opening (asterisk). Ventral is on the left/bottom. *mo*, mouth. Bars: 10µm.

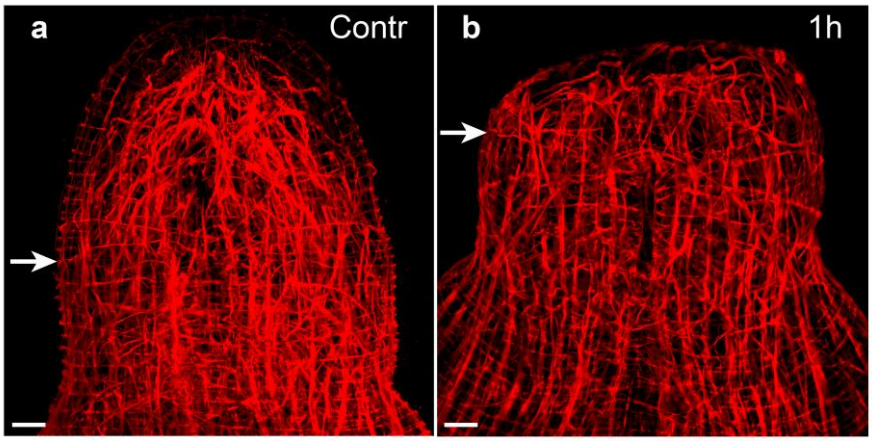

Supplementary Figure 3.S2

Immunostaining of muscle F-actin (phalloidin) after amputation of the rostrum in *M. lignano.* Confocal projections of the rostrum area after immunostaining of muscle F-actin, using TRITC-conjugated phalloidin. **a** Control animal, dorsal view. **b** 1h p-a, ventral view. Contraction of muscle fibers is visible at the level of the wound, resulting in a reduction of the wound area. Arrows indicate the level of the eyes. Anterior is on top. Bars: 10µm.

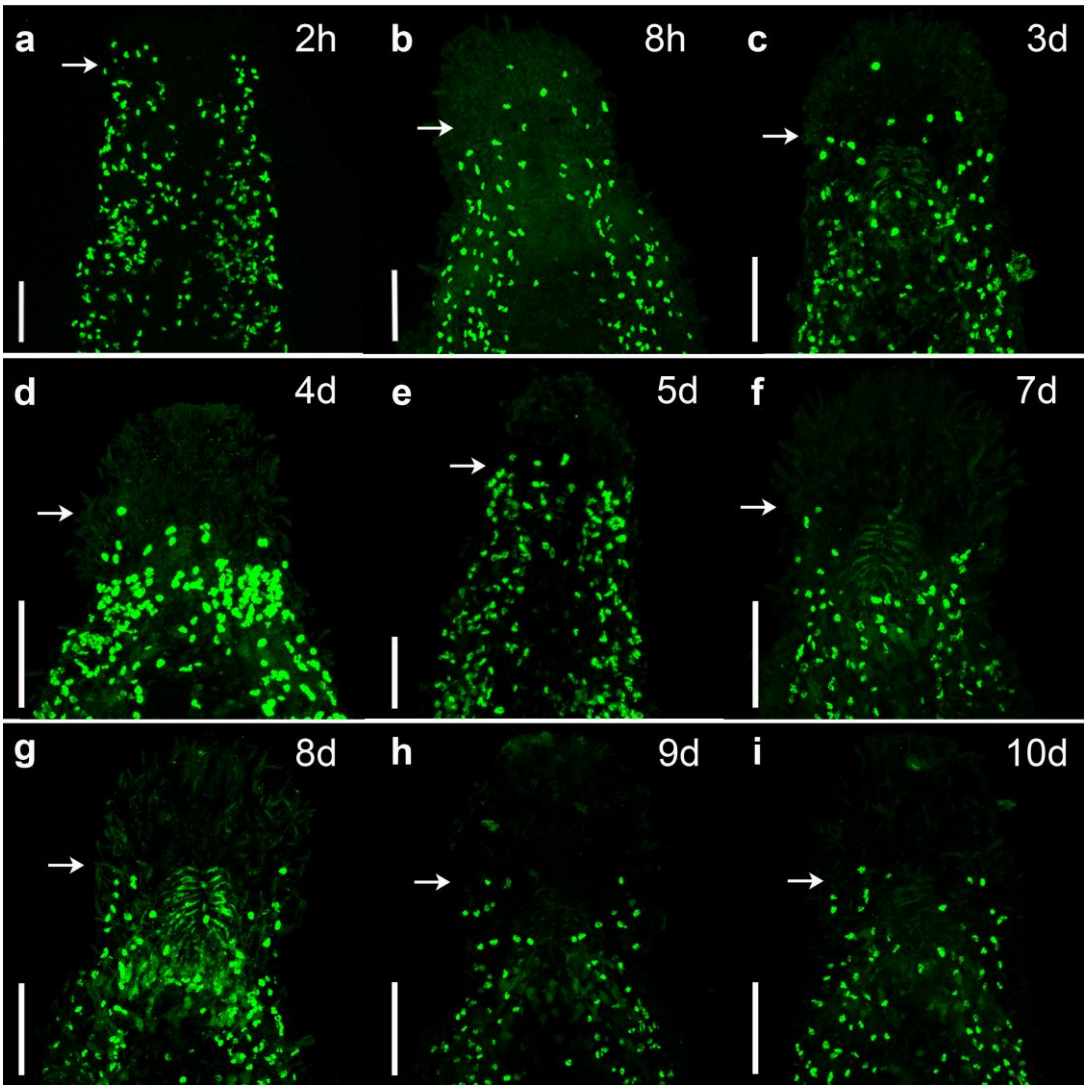

Supplementary Figure 3.S3

Spatial distribution of S-phase cells during regeneration of the rostrum in *M. lignano* (BrdU pulse). BrdU-labelling after a 30-minute BrdU pulse. **a-i** Confocal projections of the rostrum area. **a** 2h p-a. **b** 8h p-a. **c** 3d p-a. **d** 4d p-a. **e** 5d p-a. **f** 7d p-a. **g** 8d p-a. **h** 9d p-a. **i** 10d p-a. Arrows indicate the level of the eyes. Anterior is on top. Bars: 50µm.

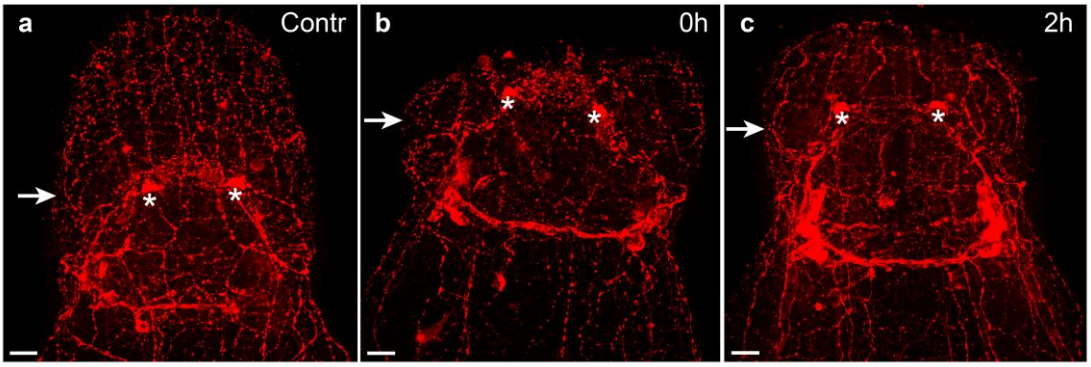

Supplementary Figure 3.S4

Immunostaining of the serotonergic nervous system (anti 5-HT) after amputation of the rostrum in *M. lignano.* Confocal projections of the rostrum after immunostaining of neurons expressing the neuropeptide serotonin. **a** Control animal. Two condensed clusters of serotonergic neurons, are present at the lateral sides of the neuropile (asterisks). Emanating from the neuropile are axons, which form a subepidermal plexus (see also Morris et al., 2007). **b** 0h p-a. The condensed clusters at the lateral sides of the neuropile are not damaged when amputation is performed at the indicated cutting level. **c** 2h p-a. Neurons of the subepidermal plexus are present in the anterior tip of the rostrum. Arrows indicate the level of the eyes. Anterior is on top. Bars: 10µm.

3.7. References

Abramoff MD, Magelhaes PJ, Ram SJ (2004) Image processing with Image J. Biophotonics Int 11:36-42

Agata K (2003) Regeneration and gene regulation in planarians. Curr Opin Genet Dev 13:492-496

Alvarado AS, Newmark PA (1998) The use of planarians to dissect the molecular basis of metazoan regeneration. Wound Repair Regen 6:413-420

Baguñà J (1976) Mitosis in intact and regenerating planarian *Dugesia mediterranea* n.sp. 2. Mitotic studies during regeneration, and a possible mechanism of blastema formation. J Exp Zool 195:65-79

Baguñà J, Saló E, Romero R, Garciafernandez J, Bueno D, Munozmarmol AM, Bayascasramirez JR, Casali A (1994) Regeneration and pattern-formation in planarians - cells, molecules and genes. Zoolog Sci 11:781-795

Bode A, Salvenmoser W, Nimeth K, Mahlknecht M, Adamski Z, Rieger RM, Peter R, Ladurner P (2006) Immunogold-labeled S-phase neoblasts, total neoblast number, their distribution, and evidence for arrested neoblasts in *Macrostomum lignano* (Platyhelminthes, Rhabditophora). Cell Tissue Res 325:577-587

Brøndsted HV (1969) Planarian Regeneration. Pergamon Press, Oxford, New York

De Mulder K, Kuales G, Pfister D, Egger B, Seppi T, Eichberger P, Borgonie G, Ladurner P (2010) Potential of *Macrostomum lignano* to recover from gamma-ray irradiation. Cell Tissue Res 339:527-542

Egger B, Gschwentner R, Hess MW, Nimeth KT, Adamski Z, Willems M, Rieger R, Salvenmoser W (2009) The caudal regeneration blastema is an accumulation of rapidly proliferating stem cells in the flatworm *Macrostomum lignano*. BMC Dev Biol 9:

Egger B, Ladurner P, Nimeth K, Gschwentner R, Rieger R (2006) The regeneration capacity of the flatworm *Macrostomum lignano* - on repeated regeneration, rejuvenation, and the minimal size needed for regeneration. Dev Genes Evol 216:565-577

Guillard R, Ryther J (1962) Studies of marine planktonic diatoms. I. *Cyclotella nana* Hustedt, and *Detonula confervacea* (Cleve) Gran. Can J Microbiol 8:229-239

Ladurner P, Rieger R, Baguñà J (2000) Spatial distribution and differentiation potential of stem cells in hatchlings and adults in the marine platyhelminth *Macrostomum* sp.: A bromodeoxyuridine analysis. Dev Biol 226:231-241

Ladurner P, Schärer L, Salvenmoser W, Rieger RM (2005) A new model organism among the lower Bilateria and the use of digital microscopy in taxonomy of meiobenthic Platyhelminthes: *Macrostomum lignano*, n. sp. (Rhabditophora, Macrostomorpha). J Zool Syst Evol Res 43:114-126

Morris J, Cardona A, De Miguel-Bonet MDM, Hartenstein V (2007) Neurobiology of the basal platyhelminth *Macrostomum lignano*: map and digital 3D model of the juvenile brain neuropile. Dev Genes Evol 217:569-584

Mouton S, Willems M, Braeckman BP, Egger B, Ladurner P, Schärer L, Borgonie G (2009) The free-living flatworm *Macrostomum lignano*: A new model organism for ageing research. Exp Gerontol 44:243-249

Newmark PA, Sánchez Alvarado A (2000) Bromodeoxyuridine specifically labels the regenerative stem cells of planarians. Dev Biol 220:142-153

Nimeth KT, Egger B, Rieger R, Salvenmoser W, Peter R, Gschwentner R (2007) Regeneration in *Macrostomum lignano* (Platyhelminthes): cellular dynamics in the neoblast stem cell system. Cell Tissue Res 327:637-646

Nimeth KT, Mahlknecht M, Mezzanato A, Peter R, Rieger R, Ladurner P (2004) Stem cell dynamics during growth, feeding, and starvation in the basal flatworm *Macrostomum* sp. (Platyhelminthes). Dev Dyn 230:91-99

Palmberg I (1986) Cell-migration and differentiation during wound-healing and regeneration in *Microstomum lineare* (Turbellaria). Hydrobiologia 132:181-188

Paulus T, Muller MCM (2006) Cell proliferation dynamics and morphological differentiation during regeneration in *Dorvillea bermudensis* (Polychaeta, Dorvilleidae). J Morphol 267:393-403

Reddien PW, Sánchez Alvarado A (2004) Fundamentals of planarian regeneration. Annu Rev Cell Dev Biol 20:725-757

Reuter M, Kreshchenko N (2004) Flatworm asexual multiplication implicates stem cells and regeneration. Can J Zool 82:334-356

Saló E (2006) The power of regeneration and the stem-cell kingdom: freshwater planarians (Platyhelminthes). Bioessays 28:546-559

Saló E, Baguñà J (1984) Regeneration and pattern-formation in planarians .1. the pattern of mitosis in anterior and posterior regeneration in *Dugesia (G) tigrina*, and a new proposal for blastema formation. J Embryol Exp Morphol 83:63-80

Saló E, Baguñà J (1985) Cell-movement in intact and regenerating planarians - quantitation using chromosomal, nuclear and cytoplasmic markers. J Embryol Exp Morphol 89:57-70

Saló E, Baguñà J (2002) Regeneration in Planarians and other worms: New findings, new tools, and new perspectives. J Exp Zool 292:528-539

Salvenmoser W, Riedl D, Ladurner P, Rieger R (2001) Early steps in the regeneration of the musculature in *Macrostomum* sp. (Macrostomorpha). Belg J Zool 131:105-109

Schärer L, Ladurner P (2003) Phenotypically plastic adjustment of sex allocation in a simultaneous hermaphrodite. Proceedings of the Royal Society of London Series B-Biological Sciences 270:935-941

Wenemoser D, Reddien PW (2010) Planarian regeneration involves distinct stem cell responses to wounds and tissue absence. Dev Biol 344:979-991

Wilson A, Laurenti E, Oser G, van der Wath RC, Blanco-Bose W, Jaworski M, Offner S, Dunant CF, Eshkind L, Bockamp E, Lio P, MacDonald HR, Trumpp A (2008) Hematopoietic stem cells reversibly switch from dormancy to self-renewal during homeostasis and repair. Cell 135:1118-1129

4. Measuring S-phase duration of adult stem cells in the flatworm *Macrostomum lignano* by double replication labelling and quantitative colocalization analysis

Freija Verdoodt, Maxime Willems, Ineke Dhondt, Wouter Houthoofd, Wim Bert, and Winnok H. De Vos

4.1. Abstract

Platyhelminthes are highly attractive models for addressing fundamental aspects of stem cell biology *in vivo*. These organisms possess a unique stem cell system comprised of neoblasts, which are the only proliferating cells during adulthood. In this study, the S-phase duration (T_s) of neoblasts was determined, both during homeostasis and regeneration in the flatworm *Macrostomum lignano*. A double immunohistochemical technique was used, performing sequential pulses with the thymidine analogs chlorodeoxyuridine (CldU) and iododeoxyuridine (IdU), separated by variable chase times in colchicine.

Due to the localized nature of the fluorescent signals (nuclei) and variable levels of autofluorescence, standard intensity-based colocalization analyses could not be applied to accurately determine the colocalization. Therefore, an object-based colocalization approach was devised to score the relative number of double-positive cells. Using this approach we found that the S-phase duration in the main population of neoblasts was approximately 13 hours. During early regeneration, no significant change in T_s was observed.

4.2. Introduction

Proliferation is a fundamental trait of stem cells, as they have the ability to continuously self-renew and generate large numbers of differentiated progeny. This dual function asserts their crucial role during development, tissue homeostasis, and regeneration, and therefore requires meticulous control (Morrison et al., 1997; Morrison and Spradling, 2008). Both external and internal stimuli affect the dynamics of stem cells, a fact that emphasizes the importance of studying these cells in their natural environment (Rando, 2006; Orford and Scadden, 2008). However, *in vivo* stem cell research is often challenging because of experimental difficulties caused by tissue depth and motion artefacts (Tsai et al., 2002; Tanaka, 2003). Mainly for this reason, Platyhelminthes have been amply

introduced as highly attractive model organisms for addressing fundamental aspects of stem cell biology *in vivo* (Newmark and Sánchez Alvarado, 2002; Sánchez Alvarado, 2004). These organisms possess a unique stem cell system within the animal kingdom, comprised of neoblasts that are the only proliferating cells in adult species (Baguñà, 1981; Saló and Baguñà, 2002; Sánchez Alvarado, 2007; Ladurner et al., 2008; Agata and Umesono, 2008). Although neoblasts are a powerful model for studying proliferation dynamics of a population of adult stem cells *in vivo*, fundamental information on specific parameters of the cell cycle is relatively limited. To our knowledge, other than the mean duration of the G2-phase in *Schmidtea mediterranea* and *Macrostomum lignano* (Newmark and Sánchez Alvarado, 2000; Nimeth et al., 2004; Nimeth et al., 2007), and the total cell cycle duration (T_c) in *S. mediterranea* (Kang and Sánchez Alvarado, 2009), no specific parameters of other phase durations are available. Furthermore, regeneration has been shown to temporarily affect the numbers of S-phase and mitotic cells in flatworms, indicating adjustment of the cell cycle kinetics (Saló and Baguñà, 1984; Newmark and Sánchez Alvarado, 2000; Nimeth et al., 2007; Wenemoser and Reddien, 2010; Verdoodt et al., 2012a). However, it is not completely understood at what stage the cell cycle is adapted during this process.

In the past, the combined use of two different thymidine analogs has been demonstrated as a valuable technique for determining kinetic parameters of cycling cells (Wimber and Quastler, 1963; David and Campbell, 1972; Miller et al., 1991; Yanik et al., 1992; Rachel et al., 2002; Hayes and Nowakowski, 2002; Burns and Kuan, 2005). Performing sequential pulses with such analogs allows for determining the duration of the S-phase (T_s) of the cell cycle. A method for immunohistochemical detection of two thymidine analogs, chlorodeoxyuridine (CldU) and iododeoxyuridine (IdU), has been established for the flatworm *Macrostomum lignano* (Verdoodt et al., 2012b). In the study presented here, this method was adapted to test the T_s of neoblasts during homeostasis and regeneration in *M. lignano*. To this end, individual worms received sequential pulses with CldU and IdU, which were separated by varying chase times in colchicine. The use of colchicine, which inhibits cell cycle progression at metaphase (Nagl, 1972), allowed analysis of a single round of cell proliferation and avoided misinterpretation due to cell doublings. To determine T_s, overlap

between the two markers was evaluated. Due to the localized nature of the fluorescent signals in limited regions (nuclei) of the image, standard intensity-based colocalization analyses which evaluate the whole image, could not be applied. Instead, an object-based colocalization approach was devised to score the relative number of double-positive cells. Using this approach, the duration of S-phase in the main population of neoblasts was determined approximately 13 hours, both during homeostasis and early regeneration.

4.3. Materials and methods

4.3.1. Animal culture and amputation of the rostrum

Cultures of *M. lignano* were reared in f/2-medium (Egger and Ishida, 2005) and fed *ad libitum* with the diatom *Nitzschia curvilineata,* as described previously (Schärer et al., 2007; Ladurner et al., 2008). To induce regeneration, the rostrum was amputated at the level anterior to the brain. Amputations were performed with a fine steel surgical blade (SM62; Swann-Morton) under a stereo microscope, while worms were relaxed in a small droplet of 1:1 $MgCl_2.6H_2O$ (7.14%) and ASW (artificial sea water). Immediately thereafter, specimens were washed in f/2-medium and pulsed with CldU.

4.3.2. Accumulation of mitotic cells after colchicine incubation

To test the efficiency and toxicity of colchicine in *M. lignano*, the accumulation of mitotic cells was analysed after incubation with different concentrations of colchicine. Adults were incubated in a colchicine-containing medium (Sigma-Aldrich) of 0.001%, 0.005%, or 0.010% (in f/2-medium). After 3h, 24h, 48h and 6d of incubation, mitotic cells were visualized using rabbit-anti-phosphorylated histone H3 (Upstate Biotechnology) and TRITC-conjugated swine-anti-rabbit (DAKO), according to the method described earlier (Verdoodt et al., 2012a). For each condition, 4 replicates were analyzed.

4.3.3. CldU- and IdU-pulse and immunocytochemistry

For the first pulse, uncut animals or regenerates were incubated in CldU (10 mM in f/2-medium, 30 min, in the dark; Sigma-Aldrich). From this moment on, animals were protected from light. Specimens were then rinsed with f/2-medium, and chased in colchicine-containing medium (0.005% in f/2; Sigma-Aldrich) for 0 h, 1 h, 2 h, 4 h, 6 h, 12 h, 24 h, and 48 h. Subsequently, the second pulse was performed with IdU (1mM in colchicine-containing medium, 30 min; Sigma-Aldrich), followed by washing with colchicine-medium (2 x 5 min). Relaxation, fixation, and indirect visualization of both CldU and IdU were performed as described previously (Verdoodt et al., 2012b). The set of antibodies used for indirect visualization of CldU were rat-anti-CldU (AbD Serotec) and FITC-conjugated donkey-anti-rat (Rockland). For indirect visualization of IdU, mouse-anti-IdU (Becton-Dickinson) and Alexa Fluor 568-conjugated goat-anti-mouse (Invitrogen) were used.

4.3.4. Image Acquisition

For the visualization of CldU- and IdU-label, a Nikon C1 (Nikon Instruments, Paris, France) confocal laser scanning microscopy system was used mounted on a Nikon TE2000 (Nikon Instruments, Paris, France) inverted epifluorescence microscope, equipped with a 488-nm Multi-line Ar laser and 543nm HeNe laser. CldU and IdU signals were sequentially excited with both laser lines (by line-scanning) and detected through a 515/30 nm bandpass filter, and a 570 long pass combined with a 593/40 nm bandpass filter, respectively. All images were acquired using identical settings of laser power, detector gain and offset. 3D-images were acquired with the pinhole set at 1AU, using a Plan Fluor 60x/1.4 oil lens at a voxel size of 0.41x0.41x1.0 µm3.

4.3.5. Image Analysis

All images were acquired with Nikon EZ-C1 software (Nikon Instruments, Paris, France). Visualization, annotation and quantification of images were performed with Fiji, a packaged version of the open source program ImageJ (W. Rasband, National Institutes of Health, Bethesda, Maryland, USA). For determination of double-positive nuclei in each specimen, an object-based colocalization analysis was developed. Assuming that a positive replication labelling yields a signal that fills up the entire nucleus, circularity and size were used as limiting parameters. The following steps were performed. First, a selection was made for analysis of the relevant 3D region of interest. In each animal, the region anterior to the testes and the region posterior to the female genital pore were analyzed. For each condition, between 4 and 7 replicates were analyzed. A sum projection was made of the Z-slices, and the individual channels were pre-processed by sequential background subtraction (radius = 20µm), Gaussian filtering (sigma = 1µm) and median filtering (radius = 2µm). Next, objects (nuclei) were specifically enhanced in both channels by applying a Laplace filter with automatic scale selection (as documented before by De Vos et al., 2010) and segmented by global isodata autothresholding. To compensate for closely-located nuclei, the resulting masks were used to extract objects, which were further separated by maxima finding and region growing. By particle analysis, those objects that did not comply with user defined nuclear shape criteria (size and circularity) were removed. Finally, colocalization was determined by scoring, per object, the amount of overlap between the binarized and coded versions of the two channels. Objects in the first channel were coded with the number 1, objects in the second channel were coded with the number 2, and so overlapping regions have code 3. Signals were said to colocalize for a given ROI, when the number of overlapping pixels (code 3) was larger than 50% of the total number of pixels of the object of interest. Finally, the raw output was visually verified and, if necessary (e.g. in spatially restricted zones of high autofluorescence), corrected using a dedicated ROI

correction/deletion tool. The workflow of the object-based colocalization analysis is summarized in Figure 4.1. The code is freely available at the following URL: http://www.limid.ugent.be/software.htm. At least 4 individuals were analysed per condition (n=4-7). For validation, the object-based analysis was compared to intensity-based colocalization methods using Pearson or Manders coefficients (Bolte and Cordelieres, 2006; Manders et al., 1992).

4.3.6. Statistical Analysis

The statistical analysis was done using Statistica 7 (StatSoft Europe GmbH, Hamburg, Germany). Normality and homogeneity of variances were tested using a Kolmogorov-Smirnov test and a Levene's test, respectively. $CldU^+$ data (absolute numbers) were square root transformed, prior to analysis. Proportions of $CldU^+$ /IdU^+ cells were first square root and then arcsinus transformed (Sokal and Rohlf, 1995). The obtained data were analyzed by means of one-way analysis of variance (ANOVA), followed by a post-hoc Bonferroni test. Linear regression analysis was performed on the individual samples assayed at 0 h, 1 h, 2 h, 4 h, and 6 h, using the proportion of double labelled cells and the chase time duration as independent and dependent variable, respectively.

Data that did not meet the assumption for homogeneity of variances were analyzed using a non-parametric Mann-Whitney U test (pair wise comparison between homeostasis and regeneration).

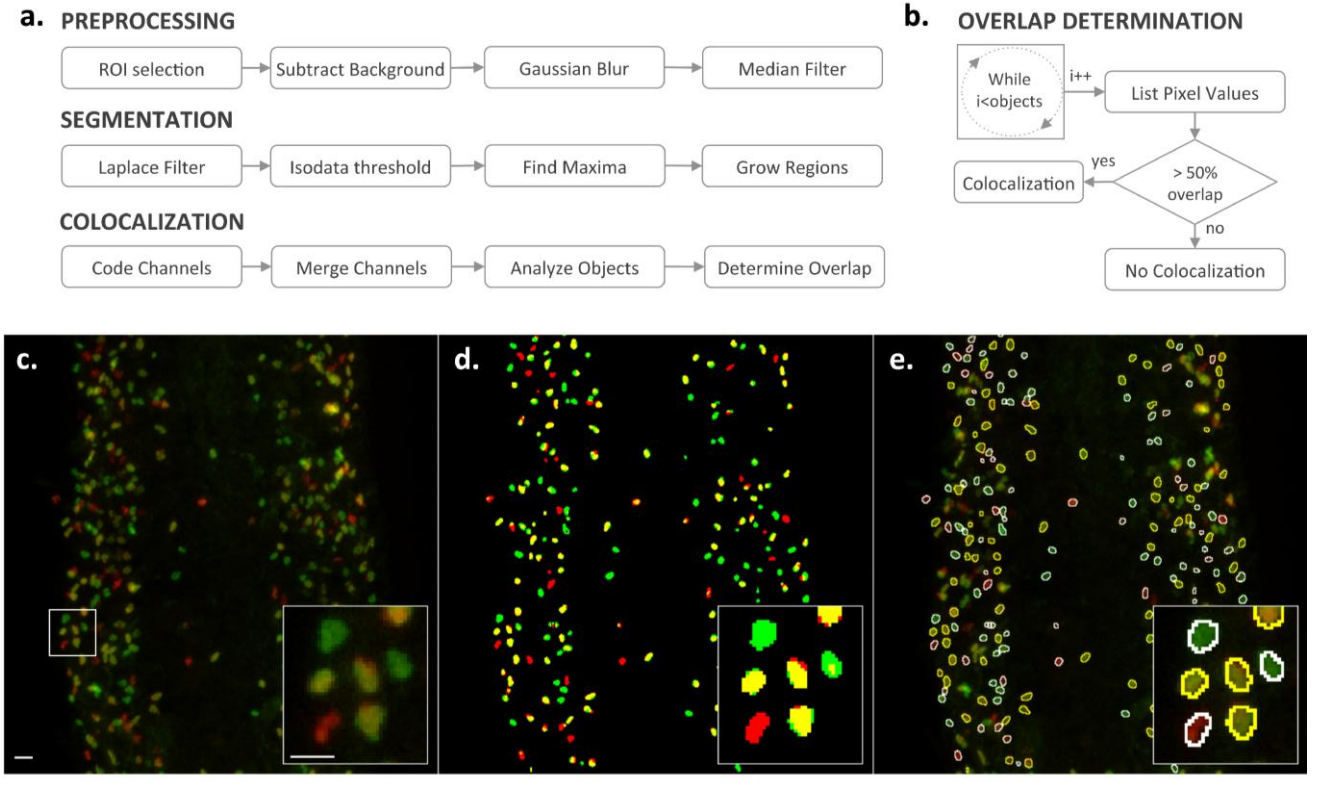

Figure 4.1:

Object-based colocalization for scoring of double-labelled nuclei in tissue sections of *M. ligano*. (a) Workflow demonstrating the major aspects of the analysis; (b) Criterion for determing overlap in a ROI; (c) Example composite image of CldU (red) and IdU (green) labelled nuclei in a gut section of *M. lignano*; (d) The same image after segmentation and binarization; (e) The same image with segmented nuclei outlined, double-positive nuclei with a yellow contour. Scale bars: 10 µm.

4.4. Results

4.4.1. Validation of the colocalization analysis

First, the colocalization analysis was validated on a number of control images, including single-pulsed samples as well as simultaneously double-pulsed samples. A comparison was made with the typical colocalization metrics Pearson correlation coefficient and Manders coefficients. While on average, the Pearson correlation coefficient was close to 0 in single stained samples and relatively high for double stained samples (0.8), the values for the Manders coefficients were not straightforward (Table 4.1). This is plausibly due to the presence of autofluorescent components, which cannot be removed in classical intensity-based analyses. Moreover, neither the Pearson nor the Manders coefficients returned the exact information that was required, namely the number of double positive nuclei, relative to the total number of labelled nuclei. The object-based method effectively segments only those objects that comply with the nuclear shape requirements and accordingly provided the necessary output. Using this method, average colocalization values of 0% in single-pulsed samples and 92% in double-pulsed samples were obtained. Comparison of the raw output with values after manual correction (Table 4.1) shows that the differences are negligible and indicates that the false-negative rate in double stained samples was not due to analytical errors but rather to labelling inefficiencies.

Metric	CldU only (n=8)	IdU only (n=6)	IdU + CldU (n=8)
Pearson [-1,1]	0.10±0.03	0.25±0.08	0.79±0.12
Manders A [0,1]	0.07±0.03	0.14±0.12	0.52±0.08
Manders B [0,1]	0.03±0.03	0.08±0.04	0.35±0.14
Object-based [0,100] raw results	1.52±1.85	0.41±0.99	88.36±10.58
Object-based corrected [0,100]	0.0±0.00	0.00±0.00	91.91±8.17

Table 4.1: Comparison of the results from different colocalization metrics after intensity- or object based colocalization analysis on control image data sets.

4.4.2. S-phase duration during homeostasis

The T_s of neoblasts was determined by performing sequential pulses with the thymidine analogs CldU and IdU, separated by varying chase times in colchicine-containing medium. Prior to performing these experiments, three concentrations of colchicine (0.001%, 0.005%, and 0.010%) were tested for their efficiency and toxicity in *M. lignano,* by analyzing the accumulation of mitotic cells. For each concentration, the number of anti-phos-H3 labeled cells was quantified, after an incubation period of 3h, 24h, 48h, and 6d (supplementary Figure 4.S1). The median concentration (0.005%) demonstrated a faster and more efficient blocking after short incubations, while no toxic effect was obvious for incubations up to 48h. The highest concentration on the other hand, demonstrated toxic effect after 24 h of incubation. In conclusion, the use of a 0.005% solution of colchicine demonstrated the best balance between efficiency of blocking cells in M-phase on one hand, and no dramatic toxic effect for exposures up to 48 h. Hence, this concentration was used for further experiments.

To estimate the T_s of neoblasts, adults were pulsed for 30 minutes with CldU, chased in CldU-free, colchicine-containing medium, and subsequently pulsed for 30 minutes with IdU. Individuals were then fixed and both analogs were visualized by double immunofluorescence labelling. First, absolute numbers of $CldU^+/IdU^+$, $CldU^+/IdU^-$, and $CldU^-/IdU^+$ nuclei were quantified (see supplementary Figure 4.S2a), using the aforementioned object-based analysis. After 12 h chase, a marginally significant increase (one-way ANOVA, $p=0.046$) was observed in the total amount of $CldU^+$ cells (single and double labelled). After 24 h chase, a highly significant increase (one-way ANOVA , $p<0.01$) was measured in the number of $CldU^+$ cells. This increase can be explained by a small proportion of cells that were unaffected by the colchicine and were able to divide.

Second, the proportion of $CldU^+/IdU^+$ neoblasts was determined by the ratio of $CldU^+/IdU^+$ nuclei over the total amount of $CldU^+$ nuclei (both single- and double-labelled). In this paradigm, nuclei from cells that have exited S-phase, during or after the first pulse, will be $CldU^+/IdU^-$ (Figure 4.2a). The chase time after which all CldU-labelled cells $CldU^+/IdU^-$ corresponds to the maximal T_s. The mean proportion of $CldU^+/IdU^+$ neoblast nuclei was quantified in individual organisms (the region anterior and posterior of the gonads) after chase times of 0 h, 1 h, 2 h, 4 h, 6 h, 12 h, 24 h, and 48 h (Figure 4.2b-c). An initial fast decrease in the proportion of double-labelled nuclei was observed. After 0 h chase, 94% (±3, n=5) $CldU^+/IdU^+$ nuclei were quantified. CldU-labelled cells that have left S-phase during the first pulse, combined with a technical margin of false-negative results (see table 4.1), explain why 0 h chase did not result in 100% $CldU^+/IdU^+$ cells. After 1 h chase, 88.26 (±2.1, n=4) were present, and after 2 h chase, this number had decreased significantly (69%±6, n=5; one-way ANOVA, $p=0.002$). The fast rate by which the proportion of $CldU^+/IdU^+$ cells diminished, was continued for chase times up to 12 h: 4 h, 6 h, and 12 h resulted in proportions of 64% (±3, n=5), 50% (±3, n=7), and 21% (±7, n=4), respectively. For chase times longer than 12 hours, the number of double-positive nuclei further decreased, albeit at a slower rate. A chase of 24 h and 48 h resulted in a proportion of 14% (±4, n=5) and 3% (±1, n=5) $CldU^+/IdU^+$ cells, respectively. The presence of this second phase in the graph is most likely linked to the increase in total number of $CldU^+$ cells (see

discussion). Therefore, for estimation of T_s, only results up to 6 h chase were taken into account. These time points (0 h, 1 h, 2 h, 4 h, and 6 h) were used in a regression analysis. The intersection of this trendline (R^2=0.93) with the X-axis was used as a measure for the duration of S-phase (Figure 4.2d). Here a duration of 12.7 hours was measured.

Figure 4.2:

Determination of T_s during homeostasis. (a) Scheme of the experimental set-up. Animals were pulsed with CldU (30 min), chased for various durations in colchicine and subsequently pulsed with IdU (30 min). Demonstrated are four hypothetical cells (I, II, III, and IV) at a different stage of S-phase during the first pulse (top panel). With longer chase times, there is an increased chance that cells have already left S-phase and therefore do not incorporate the IdU-label. (b) Visualization of CldU (green) and IdU (red) labeling in whole mount animals (confocal images) after 0h, 4h, and 24h chase. After 0h chase, the majority of cells are double labeled (yellow). Note the gradually decreasing amount of double labeled cells after 4h and 24h chase. Anterior is to the left. Scale bars: 50µm. (c) Graph representing the mean proportion (±SEM, n=4-7) of $CldU^+/IdU^+$ cells within the whole population of $CldU^+$ cells (single- and double-labelled). Note the steep decrease for chase times up to 12 hours. (d) Linear regression analysis based on data for 0 h, 1 h, 2 h, 4 h, 6 h, and 12 h chase (n=4-7). The regression line (black line) intersects with the X-as at 12.7 h, which is an estimation of T_s.

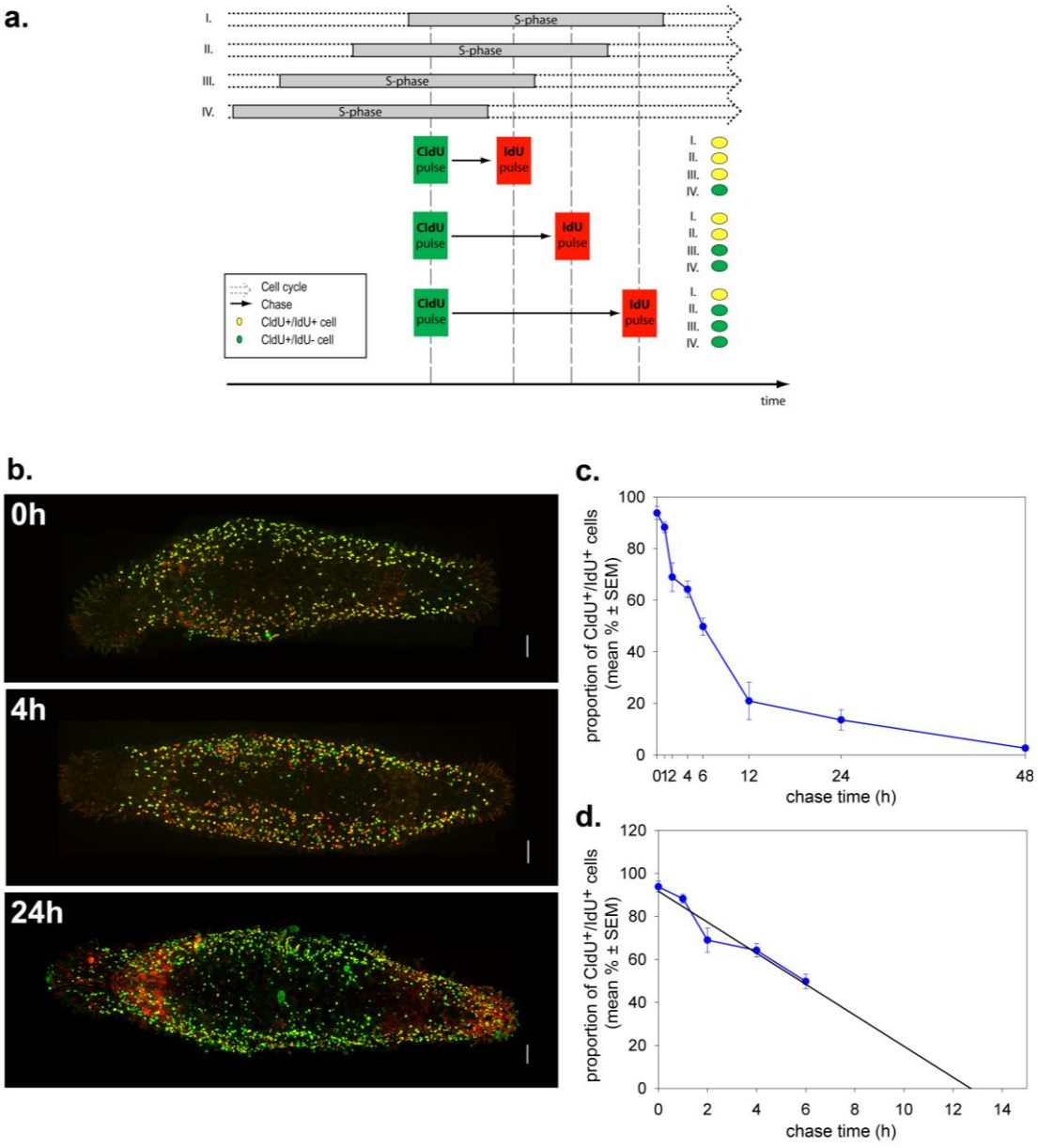
a.
I.
II.
III.
IV.
S-phase
CldU pulse
IdU pulse
Cell cycle
Chase
CldU+/IdU+ cell
CldU+/IdU- cell
time
b.
0h
4h
24h
c.
proportion of CldU+/IdU+ cells (mean % ± SEM)
chase time (h)
d.
proportion of CldU+/IdU+ cells (mean % ± SEM)
chase time (h)

4.4.3. S-phase duration during regeneration

Previously, amputation of the rostrum in *M. lignano* has been shown to cause an immediate increase in the number of S-phase cells after amputation. Thirty minutes after amputation, this number had already risen by 28%, demonstrating that a significant amount of cells were induced to enter S-phase due to amputation (Verdoodt et al., 2012a). Therefore, cells that were in S-phase during the 30-minute time interval after amputation, were followed as they progressed through the DNA synthesis phase. To this end, individuals were amputated at the level anterior to the brain (Figure 4.3a, upper panel), after which the same experimental set-up was used as for the homeostasis experiment (Figure 4.3a, lower panel). Subsequently, CldU and IdU were visualized (Figure 4.3c) and the proportion of $CldU^+/IdU^+$ neoblasts was determined (Figure 4.3b, for absolute numbers see supplementary Figure 4.S2b). Similar to the results observed during homeostasis, the proportion of double-labeled nuclei decreased rapidly for chases up to 12 hours. After 0 h, 2 h, 4 h, and 12 h chase, a proportion of 84% (±0.03, n=4), 73% (±0.08, n=4), 57% (±0.03, n=5), and 24% (±0.03, n=4) was quantified, respectively. Longer chase times demonstrated a slower decrease of the proportion of $CldU^+/IdU^+$ cells: 24 h and 48 h chase resulted in 8% (±2, n=5) and 11% (±3, n=4) double-labelled cells, respectively.

Results obtained from regenerating individuals were compared with corresponding chase time durations from the homeostasis experiment. No significant differences were found (Mann-Whitney U, $p>0.05$), except for 48 h chase ($p=0.03$). These results indicated that amputation of the rostrum did not result in an acceleration of the S-phase during early regeneration.

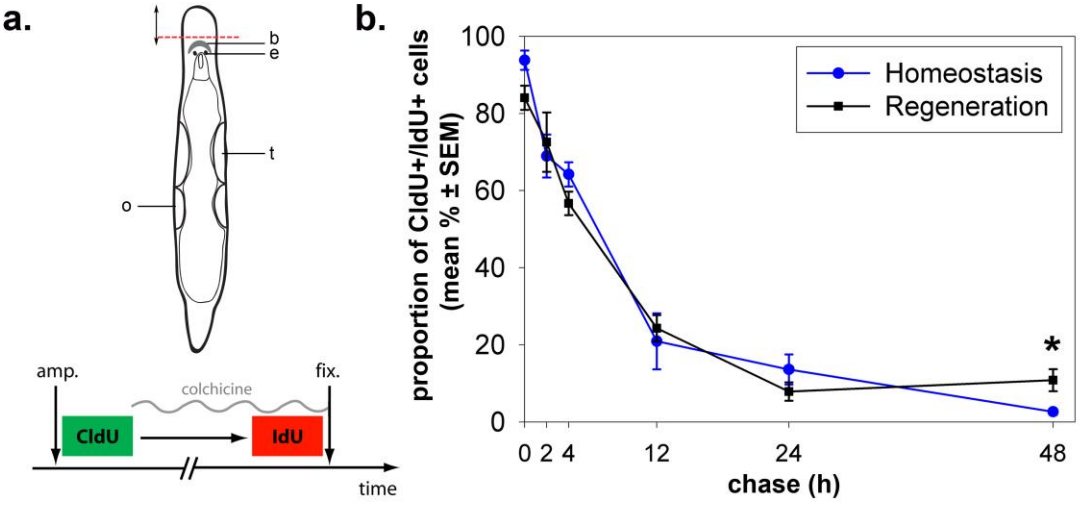
a.
b
e
t
o
amp.
colchicine
fix.
CldU
IdU
time
b.
proportion of CldU+/IdU+ cells
(mean % ± SEM)
100
80
60
40
20
0
0 2 4
12
24
48
chase (h)
Homeostasis
Regeneration
*

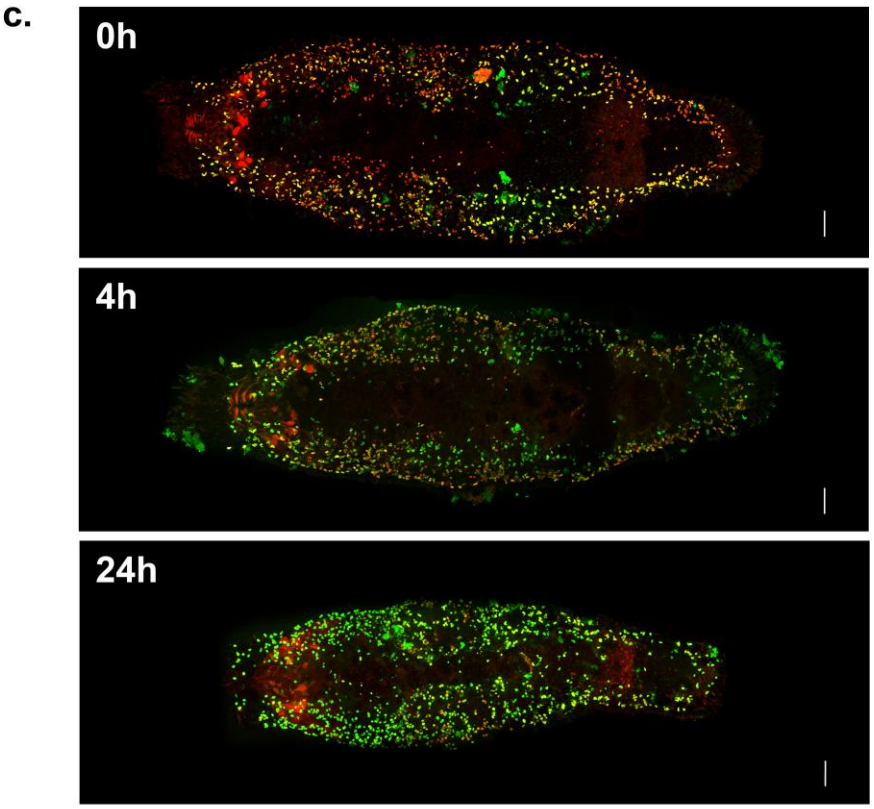
c.
0h
4h
24h

Figure 4.3:

$T_{S,}$ compared between homeostasis and early regeneration. (a) Scheme of adult *M. lignano* (upper panel) depicting the amputation level (dotted red line). The rostrum is depicted by the 2-sided arrow. b, brain; e, eye; t, testis; o, ovary. Scheme of the experimental set-up (lower panel). amp, amputation; fix, fixation. (b) Graph representing the mean proportion (±SEM, n=4-7) of $CldU^+/IdU^+$ cells after various chase times during homeostasis (blue curve) and regeneration (black curve). Note the similar course of both curves, only after 48 h of chase a significant difference (asterisk) was observed. (c.) Visualization of CldU (green) and IdU (red) labeling in whole mount animals (confocal images) after 0 h, 4 h, and 24 h chase. Note the high number of single labelled IdU^+ cells (red) after 0 h chase. These cells are activated during regeneration and entered S-phase during the second pulse (compare with 0h chase during homeostasis, Figure 4.2b). Note the gradually increasing amount of $CldU^+$ /IdU- cells (green) after 4h and 24h chase. Anterior is to the left. Scale bars: 50µm.

4.5. Discussion

In this study, the S-phase of cycling neoblasts was studied in *M. lignano* by means of a double labelling technique using two different thymidine analogs (CldU and IdU) and the mitotic blocking agent colchicine. Colchicine was used to prevent labelled cells from dividing and entering the S-phase of a subsequent cycle. The necessity of blocking the cell cycle of labelled cells is indicated by previous studies, demonstrating that (1) neoblasts cycle asynchronously, and that (2) subpopulations of neoblasts exist with different cell cycle kinetics (Ladurner et al., 2008). Given that cycling of neoblasts is not synchronized, cells that incorporate CldU during the first pulse are at different stages of the S-phase. Since T_c is unknown in *M. lignano*, $CldU^+$ cells going through mitosis while others are still in S-phase is a possibility that should be taken into account. Furthermore, diverse cell kinetics in subpopulations of neoblasts have been shown by Nimeth et al. (2007). In this study the presence of a small proportion of fast-cycling neoblasts was observed, which can traverse from the beginning of S-phase, through G2-phase, and into M-phase in merely two hours. On the other hand, the main population of neoblasts was observed to cycle much slower and needed four hours to merely traverse the G2-phase. These diverse kinetics suggest that fast-cycling $CldU^+$ cells could already go through mitosis and even enter a new S-phase, while slower cycling $CldU^+$ cells have not yet left the initial S-phase. Both processes affect the slope of $CldU^+/IdU^+$ cells in that cell division affects the total number of $CldU^+$ cells, and entrance into a new round of DNA-replication results in IdU-uptake. Therefore, in order to analyse the duration of the S-phase, it is necessary to block cells in metaphase. By comparing different concentrations, we found that a 0.005% colchicine solution demonstrated a good balance between efficiency of blocking cells in metaphase on one hand, and experiencing no dramatic toxic effects for exposures up to 48h (Supplementary Figure 4.S1). This concentration is acceptable, as it should not interfere with regular cell cycle progression. Indeed, at concentrations ranging from 0.0002% to 0.2%, colchicine has been reported to have no measurable effect on the rate of DNA synthesis, nor on the rate

of progression to M-phase in plant cells, and human cells in culture (Taylor, 1965; Borisy and Taylor, 1967; Villemont et al., 1997). Furthermore, in *M. lignano* colchicine (0.005%) has been shown to have no effect on the progression of cycling neoblasts through S-phase. This was demonstrated by similar rates of cells cycling from S-phase to M-phase in both colchicine-treated animals and non-treated animals (Nimeth et al., 2004).

To determine T_s, the number of double-labelled cells was scored in a pulse chase experiment with increasing chase times. Due to the localized nature of the fluorescent signals (nuclei) and variable levels of autofluorescence, standard intensity-based colocalization analyses could not be applied to accurately determine the colocalization. Moreover, most classical analyses fail to return the desired quantitative information, i.e. a number of double-positive nuclei. Hence, an object-based colocalization approach was devised to score the relative number of double-positive cells within a sample. This method, which is based on scoring the overlap between the segmented and binarized nuclear ROIs of both channels, proved robust and reliable, as demonstrated in both single- and double-labelled control images. With minor modifications, this method should be applicable to various biological image data-sets. Through the modification of the parameters, such as the degree of overlap, the analysis should also be able to deal with differences in labelling efficiency.

Theoretically, in this paradigm, the chase time for which all CldU-labelled cells have left S-phase, and are therefore $CldU^+/IdU^-$, corresponds to the maximum T_s (Figure 4.2a). In this study, the number of double labelled cells decreased quickly. Surprisingly, though, the initial steep decrease of the curve, was followed by a second phase with a considerably slower decrease (Figure 4.2c). The presence of this phase may be due to a subpopulation of slow-cycling cells with an extended S-phase duration (>48h) compared to the main cycling population, or due to technical factors. To evaluate the latter possibility, the efficiency of colchicine, which is reflected by absolute numbers of $CldU^+$ cells, was tested (Suppelementary Figure 4.S2). These numbers of CldU-labelled cells (both single and double labelled) were observed constant for chase times up to 6 h. Increasing the chase time by another six hours, however, resulted in a small increase ($p=0.046$), which was

observed to be even larger at 24 h chase ($p<0.01$). The expanded number of $CldU^+$ cells after long chase times, can be explained by a small amount of labelled cells that were able to divide, separating their label over two daughter cells. Double labelling of such cells, due to entry into the S-phase of a new cell cycle, explains the delayed decrease of $CldU^+/IdU^+$ cells for longer chase times. Another possible explanation for the increased number of $CldU^+$ cells is a toxic effect of colchicine after prolonged cell cycle arrest, and re-uptake of the analog by other cells. So far, it is not clear which of both hypotheses is correct. However, due to this technical constraint, results for chase times of 12 h and longer, were not used for analysis of S-phase duration. For chase times up to 6 h, though, efficient blocking of cells in metaphase is demonstrated by the constant number of $CldU^+$ cells. Hence, regression analysis was performed on results obtained from animals that were chased for 0 h, 1 h, 2 h, 4 h, and 6 h (Figure 4.2d). Based on these data points, T_s was estimated to be approximately 13 hours. Although S-phase duration varies greatly among different taxa, the phase length observed, here lies within range of the S-phase duration in, for instance, hydra (12-15 h) and rat satellite cells (14 h) (David and Campbell, 1972; Schultz and McCormick, 1994).

In *M. lignano,* the presence of a population of fast-cycling neoblasts has been described, additional to the main population of cycling neoblasts (Nimeth et al., 2007). These fast-cycling cells, although very little in absolute numbers, were observed to cycle through the whole S-, and G2-phase in merely 2 hours. The presence of a subpopulation of neoblasts with a considerably shorter S-phase compared to the main population, is expected to result in an even steeper decline in the first phase of the graph. Based on our data, however, no clear indication for such a subpopulation can be deduced. However, it should be noted that this can be caused by (1) their low incidence within the neoblast population, and (2) their extremely short Ts (1-2 h) which hampers their discrimination. Furthermore, an S-phase duration of less than 2 h has also been observed during embryonic development in *M. lignano* (Willems et al., 2009). Although separate phase durations were not determined, cell lineaging experiments have demonstrated cleavage of blastomeres approximately every one to two hours. Similar to *M. lignano*, in other models a

considerable elongation of the S-phase in adults, compared to embryos, has been observed (Alexiades and Cepko, 1996). Altogether, it can be concluded that, although a fast passage through S-phase (< 2 h) is possible in *M. lignano*, the majority of cycling neoblasts in adults need approximately 13 h.

To evaluate S-phase duration during regeneration, individuals were amputated at the level of the rostrum. Previously, during regeneration of this region, an immediate expansion of S-phase numbers was demonstrated, indicating an early-onset increase in cell proliferation (Verdoodt et al., 2012a). In this study was tested whether an acceleration at the level of the S-phase is responsible for these adjusted cell cycle kinetics. To this end, the T_s of cells that are in S-phase after amputation, was evaluated and compared to the situation during homeostasis. The data, obtained by our double labelling experiment, demonstrate that amputation did not considerably affect the S-phase duration. The curve of the proportion of double-labelled cells in regenerating animals demonstrated kinetics, comparable to those observed in non-regenerating animals (Figure 4.3b). Again, an initial steep decrease was observed, which showed no significant differences with time-point matched counterparts in homeostasis. Based on this observation, it can be concluded that S-phase was not accelerated during early regeneration. Hence, other adjustments of the cellular kinetics within the neoblast pool must occur to account for the early-onset proliferation boost after amputation. Cell production depends on the number of dividing cells and their average cell cycle duration (West et al., 2004). Thus, the fast replacement of missing tissue during regeneration in *M. lignano*, can be supported by an expansion of the pool of cycling neoblasts, an acceleration of a cell-cycle phase other than the S-phase, or both. In the same way, in mouse epidermis cells, the wave of cells entering S-phase upon induction of regeneration, is caused by a significantly shortened G1-phase, rather than a reduction of the S-phase duration. Additional studies should be done to further address cell cycle kinetics during regeneration in *M. lignano.*

In this study, for the first time, the S-phase duration was determined in a flatworm model, during both homeostasis and regeneration. These results add up to the limited knowledge

on the cell cycle dynamics of flatworms, and will contribute to a better understanding of cell cycle regulation in these organisms. Furthermore, a standardized object-based method was established for colocalization analysis. This method will be of further use when applying double immunohistochemical labelling techniques, and thus serve as a valuable expansion of the toolbox for studying flatworm stem cells *in vivo.*

Acknowledgements

We want to thank Peter Ladurner and Bernhard Egger for establishing the double labelling protocol in *M. lignano*. FV and MW received funding from the Institute for the Promotion of Innovation through Science and Technology in Flanders (IWT-Vlaanderen)

4.5. Supplementary material

Supplementary Figure 4.S1:

Accumulation of mitotic cells in *M. lignano* after incubation in colchicine. (a) Graphs representing the number of mitotic cells after incubation in three different concentrations of colchicine: low (0.001%, left panel), median (0.005%, middle panel), and high (0.010%, right panel). X-axis represents the incubation time in colchicine. Y-axis represents the mean number of mitotic cells (±SEM, n=4). For animals incubated in the median concentration, a significant higher number of mitotic cells (one-way ANOVA, p=0.01) was observed after 3h of colcichine-treatment, compared to the lowest concentration. The highest concentration was observed to cause a toxic effect for incubations longer than 24 hours, and no successful labelling could be performed. For animals treated with the middle and low concentration, such a toxic effect was not observed for incubations up to 48h. In conclusion, the use of a 0.005% solution of colchicine demonstrated a good balance between having a fast and efficient blocking of cells in M-phase on one hand, and experiencing no dramatic toxic effects for exposures up to 48h. This concentration was selected for further experiments. (b) Immunohistochemical labelling of mitotic cells using anti-phos-H3, after incubation in 0.005% colchicine.

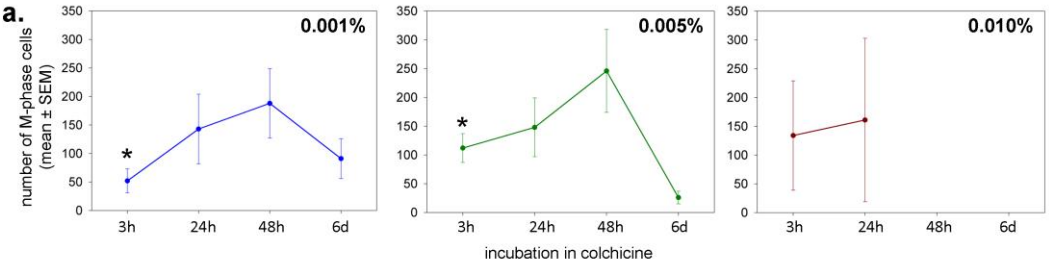
a.
number of M-phase cells
(mean ± SEM)
0.001%
0.005%
0.010%
*
*
350
300
250
200
150
100
50
0
3h
24h
48h
6d
incubation in colchicine

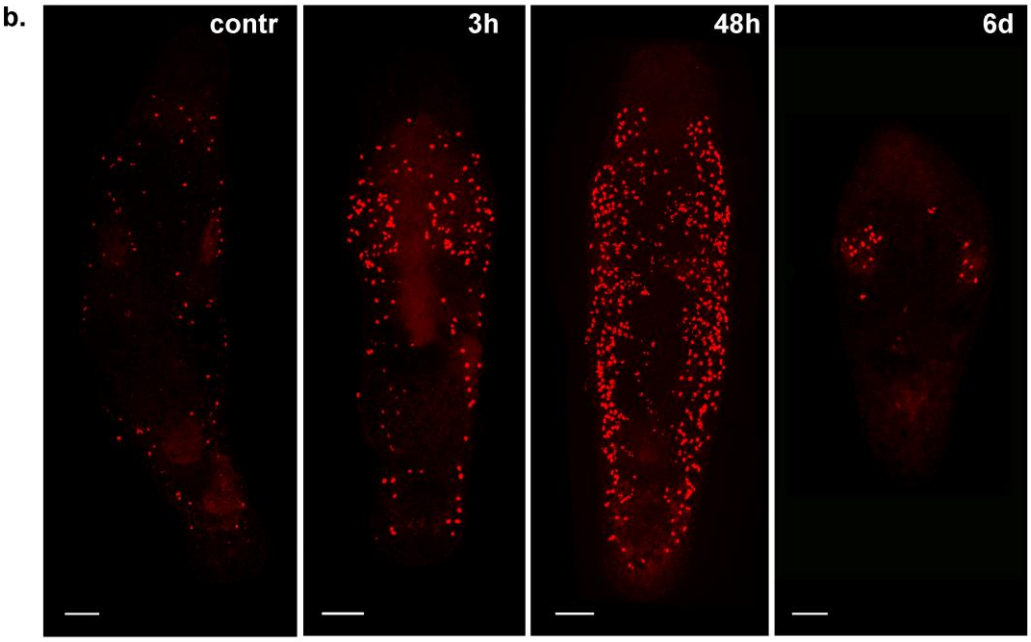
b.
contr
3h
48h
6d

a. HOMEOSTASIS

Chase	n=	CldU$^+$/IdU$^+$	CldU$^+$
		(mean ± SEM)	(mean ± SEM)
0 h	5	114,8 ± 10	123,6 ± 13
1 h	4	153 ± 20	172,3 ± 19
2 h	5	108,4 ± 5	159,2 ± 6
4 h	5	84,8 ± 13	131,4 ± 20
6 h	7	61,9 ± 6	124,9 ± 9
12 h	4	42 ± 13	216,5 ± 18
24 h	5	31,2 ± 8	253,4 ± 27
48 h	5	4,8 ± 1	194 ± 31

b. REGENERATION

Chase	n=	CldU$^+$/IdU$^+$	CldU$^+$
		(mean ± SEM)	(mean ± SEM)
0 h	4	128,3 ± 23	152,5 ± 26
2 h	4	85,5 ± 11	123,5 ± 22
4 h	5	64,8 ± 9	113,2 ± 12
12 h	4	25,8 ± 5	115,75 ± 31
24 h	5	17 ± 5	220,4 ± 17
48 h	4	26 ± 10	230,75 ± 36

Supplementary Figure S2:

Tables representing the absolute numbers of the quantification data of the CldU/IdU double labelling during homeostasis and regeneration. In the 1st and 2nd column the chase time duration and the number of replicates are given, respectively. The 3rd column represents the absolute numbers of double labelled cells (CldU$^+$/IdU$^+$). The 4th column demonstrates the total number of CldU-labelled cells (CldU$^+$), both single and double labelled. (a.) Homeostasis. Arrows and asterisks indicate significant (p=0.04, dotted arrow) and highly significant differences (p<0.01, arrows) in the number of CldU$^+$ cells. A significant increase of CldU$^+$ cells might be an indication of cell division of labelled cells, and thus inefficient blocking of cells in metaphase after prolonged incubations in colchicine (12 h). (b.) Regeneration. Significant differences in the number of CldU$^+$ cells are indicated (arrows and asterisks).

4.7. References

Agata K. and Umesono Y. (2008). Brain regeneration from pluripotent stem cells in planarian. Philos Trans R Soc B-Biol Sci *363*, 2071-2078.

Alexiades M.R. and Cepko C. (1996). Quantitative analysis of proliferation and cell cycle length during development of the rat retina. Dev Dyn *205*, 293-307.

Baguñà J. (1981). Planarian neoblasts. Nature *290*, 14-15.

Bolte S. and Cordelieres F.P. (2006). A guided tour into subcellular colocalization analysis in light microscopy. J Microsc *224*, 213-232.

Borisy G.G. and Taylor E.W. (1967). The mechanism of action of colchicine. Binding of colchincine-3H to cellular protein. J Cell Biol *34*, 525-533.

Burns K.A. and Kuan C.Y. (2005). Low doses of bromo- and iododeoxyuridine produce near-saturation labeling of adult proliferative populations in the dentate gyrus. Eur J Neurosci *21*, 803-807.

David C.N. and Campbell R.D. (1972). Cell cycle kinetics and development of *Hydra attenuata* .1. Epithelial cells. J Cell Sci *11*, 557-568.

De Vos W.H., Van N.L., Dieriks B., Joss G.H., and van O.P. (2010). High content image cytometry in the context of subnuclear organization. Cytom Part A *77*, 64-75.

Egger B. and Ishida S. (2005). Chromosome fission or duplication in *Macrostomum lignano* (Macrostomorpha, Plathelminthes) - remarks on chromosome numbers in 'archoophoran turbellarians'. J Zool Syst Evol Res *43*, 127-132.

Hayes N.L. and Nowakowski R.S. (2002). Dynamics of cell proliferation in the adult dentate gyrus of two inbred strains of mice. Dev Brain Res *134*, 77-85.

Kang H. and Sánchez Alvarado A. (2009). Flow cytometry methods for the study of cell cycle parameters of planarian stem cells. Dev Dyn *238*, 1111-1117.

Ladurner P., Egger B., De Mulder K., Pfister D., Kuales G., Salvenmoser W., and Schärer L. (2008). The stem cell system of the basal flatworm *Macrostomum lignano*. In Stem cells: from Hydra to man, Th.C.G.Bosch, ed. (Berlin - Heidelberg - New York: Springer), pp. 75-94.

Manders E.M.M., Stap J., Brakenhoff G.J., Vandriel R., and Aten J.A. (1992). Dynamics of three-dimensional replication patterns during the S-phase, analysed by double labelling of DNA and confocal microscopy. J Cell Sci *103 (Pt 3)*, 857-862.

Miller M.A., Mazewski C.M., Yousuf N., Sheikh Y., White L.M., Yanik G.A., Hyams D.M., Lampkin B.C., and Raza A. (1991). Simultaneous immunohistochemical detection of IUdR and BrdU infused intravenously to cancer patients. J Histochem Cytochem *39*, 407-412.

Morrison S.J., Shah N.M., and Anderson D.J. (1997). Regulatory mechanisms in stem cell biology. Cell *88*, 287-298.

Morrison S.J. and Spradling A.C. (2008). Stem cells and niches: Mechanisms that promote stem cell maintenance throughout life. Cell *132*, 598-611.

Nagl W. (1972). Selective-Inhibition of Cell Cycle Stages in Allium Root Meristem by Colchicine and Growth-Regulators. Am J Bot *59*, 346.

Newmark P.A. and Sánchez Alvarado A. (2000). Bromodeoxyuridine specifically labels the regenerative stem cells of planarians. Dev Biol *220*, 142-153.

Newmark P.A. and Sánchez Alvarado A. (2002). Not your father's planarian: A classic model enters the era of functional genomics. Nat Rev Genet *3*, 210-219.

Nimeth K.T., Egger B., Rieger R., Salvenmoser W., Peter R., and Gschwentner R. (2007). Regeneration in *Macrostomum lignano* (Platyhelminthes): cellular dynamics in the neoblast stem cell system. Cell Tissue Res *327*, 637-646.

Nimeth K.T., Mahlknecht M., Mezzanato A., Peter R., Rieger R., and Ladurner P. (2004). Stem cell dynamics during growth, feeding, and starvation in the basal flatworm *Macrostomum* sp. (Platyhelminthes). Dev Dyn *230*, 91-99.

Orford K.W. and Scadden D.T. (2008). Deconstructing stem cell self-renewal: genetic insights into cell-cycle regulation. Nat Rev Genet *9*, 115-128.

Rachel R.A., Dolen G., Hayes N.L., Lu A., Erskine L., Nowakowski R.S., and Mason C.A. (2002). Spatiotemporal features of early neuronogenesis differ in wild-type and albino mouse retina. J Neurosci *22*, 4249-4263.

Rando T.A. (2006). Stem cells, ageing and the quest for immortality. Nature *441*, 1080-1086.

Saló E. and Baguñà J. (1984). Regeneration and pattern-formation in planarians .1. the pattern of mitosis in anterior and posterior regeneration in *Dugesia (G) tigrina*, and a new proposal for blastema formation. J Embryol Exp Morphol *83*, 63-80.

Saló E. and Baguñà J. (2002). Regeneration in Planarians and other worms: New findings, new tools, and new perspectives. J Exp Zool *292*, 528-539.

Sánchez Alvarado A. (2004). Regeneration and the need for simpler model organisms. Philos Trans R Soc Lon Ser B-Biol Sci *359*, 759-763.

Sánchez Alvarado A. (2007). Stem cells and the planarian *Schmidtea mediterranea*. C R Biol *330*, 498-503.

Schärer L., Knoflach D., Vizoso D.B., Rieger G., and Peintner U. (2007). Thraustochytrids as novel parasitic protists of marine free-living flatworms: *Thraustochytrium caudivorum* sp nov parasitizes *Macrostomum lignano*. Mar Biol *152*, 1095-1104.

Schultz E. and McCormick K. (1994). Skeletal muscle satellite cells. Ergeb Physiol *123*, 213-257.

Sokal R.R. and Rohlf F.J. (1995). Biometry the principles and practice of statistics in biological research. (New York: W.H. Freeman and company).

Tanaka E.M. (2003). Cell differentiation and cell fate during urodele tail and limb regeneration. Curr Opin Genet Dev *13*, 497-501.

Taylor E.W. (1965). The mechanism of colchicine inhibition of mitosis. I. Kinetics of inhibition and the binding of H3-colchicine. J Cell Biol *25*, SUPPL-60.

Tsai R.Y.L., Kittappa R., and McKay R.D.G. (2002). Plasticity, niches, and the use of stem cells. Dev Cell *2*, 707-712.

Verdoodt F., Bert W., Couvreur M., De Mulder K., and Willems M. (2012a). Proliferative response of the stem cell system during regeneration of the rostrum in *Macrostomum lignano* (Platyhelminthes). Cell Tissue Res *347*, 397-406.

Verdoodt F., Willems M., Mouton S., De Mulder K., Bert W., Houthoofd W., Smith III J., and Ladurner P. (2012b). Stem cells propagate their DNA by random segregation in the flatworm *Macrostomum lignano*. Plos One *7*, e30227.

Villemont E., Dubois F., Sangwan R.S., Vasseur G., Bourgeois Y., and SangwanNorreel B.S. (1997). Role of the host cell cycle in the Agrobacterium-mediated genetic transformation of Petunia: Evidence of an S-phase control mechanism for T-DNA transfer. Planta *201*, 160-172.

Wenemoser D. and Reddien P.W. (2010). Planarian regeneration involves distinct stem cell responses to wounds and tissue absence. Dev Biol *344*, 979-991.

West G., Inzé D., and Beemster G.T.S. (2004). Cell Cycle Modulation in the Response of the Primary Root of Arabidopsis to Salt Stress. Plant Physiol *135*, 1050-1058.

Willems M., Egger B., Wolff C., Mouton S., Houthoofd W., Fonderie P., Couvreur M., Artois T., and Borgonie G. (2009). Embryonic origins of hull cells in the flatworm *Macrostomum lignano* through cell lineage analysis: developmental and phylogenetic implications. Dev Genes Evol *219*, 409-417.

Wimber D.E. and Quastler H. (1963). A ^{14}C- and ^{3}H-thymidine double labeling technique in the study of cell proliferation in *Tradescantia* root tips. Exp Cell Res *30*, 8-22.

Yanik G., Yousuf N., Miller M.A., Swerdlow S.H., Lampkin B., and Raza A. (1992). In vivo determination of cell cycle kinetics of non-Hodgkin's lymphomas using iododeoxyuridine and bromodeoxyuridine. J Histochem Cytochem *40*, 723-728.

5. Cell cycle parameters of adult stem cells in *Macrostomum lignano* (Platyhelminthes) during homeostasis and regeneration: studying actively cycling and label-retaining stem cells using flow cytometry

Verdoodt Freija, Couvreur Marjolein, Pieter Bogaert, De Meyere Kristel, Stijn Mouton Meyer Evelyne, Bert Wim, and Willems Maxime

5.1. Abstract

Cellular proliferation is a fundamental trait of stem cells. Understanding how stem cells meet the exact needs for cell renewal, requires a deeper knowledge of the cell cycle dynamics of these cells in diverse conditions, such as homeostasis and regeneration.

Flatworms have been introduced as powerful models for *in vivo* stem cell research, on account of the abundance of experimentally accessible adult stem cells (ASCs), so-called neoblasts. Although these ASCs have shown remarkable proliferative plasticity upon various environmental cues, their cell cycle dynamics are relatively understudied. Here, the cell cycle parameters of ASCs were studied *in vivo* during homeostasis and regeneration in the flatworm *Macrostomum lignano.* To this end, flow cytometry methods were adapted for use in this flatworm. During homeostasis, the distribution of cells within different phases of the cell cycle was tested, using the DNA-binding fluorochrome DAPI. By combining DAPI with ethynyldeoxyuridine (EdU), the progress of a cohort of EdU-labelled cells through the cell cycle was monitored and a cell cycle duration of approximately 30 h was estimated for the main population of neoblasts in *M. lignano*. During regeneration, an altered cell cycle distribution was observed, characterized by increased S-phase activity and a decreased number of cells in G0/G1-phase. Furthermore, a special subset of Label-Retaining Cells (LRCs), which were shown to be relatively quiescent during homeostasis, demonstrated increased cell cycle activity upon amputation.

5.2. Introduction

Proliferation is a primary function of stem cells (Orford and Scadden, 2008). Hence, to fully understand stem cell biology and exploit the therapeutic potential of these cells, it is essential to gain detailed knowledge of the cell cycle parameters of these cells under various physiological conditions (e.g., homeostasis, regeneration, nutrient deprivation). The eukaryotic cell cycle is a highly ordered process which has, classically, been divided

into four phases, the DNA-synthesis (S) phase and the mitotic segregation (M) phase, respectively preceded by gap phases G1 and G2 (Israels and Israels, 2001). In addition, a fifth phase, referred to as the G0-phase, is described as a post-mitotic phase in which cells reside in a quiescent state. The cells in this phase are not part of the cycling population, but may resume cycling after having received activating stimuli (Johnson and Walker, 1999).

When analyzing the cell cycle of stem cells, the need for *in vivo* studies is stressed by reports demonstrating highly affected cycling behaviour upon placing individual cells in a new environment (Joseph and Morrison, 2005; Orford and Scadden, 2008). This is exemplified by adult stem cells, which are typically quiescent *in vivo* but are driven to cycle under *in vitro* culture conditions (Morshead et al., 1998). Furthermore, environmental cues such as tissue loss or damage, have been demonstrated to directly affect the cell cycle (Wilson et al., 2008; Orford and Scadden, 2008; Spradling et al., 2001; Hong and Stambrook, 2004). Hence, studying stem cells in their natural habitat serves to better understand their cycling behavior in diverse physiological conditions.

In contrast to many other *in vivo* models, flatworms possess a highly abundant population of experimentally accessible adult stem cells (ASC), which have been shown to be pluripotent (Wagner et al., 2011). Therefore they promise to be highly valuable for studying the cell cycle of ASCs. The stem cells in flatworms, so-called neoblasts, are the only cells in the adult individual in which mitotic activity can be observed, and they are responsible for the remarkable plasticity that is demonstrated by these animals under diverse experimental conditions (Gentile et al., 2011; Ladurner et al., 2008 and references therein). This plasticity is most clear during regeneration, which leads to a vast increase in proliferation activity (Newmark and Sánchez Alvarado, 2000; Nimeth et al., 2007; Verdoodt et al., 2012a), indicating changes in the cell cycle parameters of the ASCs, or a subset thereof. Nevertheless, although flatworm stem cells are subject to a wide range of studies, their cell cycle parameters are relatively understudied.

Because of the ability to rapidly analyze properties of cells in suspension, flow cytometry offers a range of valuable applications to study cell cycle kinetics (Yanpaisan et al., 1998).

Uniparametric flow cytometry methods using stoichiometrically binding DNA stains such as propidium iodide (PI) and 4'-6-diamidino-2-phenylindole (DAPI) are routinely used for this purpose. These techniques rely on the fact that such staining molecules emit a signal directly proportional to the amount of DNA present in a cell, and varying DNA content is linked to progression through the cell cycle. Individual cells can therefore be assigned to different phases of the cell cycle (G0/G1, S, and G2/M) (Nunez, 2001). This method has resulted in a detailed analysis of the distribution of cells within the different phases of the cell cycle in various model systems (yeast: Haase and Reed, 2002; plants: Galbraith et al., 1983; triclad flatworms: Ermakov et al., 2011; hydra: Ulrich and Tarnok, 2005). Furthermore, biparametric flow cytometry methods have been developed, using a quantitatively binding DNA-fluorochrome in combination with a thymidine analog, which labels cells in the S-phase of the cell cycle. Using this technique, a cohort of pulse-labelled cells can be monitored as they progress through the cell cycle. In this way, actively cycling cells can be distinguished from non-cycling cells, resulting in a considerable increase in the resolution of the analysis of cell cycle characteristics (Yanpaisan et al., 1998; Lucretti et al., 1999; Kang and Sánchez Alvarado, 2009; Clausen et al., 1986a; Clausen et al., 1986b; Fluckiger et al., 2006).

In the study presented here, cell cycle parameters of ASCs are studied in the flatworm *Macrostomum lignano,* using flow cytometry. Working with *M. lignano* has the advantage over other flatworm species that, under normal culture conditions (continuous and unlimited access to food), a constant proliferation rate is maintained (Ladurner et al., 2000), which greatly facilitates analysis of the cell cycle. Furthermore, soaking the individuals in a thymidine analog-containing medium is sufficient for successful and uniform labelling of the whole animal, thereby allowing meticulous timing of pulse-chase experiments (Ladurner et al., 2000). Invasive techniques that have been demonstrated to directly affect the cell cycle (e.g. feeding or injection of the analog), can be avoided. In the past, a wide range of diverse pulse-chase and continuous pulse experiments have been conducted on this species, demonstrating kinetic heterogeneity amongst the ASC population. For instance, extended chase time durations (up to six months) have proven

the existence of a subpopulation of quiescent, label-retaining stem cells (Verdoodt et al., 2012b). Besides this stem cell subpopulation with limited cell cycle activity, the majority of ASCs are demonstrated to be actively cycling (Ladurner et al., 2000; Nimeth et al., 2004; Nimeth et al., 2007).

In this study, three *in vivo* approaches were performed using flow cytometry. First, the cell cycle distribution of ASCs was analyzed during homeostasis and regeneration, performing uniparametric analysis of DNA content (DAPI). Second, the cell cycle duration of the actively cycling population of ASCs was determined, conducting a biparametric flow cytometry method with the thymidine analog EdU (5-ethynyl-2´-deoxyuridine). Third, the cycling activity of quiescent ASCs was determined during homeostasis and regeneration by combining label-retention analysis with DNA content analysis.

5.3. Materials & Methods

5.3.1. Animal culture and amputation of the rostrum

Cultures of *M. lignano* were reared in artificial seawater medium (f/2) (Egger and Ishida, 2005) and fed *ad libitum* with the diatom *Nitzschia curvilineata*, as described previously (Schärer et al., 2007; Ladurner et al., 2008). To obtain animals of a standardized age, adult worms were put together for 24 hours, after which the eggs were collected. At the start of each experiment, animals were between one and three months old. Animals that were pulsed with a thymidine analog were protected from light.

Amputations of the rostrum were performed with a fine steel surgical blade (SM62; Swann-Morton) under a stereo microscope at a cutting level anterior to the brain. During this procedure, individuals were relaxed in a small droplet of 1:1 $MgCl_2.6H_2O$ (7.14%) and ASW (artificial sea water). Immediately thereafter, regenerates were washed in f/2 medium and transferred to culture dishes filled with f/2 medium and diatoms for three days, after which they processed for flow cytometric analysis.

5.3.2. Preparation of samples for uniparametric flow cytometry

Ten individuals were pooled in a small eppendorf tube, f/2-medium was removed, and 75µl of buffer A (0.1 M citric acid, 0.5% Tween 20) was added. After 10 min incubation in buffer A, mechanical dissociation of animals into single cells was performed by careful pipetting (50x). Finally 150µl of buffer B (0.4 M NaH_2PO_4, 2 µg/ml DAPI; Sigma-Aldrich) was added to the cell suspension, which was then filtered through a nylon filter (pore size: 37µm; Sefar) and finally analyzed using flow cytometry.

5.3.3. EdU-labelling and preparation of samples for biparametric flow cytometry

Animals were pulsed with EdU (1mM in f/2, 30 min; Invitrogen). For the LRC-experiment, animals were pulsed with EdU (20µM in f/2, 7 d, changing the medium daily). Immediately after pulsing, animals were washed with f/2 (3x), and transferred to culture dishes filled with f/2 and diatoms for the appropriate chase time. Thirty specimens were pooled to form one replica, and for each condition, at least 5 replicas were measured. For visualization of EdU, individuals were relaxed in $MgCl_2$ (1:1 $MgCl_2.6H_2O$ (7.14%):f/2, 5 min – $MgCl_2.6H_2O$ (7.14%), 5 min), fixed in 4% PFA (paraformaldehyde, 30 min; Scharlau), and rinsed in PBS-T (phosphate-buffered saline + 0.1% Triton X-100, 3 x 10 min). Blocking was then performed with BSA-T (1% bovine serum albumine in PBS-T, overnight, 4 °C), followed by incubation in Click-iT EdU reaction cocktail (concentrations according to manufacturer's instructions, 2 h, 4 °C; Invitrogen). Animals were then washed thoroughly with PBS (5 x 5 min), transferred into a small eppendorf tube, and washed with CMF-SW (calcium- and magnesium-free artificial sea water; 3.1% NaCl, 0.08% KCl, 0.16% Na_2SO_4, 0.02% $NaHCO_3$ in dH_2O; 2 x 0.5 min) (Mitsuhashi, 2002). Subsequently, animals were treated with trypsine (1.5% trypsine in CMF-SW, 50 µl, 90 min, 37°C) while every 15 min mechanical dissociation was performed by careful pipetting (50 x). Cell suspensions were then diluted with 200 µl of measuring buffer (1 unit of buffer A, 2 units of buffer B), filtered through a nylon filter (pore size: 37µm; Sefar), and analyzed using flow cytometry.

5.3.4. Flow cytometry

Samples were analyzed with a 3-laser LSR-II flow cytometer (BD Biosciences, San Jose, CA), using a 405 nm and a 488 nm laser for the excitation of DAPI and Alexa Fluor 488, respectively. Emission of DAPI and Alexa Fluor 488 was detected at 450/50 nm , and 525/50 nm respectively. To discriminate for autofluorescence, control samples were treated equally as experimental samples, except the use of Alexa Fluor 488 was omitted. Autofluorescent particles could be gated from EdU^+ particles based on their lower signal intensity, and this border was used to set the EdU-threshold value. To discriminate for non-specific binding of Alexa Fluor 488 azide, control samples were similarly processed as EdU-treated samples, except the EdU-pulse was omitted. Non-specific staining was observed in a small population of particles that were characteristic in their large size (forward scatter - FSC) and complex internal structure (side scatter - SSC). Based on these characteristics, non-specifically stained particles were gated on FSC-SSC dot plots and thus excluded from analysis. To discriminate against cell debris and aggregates of two nuclei (doublets) or more, acquired data were gated, based on dot plots of 'total DAPI-fluorescence of a particle' (DAPI-area) vs. 'transit time of a particle' (DAPI-width) (Nunez, 2001).

5.3.5. Data analysis and Statistics

Uniparametric analysis of the distribution of cells within the cell cycle was performed on DAPI-histograms, using FACSdiva (BD Bioscience) and Flow Jo (Treestar, San Carlos, CA). Biparametric cell cycle analysis was performed using FACSdiva (BD Bioscience). Spectral overlap, for combined use of DAPI and EdU (Alexa Fluor 488), was corrected based on single stained samples. The horizontal separating line, distinguishing between EdU^+ and EdU^- cells, was based on the EdU-threshold value (as described earlier). The vertical line, separating the area of 2n and 4n DNA, was determined based on the DAPI histogram of all particles. On this histogram, the right border of the G0/G1-peak was used as a landmark. Mean proportions (± SEM) are shown of a minimum of 6 replicates for each condition (n=6-11). The statistical analysis was done using Statistica 7 (StatSoft Europe GmbH, Hamburg,

Germany). Given that the data of the EdU pulse-chase experiment as well as the LRC-experiment failed to meet the assumption for homogeneity of variances (Levene's test and Brown & Forsythe test), non-parametric tests were performed. EdU pulse-chase data were analysed using Kruskal-Wallis non-parametric ANOVA and the Dunn multiple comparison test. Uniparametric data, and biparametric LRC-data were analyzed by means of Mann-Whitney U tests, comparing homeostasis and regeneration.

5.4. Results

5.4.1. Cell cycle distribution of ASCs during homeostasis, and regeneration

To evaluate the cell cycle distribution of cells in *M. lignano* during homeostasis and regeneration, a uniparametric flow cytometry method was established to analyze DNA content. For the preparation of cell suspensions of *M. lignano*, a method was used based on the procedure originally described for plant cells by Otto et al. (1990), and later modified for triclad flatworms (planarians) by Ermakov et al. (2011). Compared to the maceration protocol that has been published for *M. lignano* (Ladurner et al., 2000), this new technique was evaluated to be better adapted for flow cytometry, as it resulted in better disintegration of the animals into single cells and led to DNA histograms with lower coefficients of variation. DAPI was used to quantitatively evaluate the amount of DNA, present in the cells: based on the intensity of the fluorescent signal of individual cells, DNA content histograms were constituted. During analysis, discrimination for cell doublets was performed to avoid an overestimation of the proportion of cells in G2/M-phase (see materials and methods). Finally, automatic cell cycle analysis was performed using specialized software (Flow Jo).

In intact individuals, a predominant G0/G1 peak was observed, consisting of a mixture of non-cycling (terminally differentiated cells, and quiescent G0 stem cells) and cycling cells (G1 cells) with DNA content corresponding to 2n (Figure 5.1A). A considerably smaller

amount of cells was observed to have twice as much DNA (4n), which represents actively cycling cells that have passed the DNA synthesis phase and therefore are in G2/M-phase. The intermediate region included actively cycling cells possessing various amounts of DNA, and which are at different stages of the S-phase. This confirms that proliferation in *M. lignano* is not synchronized *in vivo* (see also Ladurner et al., 2000). Automatic cell cycle analysis of intact individuals demonstrated that 96% (±3, n= 9), 1.5% (±2.5, n=9), and 4.3% (±0.2, n=9) of the cells, respectively, had DNA content corresponding to the G0/G1-, S-, and G2/M-phase (Figures 5.1B, C). Based on the proportions of cells in the S-, and G2/M-phases, cycling cells were observed to comprise at least 5.8% (±2.5, n=9) of the total cell number in *M. lignano.* The proportion of S-phase cells observed here (1.2%) is in line with a previous estimation of 2% S-phase cells, demonstrated after a 30-minute BrdU pulse and whole-mount labelling (Ladurner et al., 2000).

In regenerating animals, cell cycle distribution was analyzed three days after amputation. Previously it has been shown that, at this time step during the regeneration process, S-phase activity peaked. Although the effect was spatially limited, the impact on cell cycle dynamics exceeded that of the preceding systemic phase (Verdoodt et al., 2012a). DNA content histograms demonstrated a considerably reduced G0/G1 peak and an increased amount of cycling cells (S, G2/M). Performing automatic cell cycle analysis confirmed a significantly decreased proportion of cell in G0/G1 (87.5%± 2.3, n=9, p=0.03), along with a significantly increased amount of cells in S-phase (8.4% ± 2.1, n=9, p=0.04) (Figures 5.1B, D). G2/M was observed to comprise 4.8 % (±0.2, n=9, p=0.07) of the cell suspension.

Figure 5.1

Cell cycle distribution of cells in *M. lignano*, performing uniparametric flow cytometric analysis of DNA content (DAPI). Individuals were dissociated into single cells during homeostasis and regeneration, and then stained with DAPI. Subsequently DNA content histograms were generated using flow cytometry, and automatic cell cycle analysis was performed using Flow Jo. **(A)** Representative DNA content histogram of *M. lignano* (homeostasis), based on the intensity of the DAPI-signal. Note the predominant G0/G1-peak, for the largest part consisting of non-cycling, differentiated cells. **(B, C)** Automatic analysis of cell cycle distribution in *M. lignano*. **(B)** Graph representing the proportion of cells in G0/G1-, S-, and G2/M-phase of the cell cycle (mean ± SEM, n=9-11) during homeostasis (black), and regeneration (grey). Significant differences to the corresponding proportion during homeostasis are indicated (asterisks). Note the decreased and increased proportions of cells in G0/G1, and S, respectively, during regeneration. **(C-D)** Representative cell cycle profiles of *M. lignano***.** The proportion of cells in G0/G1- (green curve), S- (yellow curve), and G2/M-phase (blue curve) of the cell cycle are demonstrated (upper pannels). Enlargement of the base of the histogram (lower panels). **(C)** Homeostasis. **(D)** Regeneration. A smaller G0/G1 peak was observed, while the S-region was enlarged.

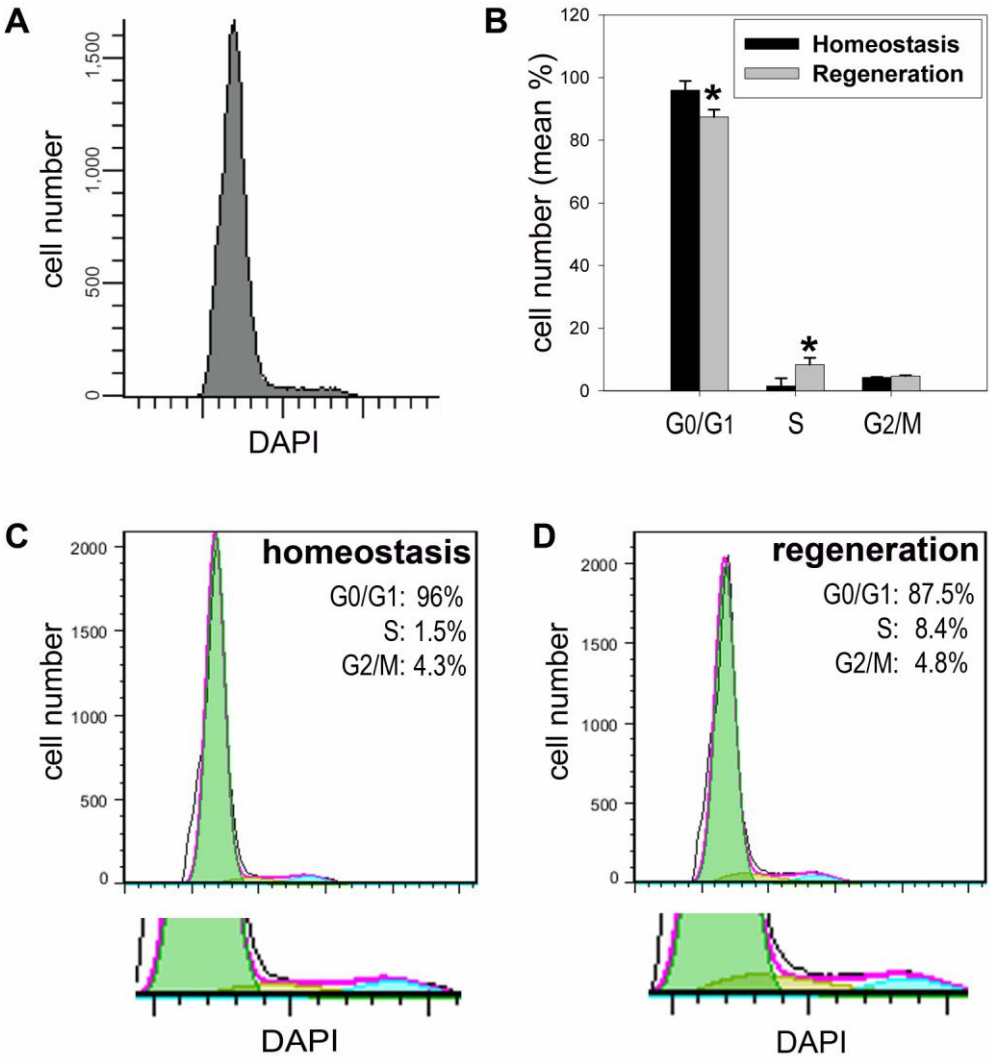
A
cell number
1.500
1.000
500
0
DAPI
B
cell number (mean %)
120
100
80
60
40
20
0
Homeostasis
Regeneration
*
*
G0/G1
S
G2/M
C
homeostasis
G0/G1: 96%
S: 1.5%
G2/M: 4.3%
cell number
2000
1500
1000
500
0
DAPI
D
regeneration
G0/G1: 87.5%
S: 8.4%
G2/M: 4.8%
cell number
2000
1500
1000
500
0
DAPI

5.4.2. Progression of EdU-labelled cells through the cell cycle

Although uniparametric flow cytometric analysis of DNA content is a valuable method for studying the global effect of environmental changes on cycling cells, it does not provide information on cycle traverse rates or phase transit times. To improve the resolution of the analysis of cell kinetic parameters in *M. lignano*'s asynchronous cell population, a biparametric flow cytometry method was applied to discriminate active from non-active cells. Using EdU, a thymidine analog that is incorporated into newly synthesized DNA during S-phase, the progress of a cohort of EdU^+ cells through the cell cycle was analyzed. In this study, EdU was preferred over other, more frequently used analogs such as BrdU, IdU, or CldU, due to the considerably shorter visualization technique, but mostly due to the highly improved signal to noise ratio (data not shown). However, fixation of the animals with PFA, a necessary step in the visualization of EdU, was observed to hamper dissociation of the animals into single cells. Therefore, the dissociation technique that was proved efficient for unfixed animals in the uniparametric flow cytometric analysis, needed to be adjusted for this experiment. Enzymatic dissociation using trypsine was observed to give the best balance between yield of single cells and quality of the DNA content histogram.

For cell cycle analysis, animals were pulsed for 30 minutes with EdU. After various chase times, EdU was visualized and individuals were dissociated into single cells and stained with DAPI (Figure 5.2A).

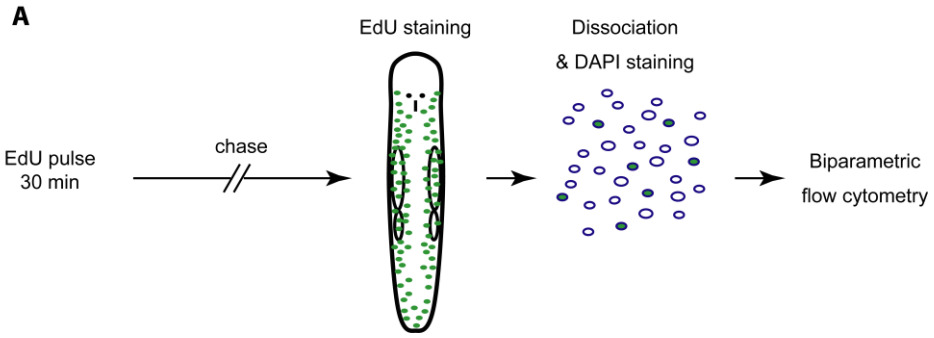

Figure 5.2A

Scheme of experimental set-up. Adult individuals were pulsed with EdU (30 min), chased for various durations, and stained for EdU. Subsequently, they were dissociated into single cells, stained with DAPI, and finally processed for biparametric analysis of DNA content (DAPI) and EdU-signal, using a flow cytometer.

For each chase time, biparametric DNA-EdU distributions were measured using flow cytometry, and the proportion of EdU^+ cells in the 2n-region and in the 4n-region of the histogram was determined (see Materials & Methods). The proportion of labelled cells in S-phase could not be determined separately, since overlap with the G0/G1- and the G2/M-region was observed because of the breadth of the DNA-histogram peaks of fixed cell suspensions (see Hamelik and Krishan, 2009). Therefore, cells in the 2n region of the histogram correspond to cells in the G0/G1 + early S-, and the 4n region holds cells in late S + G2/M. The proportions of 2n and 4n cells for diverse chase times are shown in Figure 5.2B. After a chase time of 0 h, 52.0% (±4.3, n=11) and 45.6% (±4.0, n=11) of the EdU^+ cells had DNA content corresponding to 2n and 4n, respectively. Cells were distributed around the division line between the 2n and 4n region of the histogram (Figure 5.2C, top/right panel), indicating that proliferation is not synchronized and that these labelled cells were at different stages of the S-phase at the time of EdU delivery. After 12 h chase, 47.6% (±1.3, n=11) and 50.8% (±1.4, n=11) of EdU^+ cells had a DNA content of 2n and 4n, respectively (Figure 5.2C, bottom/left panel). After 24 h chase, a marked accumulation of EdU^+ cells was observed in G0/G1 + early S, due to the generation of labelled progeny

during the preceding M-phase (Figure 5.2C, bottom/right panel). Respectively, 85.1% (±4.3, n=8, p=0.008) and 14.2% (±4.2, n=8, p=0.008) of labelled cells had a DNA content of approximately 2n and 4n. Based on this observation, the cell cycle duration was observed to be at least 24 h (see discussion section). After 48 h chase, a proportion of EdU^+ cells was observed to have shifted to the 4n region again, entering late S + G2/M of the second cell cycle after pulsing. The proportion of labelled cells in the 2n region decreased from 85.1% to 57.4% (±1.1, n=6) and rose in the 4n region to 41.4% (±1.0, n=6). Still, the fraction of labelled cells in G0/G1 + early S remained higher when compared to corresponding times during the first cycle, indicating that not all cells cycled further through the cell cycle, at least not immediately (Figure 5.2B). After 72h chase, again a peak of cells with 2n DNA (89%±3.6, n=7, p=0.003) was seen, together with a decrease in the proportion of cells with 4n DNA (10.5%±0.4, n=7, p=0.004).

Figure 5.2B,C

Monitoring the progression of a cohort of EdU-labelled cells through the cell cycle in *M. lignano.* (B) Graph representing the proportion of EdU^+ cells (mean ± SEM) in the 2n-region of the DNA content histogram (black curve) and the 4n-region (grey curve) at various chase times after pulsing (n=6-11) . Cells in the 2n-region of the histogram correspond to cells in G0/G1 + early S and , and the 4n-region holds cells in late S + G2/M. (C) Representatives of contour plots of green fluorescence (EdU, Y-axis) and DNA content (DAPI, X-axis) after various chase times. Based on EdU-unlabelled samples the horizontal separation line between EdU^+ and EdU^- cells was set. In the upper part of each plot (green rectangle), cells are present in which robust EdU-signal can be detected. The line perpendicular to the X-axis separates cells in G0/G1 + early S (2n, left), and cells in late S + G2/M (4n, right). The location of this separation line, was determined using the right border of the G0/G1-peak in the DAPI histogram as a landmark. Percentages represent the proportion of 2n, or 4n cells, relative to the total amount of EdU^+ cells.

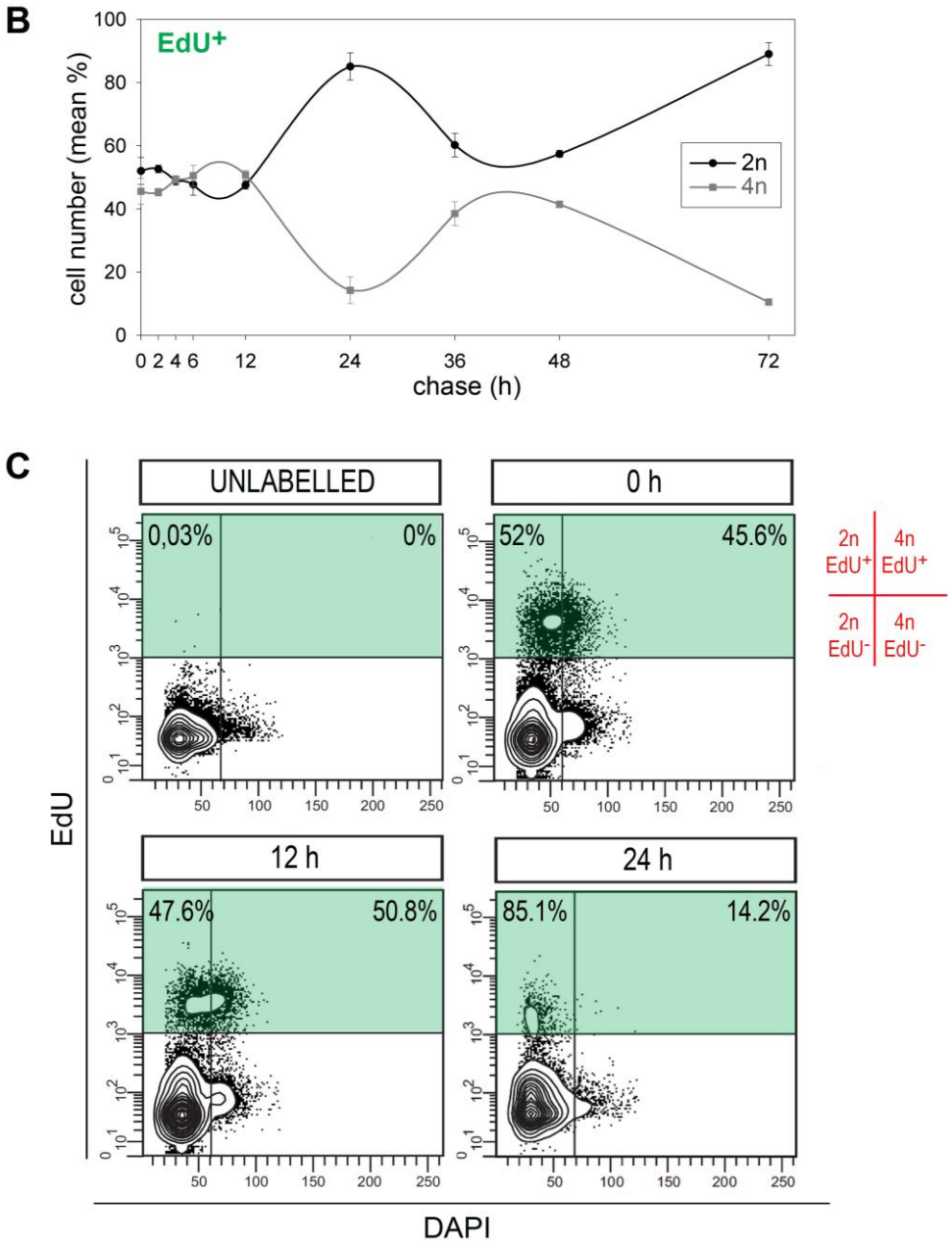
B
EdU+
cell number (mean %)
100
80
60
40
20
0
0 2 4 6
12
24
36
48
72
chase (h)
2n
4n
C
UNLABELLED
0 h
12 h
24 h
0,03%
0%
52%
45.6%
47.6%
50.8%
85.1%
14.2%
2n EdU+
4n EdU+
2n EdU-
4n EdU-
EdU
DAPI

5.4.3. Cycling activity of label-retaining cells during homeostasis and regeneration

In *M. lignano*, pulsing with thymidine analogs during development and homeostasis has been demonstrated to result in cells that retained label for extended chase time durations of up to six months (Verdoodt et al., 2012b). Among these LRCs, post-mitotic differentiated cells were identified, as well as neoblasts in which label-retention was argued to be caused by cellular quiescence that prevented dilution of label (Verdoodt et al., 2012b). In this study, a population of LRCs was established by performing an EdU pulse (7 d continuously) in adult individuals. After a chase time of three months, animals were stained for EdU, dissociated into single cells, and stained with DAPI. Cell suspensions were subjected to flow cytometry, determining the DNA content and EdU signal of individual cells (Figure 5.3A). Within the population of LRCs, on average 96.7% (±0.4, n=7) of the cells had a DNA content of 2n. Merely 3.1% (±0.4, n=7) of the cells was observed to have a DNA content of 4n, demonstrating little cell cycle activity among LRCs (Figure 5.3B).

To test whether regeneration induces increased cycling activity within the population of LRCs, amputation of the rostrum was performed in individuals that had been pulsed with EdU (7 d continuously, 20 µM) and then chased for 3 months (Figure 5.3A). Three days after amputation, biparametric flow cytometry demonstrated that 92.3% (±0.8, n=6, p=0.0008) and 7.0% (±0.7, n=6, p=0.0006) of the LRCs had a DNA content corresponding to 2n and 4n, respectively (Figures 5.3C, D). In conclusion, the proportion of EdU^+ cells with a DNA content of 4n had increased significantly (7.0% vs. 3.1%) compared to uncut animals, demonstrating that amputation did induce increased cycling activity among the population of LRCs.

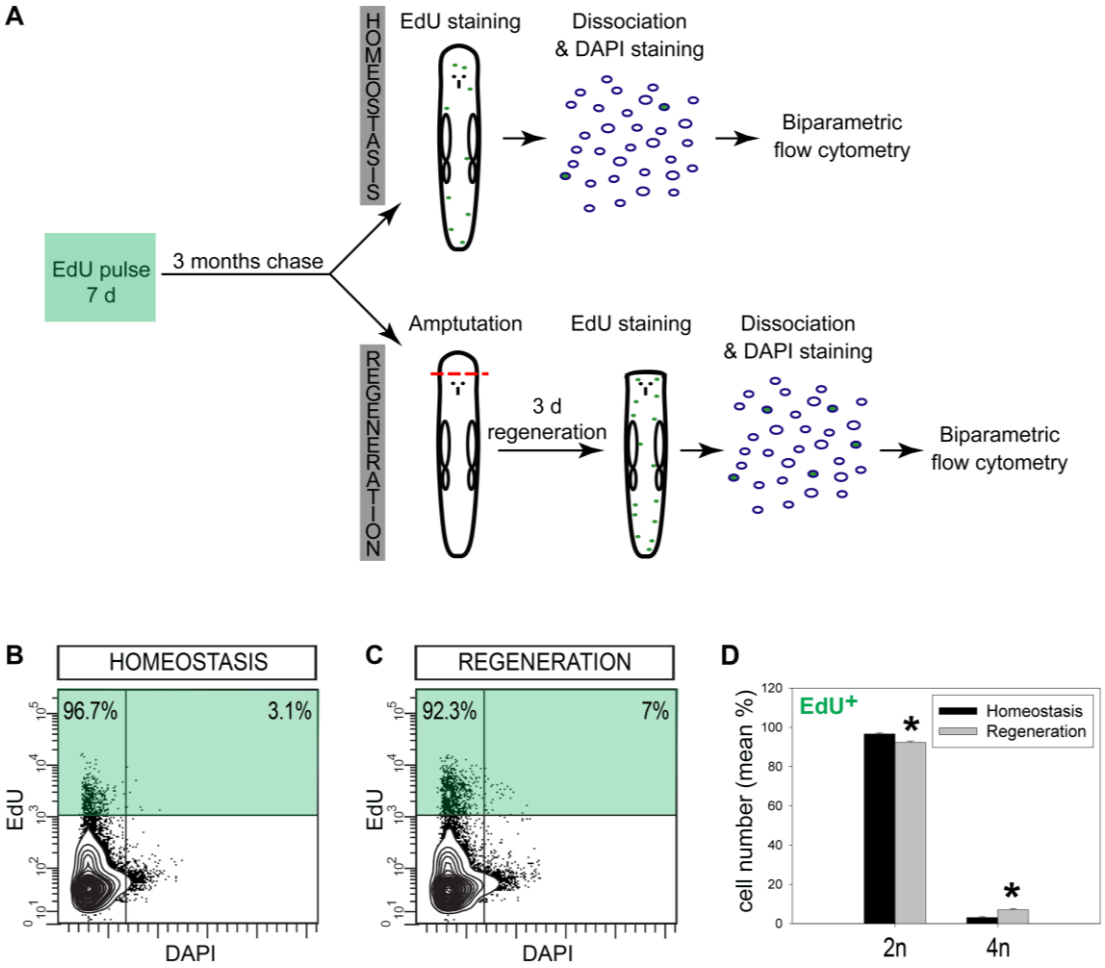

Figure 5.3

Analysis of cell cycle activity in a population of LRCs during homeostasis and regeneration. (A) Scheme of experimental set-up. Adult individuals were pulsed with EdU for 7 d continuously, after which they were chased for 3 months. To test cell cycle activity during homeostasis, individuals were then stained for EdU, dissociated into single cells, stained with DAPI, and subjected to biparametric flow cytometry. For our regeneration experiment, individuals were amputated at the rostrum (red dotted line) and left to regenerate for 3 d, prior to EdU staining. (B,C) Contour plots, showing green fluorescence (EdU) against DNA content

(DAPI). The green rectangle represents the region of the plot in which robust EdU-signal can be detected. Left of the vertical separation line are cells in G0/G1 + early S (2n), right are cells in late S + G2/M (4n). (B) Homeostasis. A population of cells (100%) have retained EdU-label for 3 months, and are for the largest part concentrated in the 2n region of the plot (96.7%). Merely a small proportion of cells is observed in the 4n-regions, which holds cycling cells (3.1%). (C) Regeneration. The proportion of LRCs in the 4n-region right is increased (7% vs. 3.1%), indicating increased cell cycle activity among the LRCs during regeneration. (D) Graph representing the proportion of LRCs in the 2n-region and 4n-region of the DNA content histogram during homeostasis (black bars) and regeneration (grey bars). During regeneration, the proportion of LRCs in 4n-region which contains cycling cells has increased, compared to homeostasis. Significant differences to the corresponding proportion during homeostasis are indicated (asterisks).

5.5. Discussion

5.5.1. Uniparametric flow cytometry to study cell cycle distribution of ASCs in *M. lignano*

A univariate flow cytometry technique was established to determine the DNA content of individual cells in suspension. This allowed us to rapidly measure the distribution of cells within the cell cycle during homeostasis and regeneration in *M. lignano.* The fluorochrome DAPI was used to bind quantitatively to DNA, as it was observed to have several advantages over the use of PI. (1) DAPI resulted in higher yields of labelled cells when compared to PI, most likely due to better permeability of the cells. (2) Reduced clumping was observed as additional washing and centrifugation steps, which are inevitably linked to the use of PI, are made unnecessary using DAPI due to the low autofluorescence of unbound DAPI. Finally (3), in contrast to PI, DAPI does not intercalate with double-stranded RNA, which rendered pre-treatment with RNase unnecessary (Yanpaisan et al., 1999). These advantages account for the fact that DAPI resulted in DNA content histograms with lower coefficients of variation, enabling more accurate analysis of cell cycle distribution.

Although no specific cell cycle parameters can be deduced, this method is promising as it allows rapid measurement of large numbers of samples, as opposed to highly time-consuming microscopic analysis of whole-mount individuals. It can be further deployed to quickly monitor the effect of various environmental changes on the proliferative dynamics of stem cells in *M. lignano*. Furthermore, in combination with RNA interference (see Pfister et al., 2008; De Mulder et al., 2009) and the use of specific antibodies, it has the potential to contribute to the characterization of cell cycle phenotypes. Therefore, this method serves as a valuable expansion of the growing toolkit being developed to study stem cell biology in this flatworm (Ladurner et al., 2008 and references therein; Pfister et al., 2008; Willems et al., 2009; De Mulder et al., 2010).

5.5.2. Progression of EdU-labelled cells through the cell cycle

Using DNA content as a single parameter in the analysis of the cell cycle, no specific cell cycle parameters can be deduced because cycling cells cannot be distinguished from differentiated cells. To improve the resolution of cell cycle measurement, the thymidine analog EdU, which labels actively cycling cells, was introduced as a second parameter. In this way, a cohort of EdU-labelled ASCs could be followed as they progress through the cell cycle. This recently developed EdU-based method can be a superior alternative to BrdU-based flow cytometry (Kotogany et al., 2010; Darzynkiewicz et al., 2011). Firstly, when using EdU, denaturation of the DNA, a step which is observed to compromise the quality of the nuclei, is rendered unnecessary (Sasaki et al., 1988; Lucretti et al., 1999). Moreover, due to increased fluorescent intensity, EdU does not require the use of complex signal-amplification methods, in contrast to flow cytometric analysis of BrdU-signal in triclad flatworms (Kang and Sánchez Alvarado, 2009).

After 24 h chase, EdU^+ cells were observed to have accumulated in the 2n region, indicating that these cells were in G1- or early S-phase of the second cell cycle after pulsing. At this time, the cohort of EdU-labelled cells started to enter the 4n-region, and thus the cells that were most advanced in their cell cycle started to shift to late S-phase. Based on this observation, one could conclude that in 24 h, cells have traversed a complete cell cycle (from the S-phase during which they were pulsed, to the next S-phase). However, the cells that are farthest along their cell cycle and are now entering late S-phase, were most likely pulsed at the utter end stage of the previous S-phase. Hence, these cells still need to traverse a part of S-phase to have completed a full cell cycle (Figure 5.4).

Therefore, we conclude that the cell cycle duration of neoblasts in *M. lignano* is more than 24 h. To estimate the exact duration, the time needed for neoblasts to traverse the part of the S-phase that is spent in the 4n-region, should be measured. In this study, our 0 h chase experiment demonstrated that approximately half (52%) of the S-phase cells were in the 2n region, and the other half (45%) in the 4n region. Based on this observation and the fact

that neoblast proliferation is asynchronized, we can assume that cells spend roughly half of the S-phase in the 2n region of the histogram, and the other half in the 4n region. Hence, cells entering the 4n region after 24h, still need to traverse approximately half of the total S-phase duration to reach the stage in which they were pulsed during the preceding cell cycle. We previously have estimated the duration of S-phase to be 13 h in *M. lignano* (Chapter 4). Therefore, the cell cycle duration of neoblasts in *M. lignano* is approximately 30h (24h + 13h/2).

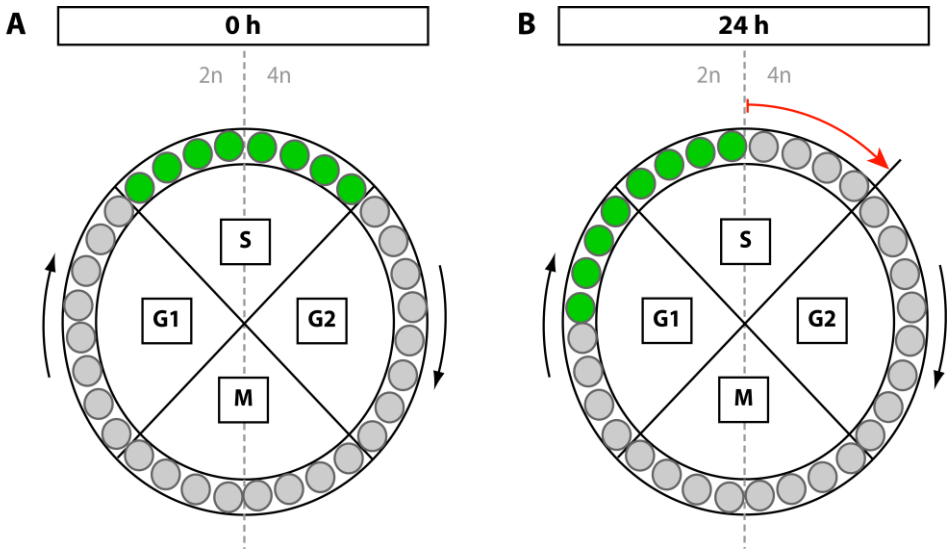

Figure 5.4

Scheme, explaining the course of EdU-labeled cells through the cell cycle. Small, colored circles represent an asynchronous population of cells, distributed within the distinct phases of the cell cycle: G1-, S-, G2-, and M-phase. For clarity, in this scheme, each phase occupies exactly one quarter of the circle. This does not relate to their exact duration within the cell cycle. Cells with a DNA content corresponding to 2n are separated from cells with a DNA content of 4n by the vertical line (dotted, gray line). An EdU pulse is performed, which labels cells in S-phase of the cell cycle (green circles), while other cells remain unlabelled (gray circles). (A) After 0 h chase, EdU-labelled cells are distributed equally around the 2n-4n division line. (B) After 24 h chase, EdU-labeled cells, which had accumulated in the 2n-region, are now entering the 4n-region. This indicates that, in 24 h, they have traversed a complete cell cycle minus a part of the S-phase (red arrow). Therefore, cell cycle duration of neoblasts was concluded to be little over 24 h.

The estimated cell cycle duration of 30 h, however, reflects on a population of the main population of neoblasts. In the past, the presence of a subpopulation of fast-cycling neoblasts has been described in *M. lignano* (Ladurner et al., 2000; Nimeth et al., 2004; Nimeth et al., 2007). These cells were observed to pass the complete duration of S-, G2-phase in 2 h (Nimeth et al., 2007), and therefore, potentially, have a cell cycle duration of merely a few hours. We hypothesize that the presence of such cells, which quickly switch from the 2n- to the 4n region, explains the relatively equal distribution of labelled cells around the 2n-4n division, line for chase times up to 12 h. Merely, when the main population of cycling neoblasts traversed M-phase and subsequently accumulated in G1, a significantly changed distribution was observed, suggesting that this population considerably outnumbers the fast-cycling population. Based on these results, however, the cell cycle duration of fast cycling neoblasts could not be determined. In the future, further molecular and structural characterization of neoblasts, aimed at distinguishing among different subpopulations, should reveal more details of the cell cycle of the population of fast-cycling cells.

All through the second cycle, the proportion of labelled cells in G0/G1 remained higher compared to the first cycle. This observation indicates that a proportion of the daughter cells exits the cell cycle to eventually differentiate and execute a specific function, or remains longer in G1-phase and does not immediately enter a new round of DNA synthesis.

5.5.3. Cell cycle distribution of ASCs during regeneration

In this study, the cell cycle distribution of ASCs was analyzed in 3d-regenerates using uni-parametric flow cytometry. A significant increase in the proportion of cells in S-phase was observed, together with a decrease of cells in G0/G1 and a relatively constant proportion of cells in G2/M. We argue that this is the result of an increased proportion of cycling cells in the cell population. This is confirmed by our LRC experiment, which demonstrated the re-entrance of long-term quiescent cells into the cell cycle upon amputation (see below).

However, assuming that an increased participation of cells in the cell cycle is solely responsible for the altered cell cycle distribution in regenerates, one would expect an increase in G2/M numbers as well. Therefore, an additional explanation for the observed changes in the DNA content histogram should be taken into account, such as alterations in the duration of one or more cell cycle phases. In an asynchronous population, the shortening of a particular phase lowers the chance of a cell to be in that particular phase resulting in an altered cell cycle distribution. In the past, an acceleration of the cell cycle at the level of G1 and G2 has been demonstrated in diverse regeneration models (Ford and Young, 1963; Clausen et al., 1986a; Wenemoser and Reddien, 2010). In our study, the significant decrease (8.5%) in the proportion of cells in the G0/G1-peak indicates that a reduction of the duration of G1, together with an increased participation of G0 cells in the cell cycle, is likely to account for the changed DNA content histogram. However, a reduction of the duration of G2 is a valid hypothesis as well. It would furthermore explain why the proportion of cells in G2/M does not increase, as opposed to the amount of S-phase cells, given that the decreased amount of cells in G2 is counterbalanced by an increased amount of cells in M-phase. This is confirmed by a previous study in which a doubling of mitotic numbers was demonstrated in 2d-regenerates of *M. lignano* (Nimeth et al., 2007). Still, it should be noted that no acceleration at the level of G2 was observed during the first four hours of regeneration in *M. lignano* (Nimeth et al., 2007). In this study, a G2 shortening remains possible given that 3 d-regenerates were used, although the reason for a postponed effect is not clear. A subsequent step to confirm this hypothesis, would be to combine our flow cytometry method with a mitosis marker (e.g. anti-phosphorylated histone H3). Still, we can conclude that during regeneration in *M. lignano*, the additional need for cell proliferation is met by an increased amount of cycling cells, combined with an acceleration of the cell cycle.

5.5.4. Quiescent neoblasts participate in the regeneration process

Previously, the establishment of LRCs has been described in *M. lignano*. Among these labelled cells, neoblasts were identified that were shown to retain label due to their long-term quiescence (Verdoodt et al., 2012b). In the current study, a population of LRCs was established after performing a pulse in adult individuals. DNA content analysis demonstrated that these EdU^+ cells were, for the most part (97%), located in the G0/G1-region (2n) of the histogram. Based on their DNA content, the labelled cells in this region are either the differentiated progeny of labelled neoblasts, quiescent neoblasts in G0-phase, or cycling neoblasts in G1- or early S-phase. A relatively small proportion (3%) of the LRCs were observed to have a DNA content of 4n, which indicates cell cycle activity among LRCs during homeostasis. These observations point out that the population of cells that retain label is a mixture of differentiated cells and neoblasts that retain long periods of quiescence and occasionally participate in the cell cycle. Our regeneration experiment demonstrates that after amputation, the number of cycling LRCs had increased. This proves that a fraction of the LRC population are neoblasts, which can be activated to re-enter the cell cycle upon amputation. Given that no conclusive evidence for dedifferentiation of terminally post-mitotic cells in flatworm regeneration exists, this process is unlikely to account for the increased number of cycling cells (for references see: Reddien and Sánchez Alvarado, 2004; Egger et al., 2009). Hence, a population of quiescent cells in *M. lignano* appears to form a relatively silent reservoir that is activated after wounding. Similar examples of the activation of a quiescent stem cell population upon injury have been amply observed in mice (Tumbar et al., 2004; Wilson et al., 2008; Li et al., 2010). Furthermore, our observation of the activation of quiescent cells is in line with a previous study on *M. lignano*, demonstrating repopulation of the neoblasts pool after sublethal irradiation (De Mulder et al., 2010). The authors suggested that a small proportion of neoblasts with a higher irradiation resistance, possibly G0-arrested neoblasts, were responsible for the recovery of the proliferative compartment of the

individual. How the quiescent state is maintained and what the molecular mechanisms are that regulate transitions into and out of that state remain important considerations for the future.

5.5.6. Conclusions

In this study, three *in vivo* methods were established using flow cytometry as a means to study cell cycle parameters of quiescent and actively cycling ASCs in *M. lignano.* Using these techniques, an approximation of the cell cycle duration within the main population of neoblasts in *M. lignano* was measured and, for the first time, the participation of quiescent cells in the regeneration process was demonstrated. Being rapid, reproducible, and highly informative, these methods promise to further generate knowledge on stem cell heterogeneity and cycling dynamics in *M. lignano*. Furthermore, combined with the intriguing population of abundant and experimentally accessible ASCs in this flatworm, they provide an interesting opportunity to test stem cell behavior upon diverse environmental cues.

Acknowledgements

This work was supported by a Ghent University Methusalem BOF09/01M00709 Grant. FV and MW received funding from the Institute for the Promotion of Innovation through Science and Technology in Flanders (IWT-Vlaanderen).

5.6. References

Clausen O.P.F., Kirkhus B., and Schjolberg A.R. (1986a). Cell cycle progression kinetics of regenerating mouse epidermal cells: An *in vivo* study combining DNA flow cytometry, cell sorting, and [^{3}H] dThd autoradiography. J Invest Dermatol *86*, 402-405.

Clausen O.P.F., Kirkhus B., Thorud E., Schjolberg A., Moen E., and Cromarty A. (1986b). Evidence of mouse epidermal subpopulations with different cell cycle times. J Invest Dermatol *86*, 266-270.

Darzynkiewicz Z., Traganos F., Zhao H., Halicka H.D., and Li J.W. (2011). Cytometry of DNA replication and RNA synthesis: Historical perspective and recent advances based on "Click Chemistry". Cytometry A *79A*, 328-337.

De Mulder K., Kuales G., Pfister D., Egger B., Seppi T., Eichberger P., Borgonie G., and Ladurner P. (2010). Potential of *Macrostomum lignano* to recover from gamma-ray irradiation. Cell Tissue Res *339*, 527-542.

De Mulder K., Pfister D., Kuales G., Egger B., Salvenmoser W., Willems M., Steger J., Fauster K., Micura R., Borgonie G., and Ladurner P. (2009). Stem cells are differentially regulated during development, regeneration and homeostasis in flatworms. Dev Biol *334*, 198-212.

Egger B., Gschwentner R., Hess M.W., Nimeth K.T., Adamski Z., Willems M., Rieger R., and Salvenmoser W. (2009). The caudal regeneration blastema is an accumulation of rapidly proliferating stem cells in the flatworm *Macrostomum lignano*. BMC Dev Biol *9*.

Egger B. and Ishida S. (2005). Chromosome fission or duplication in *Macrostomum lignano* (Macrostomorpha, Plathelminthes) - remarks on chromosome numbers in 'archoophoran turbellarians'. J Zool Syst Evol Res *43*, 127-132.

Ermakov A.M., Ermakova O.N., Kudravtsev A.A., and Kreshchenko N.D. (2011). Study of planarian stem cell proliferation by means of flow cytometry. Mol Biol Rep *39*, 3073-3080.

Fluckiger A.C., Marcy G., Marchand M., Negre D., Cosset F.L., Mitalipov S., Wolf D., Savatier P., and Dehay C. (2006). Cell cycle features of primate embryonic stem cells. Stem Cells *24*, 547-556.

Ford J. and Young R. (1963). Cell proliferation and displacement in the adrenal cortex of young rats injected with tritiated thymidine. Anat Rec *146*, 125-137.

Galbraith D.W., Harkins K.R., Maddox J.M., Ayres N.M., Sarma D.P., and Firoozabady E.B.R.A. (1983). Rapid flow cytometric analysis of the cell cycle in intact plant tissues. Science *220*, 1049-1051.

Gentile L., Cebria F., and Bartscherer K. (2011). The planarian flatworm: an *in vivo* model for stem cell biology and nervous system regeneration. Dis Model Mech *4*, 12-19.

Haase S.B. and Reed S.I. (2002). Improved flow cytometric analysis of the budding yeast cell cycle. Cell Cycle *1*, 132-136.

Hamelik R.M. and Krishan A. (2009). Click-iT (TM) assay with improved DNA distribution histograms. Cytom Part A *75A*, 862-865.

Hong Y.L. and Stambrook P.J. (2004). Restoration of an absent G1 arrest and protection from apoptosis in embryonic stem cells after ionizing radiation. Proc Natl Acad Sci U S A *101*, 14443-14448.

Israels E.D. and Israels L.G. (2001). The cell cycle. Stem Cells *19*, 88-91.

Johnson D.G. and Walker C.L. (1999). Cyclins and cell cycle checkpoints. Annu Rev Pharmacol Toxicol *39*, 295-312.

Joseph N.M. and Morrison S.J. (2005). Toward an understanding of the physiological function of mammalian stem cells. Dev Cell *9*, 173-183.

Kang H. and Sánchez Alvarado A. (2009). Flow cytometry methods for the study of cell cycle parameters of planarian stem cells. Dev Dyn *238*, 1111-1117.

Kotogany E., Dudits D., Horvath G.V., and Ayaydin F. (2010). A rapid and robust assay for detection of S-phase cell cycle progression in plant cells and tissues by using ethynyl deoxyuridine. Plant Methods *6*.

Ladurner P., Egger B., De Mulder K., Pfister D., Kuales G., Salvenmoser W., and Schärer L. (2008). The stem cell system of the basal flatworm *Macrostomum lignano*. In Stem cells: from Hydra to man, Th.C.G.Bosch, ed. (Berlin - Heidelberg - New York: Springer), pp. 75-94.

Ladurner P., Rieger R., and Baguñà J. (2000). Spatial distribution and differentiation potential of stem cells in hatchlings and adults in the marine platyhelminth *Macrostomum* sp.: A bromodeoxyuridine analysis. Dev Biol *226*, 231-241.

Li F.S., Lu L.L., and Lu J.J. (2010). Identification and location of label retaining cells in mouse liver. J Gastroenterol *45*, 113-121.

Lucretti S., Nardi L., Nisini P.T., Moretti F., Gualberti G., and Dolezel J. (1999). Bivariate flow cytometry DNA/BrdUrd analysis of plant cell cycle. Methods Cell Sci *21*, 155-166.

Mitsuhashi J. (2002). Porifera. In Invertebrate tissue culture methods, (Tokyo: Springer), pp. 231-236.

Morshead C.M., Craig C.G., and van der K.D. (1998). *In vivo* clonal analyses reveal the properties of endogenous neural stem cell proliferation in the adult mammalian forebrain. Development *125*, 2251-2261.

Newmark P.A. and Sánchez Alvarado A. (2000). Bromodeoxyuridine specifically labels the regenerative stem cells of planarians. Dev Biol *220*, 142-153.

Nimeth K.T., Egger B., Rieger R., Salvenmoser W., Peter R., and Gschwentner R. (2007). Regeneration in *Macrostomum lignano* (Platyhelminthes): cellular dynamics in the neoblast stem cell system. Cell Tissue Res *327*, 637-646.

Nimeth K.T., Mahlknecht M., Mezzanato A., Peter R., Rieger R., and Ladurner P. (2004). Stem cell dynamics during growth, feeding, and starvation in the basal flatworm *Macrostomum* sp. (Platyhelminthes). Dev Dyn *230*, 91-99.

Nunez R. (2001). DNA measurement and cell cycle analysis by flow cytometry. Curr Issues Mol Biol *3*, 67-70.

Orford K.W. and Scadden D.T. (2008). Deconstructing stem cell self-renewal: genetic insights into cell-cycle regulation. Nat Rev Genet *9*, 115-128.

Otto F.J., Schumann J., and Zante J. (1990). High-resolution DNA flow cytometry in malignant melanoma. Cytom Suppl *4*, 55.

Pfister D., De Mulder K., Hartenstein V., Kuales G., Borgonie G., Marx F., Morris J., and Ladurner P. (2008). Flatworm stem cells and the germ line: Developmental and evolutionary implications of macvasa expression in *Macrostomum lignano*. Dev Biol *319*, 146-159.

Reddien P.W. and Sánchez Alvarado A. (2004). Fundamentals of planarian regeneration. Annu Rev Cell Dev Biol *20*, 725-757.

Sasaki K., Adachi S., Yamamoto T., Murakami T., Tanaka K., and Takahashi M. (1988). Effects of denaturation with HCl on the immunological staining of bromodeoxyuridine incorporated into DNA. Cytometry *9*, 93-96.

Schärer L., Knoflach D., Vizoso D.B., Rieger G., and Peintner U. (2007). Thraustochytrids as novel parasitic protists of marine free-living flatworms: *Thraustochytrium caudivorum* sp nov parasitizes *Macrostomum lignano*. Mar Biol *152*, 1095-1104.

Spradling A., Drummond-Barbosa D., and Kai T. (2001). Stem cells find their niche. Nature *414*, 98-104.

Tumbar T., Guasch G., Greco V., Blanpain C., Lowry W.E., Rendl M., and Fuchs E. (2004). Defining the epithelial stem cell niche in skin. Science *303*, 359-363.

Ulrich H. and Tarnok A. (2005). Quantification of cell-cycle distribution and mitotic index in Hydra by flow cytometry. Cell Prolif *38*, 63-75.

Verdoodt F., Bert W., Couvreur M., De Mulder K., and Willems M. (2012a). Proliferative response of the stem cell system during regeneration of the rostrum in *Macrostomum lignano* (Platyhelminthes). Cell Tissue Res *347*, 397-406.

Verdoodt F., Willems M., Mouton S., De Mulder K., Bert W., Houthoofd W., Smith III J., and Ladurner P. (2012b). Stem cells propagate their DNA by random segregation in the flatworm *Macrostomum lignano*. Plos One *7*, e30227.

Wagner D.E., Wang I.E., and Reddien P.W. (2011). Clonogenic neoblasts are pluripotent adult stem cells that underlie planarian regeneration. Science *332*, 811-816.

Wenemoser D. and Reddien P.W. (2010). Planarian regeneration involves distinct stem cell responses to wounds and tissue absence. Dev Biol *344*, 979-991.

Willems M., Boone M., Couvreur M., De Mulder K., Van Ranst J., Artois T., and Borgonie G. (2009). Use of freeze-cracking in ontogenetic research in *Macrostomum lignano* (Macrostomida, Rhabditophora). Dev Genes Evol *219*, 273-279.

Wilson A., Laurenti E., Oser G., van der Wath R.C., Blanco-Bose W., Jaworski M., Offner S., Dunant C.F., Eshkind L., Bockamp E., Lio P., MacDonald H.R., and Trumpp A. (2008). Hematopoietic stem cells reversibly switch from dormancy to self-renewal during homeostasis and repair. Cell *135*, 1118-1129.

Yanpaisan W., King N.J.C., and Doran P.M. (1998). Analysis of cell cycle activity and population dynamics in heterogeneous plant cell suspensions using flow cytometry. Biotechnol Bioeng *58*, 515-528.

Yanpaisan W., King N.J.C., and Doran P.M. (1999). Flow cytometry of plant cells with applications in large-scale bioprocessing. Biotechnol Adv *17*, 3-27.

6. General discussion

6.1. Adult stem cells in *M. lignano*

The research that has been done to extend the knowledge on neoblasts in *M. lignano* has demonstrated a remarkable and intriguing population of adult stem cells. Although we are far from understanding neoblasts to their full extent, important steps have already been made (see Chapter 1-5).

During this PhD, several approaches have been undertaken with the intention to further unravel the organization of the neoblast system and its dynamics. We have demonstrated kinetic heterogeneity within the neoblast population by providing evidence for the presence of a subpopulation of long-term quiescent neoblasts (Chapter 2). These quiescent neoblasts were found to be activated during the regeneration process (Chapter 5). The proliferative response of the neoblast population upon amputation of the rostrum was evaluated and revealed interesting differences to the situation described for tail plate regeneration (Chapter 3). Furthermore, this thesis has extended the information on the cell cycle in flatworms, by providing specific data on cell cycle distribution, and S-phase and total cell cycle duration (Chapter 4, 5). In Box 6.1 the main conclusions of Chapter 2 to 5 are assembled. These results will contribute to a better understanding of the biology of neoblasts, specifically, and adult stem cells, in general (see Chapter 6.2.).

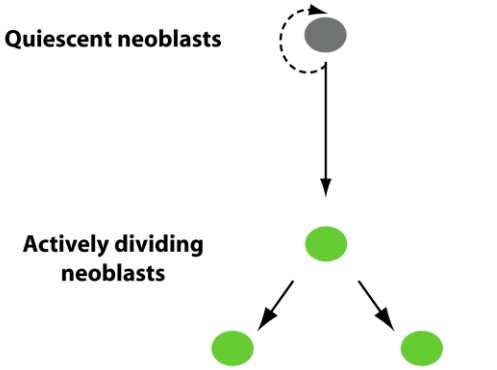

- set aside during development
- long- term survival
- distributed among actively cycling neoblasts
- relatively inactive during homeostasis
- activated during regeneration

- at least 2 subpopulations with diverse kinetics:
  fast-cycling neoblasts
  main population of slower cycling neoblasts
- main population:
  S-phase 13 h
  cell cycle ± 30 h
- increased proliferation activity during regeneratrion:
  - expansion of population (due to increased input from quiescent neoblasts)
  - shortening of G1-phase (and/or G2)
- during regeneration of the rostrum: mitotic division in the otherwise non-proliferative region anterior to the eyes

Box 6.1

6.1.1. Studying stem cell dynamics in *M. lignano*: an expanding toolbox

In this study, a range of techniques and quantification methods have been used and/or established to study the dynamics of stem cells, all having their specific merits and drawbacks. First, single labelling of S-phase cells (anti-BrdU) or mitotic cells (anti-phos-H3) was performed, conducting manual quantification of labelled cells (Chapter 3). These techniques have led to important information on stem cell proliferation during homeostasis and regeneration (Ladurner et al., 2000; Nimeth et al., 2004; Nimeth et al., 2007; Egger et al., 2009; Verdoodt et al., 2012). Subsequently, the resolution of the analysis of cell cycle kinetics considerably improved, by being able to perform double labelling with two different thymidine analogs (CldU, and IdU) (Chapter 2, 4). However,

visual evaluation of overlapping labels is difficult, and this required the establishment of a standardized method for automatic analysis of colocalization and quantification. The plug-in created for the freeware program Image J is a valuable addition to the toolbox for studying stem cells in *M. lignano,* especially for diverse future whole-mount double labelling techniques. Further methodological advances were made by introducing flow cytometry to study stem cell dynamics in *M. lignano* (Chapter 5). Using this instrument, single cells could be assigned to distinct cell cycle phases, based on their DNA content. Furthermore, flow cytometry offers the capability of rapid and accurate measurement of cell characteristics, and allows quantitative analysis of a combination of multiple characteristics (Shapiro, 1983; Darzynkiewicz et al., 2011), including a high number of replicates. In comparison, whole mount immunohistochemical labelling requires confocal imaging and quantification of individuals, one by one. On the other hand, whole-mount immunohistochemical labelling cannot be renounced completely, given its value for spatial information. For instance, whole mount labelling in Chapter 3 has demonstrated for the first time that neoblasts appear to be able to divide within in the rostrum upon amputation, as opposed to previous data on homeostasis, starvation and regeneration of the tail plate.

In the course of this study, diverse thymidine analogs (e.g. BrdU, IdU, CldU, and EdU) have been used to label cells in S-phase. The most commonly used analog, BrdU, was employed for most single labellings (chapter 2, 3). Double labelling was performed by means of IdU and CldU, because of the ability to separately visualize them, using commercially available antibodies (chapter 2, 4). Finally, the newly available analog EdU was used in several occasions due to its simplified visualization technique (chapter 2, 5). The gentle preparation conditions of EdU facilitate the preservation of both protein epitopes and the cells' integrity, which allowed combined use with the antibody for Macvasa protein. The concentrations that were used for a 30-minute pulse of each of the analogs, were based on previously published protocols. For extended pulse durations (e.g. LRC experiments) the

concentration was diluted with a factor 10 to 50, depending on the exact duration of the pulse and the following chase time.

Using diverse thymidine analogs, it is a critical requirement for qualitative, and even more for quantitative studies of cell proliferation, that at the used concentration, DNA synthesis is detected with the same efficiency. The data obtained during this study did not demonstrate dramatic differences in labelling efficiency. For instance, a comparison between BrdU and EdU was made in chapter 2, performing double labelling with both analogs (supplementary Figure 2.S1). Inidividuals were sequentially pulsed with EdU and BrdU, which resulted in complete overlap of both labels in the majority of labelled cells, and an expected amount of single labelled cells (as pulses could not be performed separately). Previous studies in mice have demonstrated similar results (Lentz et al., 2010; Zeng et al., 2010). In the same way, sequential pulses of CldU and IdU in chapter 4 demonstrate almost complete colocalization of CldU and IdU-labelled cells (94% $CldU^+$ /IdU^+ cells after 0 h chease). These data suggest that (1) BrdU and EdU, and (2) CldU and IdU staining methods detected DNA synthesis with the same efficiency.

6.1.2. Stem cell protection in *M. lignano*

Neoblasts have an extreme potential and plasticity in *M. lignano*, as shown by differentiation into diverse somatic and germ line cell types (Ladurner et al., 2000; Bode et al., 2006), their contribution to a remarkable regeneration capacity (Egger et al., 2006; Nimeth et al., 2007; Egger et al., 2009; Verdoodt et al., 2012), and recovery after chemical (Nimeth et al., 2004) and irradiation treatments (Pfister et al., 2007; De Mulder et al., 2010). Together with the high cell turnover during homeostasis, and the low incidence of problematic outcome, it is intriguingly clear that neoblasts must be subject to a rigorous control mechanism, or several thereof.

In Chapter 2, the highly debated immortal strand hypothesis was tested in *M. lignano*. This hypothesis states that stem cells, as a means to protect genome integrity, segregate their DNA strands in a non-random fashion (Cairns, 1975). The diverse *in vivo* approaches that were undertaken in Chapter 2, did not support non-random segregation of DNA strands.

Hence, it was concluded that the vast majority of neoblasts is not protected by 'immortal strands'. However, our label-retention analysis produced evidence for long-term cellular quiescence within a portion of the neoblast population. The long-term pulse chase experiments that were performed in this study (Chapter 2, 5) have demonstrated, for the first time, the large extent to which cellular quiescence is characteristic to a subset of neoblasts. Firstly, the foundation of a pool of quiescent neoblasts was shown to be formed, already during the earliest stages of development. And, secondly, these G0-arrested cells were shown to be long-lived since they were still present in animals that were chased for as long as six months, which is the median lifespan of *M. lignano* (Mouton et al., 2009). Consequently, it was concluded that cellular quiescence is an important aspect of the protection of the neoblast pool. Given the error prone nature of DNA replication, limiting the number of DNA synthesis rounds seems a logical solution (Cairns, 2002; Cairns, 2006). Using a hypothetical example, Cairns has elegantly measured that the presence of slow-cycling cells which replenish a population of faster cycling cells, significantly decreases the overall number of cell divisions in the population (Cairns, 2006). Nonetheless, it is clear that, despite these dormant cells, a large number of cell divisions do occur in *M. lignano* during homeostasis (Chapter 5), and even more during regeneration (Chapter 3). Next to this population of quiescent cells, *M. lignano* is known to possess a population of highly active neoblasts that account for the high cell turnover during homeostasis in this flatworm (for references see Ladurner et al., 2008). Hence, besides cellular quiescence, most likely complementary mechanisms exist to protect neoblasts, or a subset thereof. A wide range of diverse DNA repair mechanisms have been described in various model organisms (plants: Kimura and Sakaguchi, 2006; yeast: Lee et al., 2002; insects: Sekelsky et al., 2000; mammalia: Sancar et al., 2004; Lombard et al., 2005; Milyavsky et al., 2010), and defects in these mechanisms have been associated with stem cell abnormalities (Hanahan and Weinberg, 2000; Park and Gerson, 2005). In flatworms, DNA-repair mechanisms have been described, although information is limited (Boorstein et al., 1989; Hollenbach et al., 2011). For instance, in *S. meditterranea*, a homolog of a human DNA mismatch repair gene (*Smed-*

msh2) is expressed in neoblasts and some progeny (Hollenbach et al., 2011). The relevance of such mechanisms remains to be tested in *M. lignano*.

In conclusion, by demonstrating the significance of cellular quiescence in *M. lignano*, a considerable contribution is made to the study of mechanisms that guard the functionality of the neoblasts in flatworms.

6.1.3. Neoblasts, a heterogeneous population of adult stem cells

6.1.3.1. Subpopulations of stem cells with different cell cycle kinetics

Our results demonstrate that the adult neoblast pool exists of at least two subpopulations with different cell cycle kinetics: (1) a population of long-term quiescent neoblasts (Chapter 2) that can be induced to proliferate upon amputation (Chapter 5), and (2) actively cycling neoblasts with an S-phase duration of 13h and a total cell cycle duration of approximately 31h (Chapter 4,5). Furthermore, the presence of an additional subpopulation of fast-cycling cells was indicated in a previous study, in which a limited number of cells was suggested to cycle through the whole S- and G2-phase in merely two hours (Nimeth et al., 2007). Additionally, the presence of cells with a significant longer G2-phase compared to the main cycling population has been suggested as well (Nimeth et al., 2004). However, in a later publication this observation was attributed to the fact that animals were intentionally starved when the experiments were performed (Nimeth et al., 2007). Therefore, the presence of a subpopulation with a longer G2 is most likely an environmental effect, rather than that these cells make up a distinct subpopulation with different cell cycle kinetics. The fast entrance into M-phase, caused by feeding after a prolonged starvation period, is a confirmation thereof (Nimeth et al., 2004). Moreover, in other model systems, cell cycle arrest in G2 has often been linked to feeding status as well (Cameron and Cleffmann, 1964; Baguñà, 1976).

Taken together, it can be concluded that the neoblasts system in *M. lignano* is subdivided in three populations with distinct cell cycle kinetics: quiescent, main cycling, and fast cycling cells.

In contrast, neoblasts of the planarian flatworm *Schmidtea mediterranea* have long been considered to cycle regularly, without indications for a significant subset of slow cycling or arrested neoblasts. This conclusion was based on the fact that after three days of continuous pulsing with BrdU, ~99% of all neoblasts were labelled (Newmark and Sánchez Alvarado, 2000). However, it should be noted that neoblasts were identified based on their morphology in cell suspensions, and a more accurate way to distinguish neoblasts from differentiated cells might lead to re-interpretation of these results. More recently, the presence of a distinct population of G0-arrested cells was suggested in a related planarian flatworm, *Dugesia japonica*. This was demonstrated in several studies, based on a combination of gene expression data of stem cell related genes (*djpiwi* and *djpcna*), the inability to incorporate BrdU during continuous pulsing, and a higher radiation tolerance of these cells (Orii et al., 2005; Sato et al., 2006; Rossi et al., 2006; Higuchi et al., 2007; Salvetti et al., 2009). Interestingly, quiescent neoblasts seemed to be clustered and localized only at the pre-pharyngeal dorsal midline, while active neoblasts are dispersed throughout the body (with the exception of the pharynx region, and the region anterior to the eyes) (Orii et al., 2005; Rossi et al., 2006; Salvetti et al., 2009). However, in our study quiescent cells in *M. lignano* could not be distinguished from actively cycling neoblasts based on their distribution. Instead, our Macvasa-LRC experiment (Chapter 2), indicated that quiescent stem cells are dispersed among active neoblasts, this within the bilateral pattern that holds all cycling cells. Thus, based on this discrepancy, species-specific differences in the organization of the neoblast system in flatworms should be taken into account. This demonstrates the added knowledge that might come from studying stem cells in different flatworm models.

6.1.3.2. Subpopulations of stem cells with a different functionality?

It is not known if the kinetic heterogeneity of neoblasts reflects functional heterogeneity as well. Although this largely remains to be elucidated for *M. lignano*, different subpopulations reflecting diverse functionality and potentiality is a common aspect of stem cell populations.

Classically, stem cell pools have been believed to be organized in a hierarchical structure, although this hypothesis is not generally accepted (Quesenberry, 2006). Nevertheless, an interesting example of such an organization is delivered by —probably the best studied stem cell system— the hematopoietic system in mammals (reviewed in Trumpp et al., 2010). In this well documented stem cell system, a limited number of stem cells that are mostly dormant and have high repopulation potential upon transplantation *in vivo* are observed to fill up the top layer of the hierarchy (Cheshier et al., 1999). These cells replenish a series of progenitor cells that are shorter-lived, have a more limited potential, and are often rapidly-dividing (Passegué et al., 2005). Other examples of mammalian stem cell systems with a similar organization are the hair follicle and the gut epithelium (reviewed in Fuchs, 2009). When applying such an organization to the stem cell population in *M. lignano*, the quiescent stem cells, which are demonstrated in our study, are the most appropriate candidates to fill the highest spots in the hierarchy. The kinetic properties of these cells demonstrate striking similarities with occupants of these regions in other stem cell systems (Mohrin et al., 2010): (1) their largely inactive state during homeostasis, which can be lifted during regeneration (Chapter 2, 5), and (2) their long-term survival, as shown by the long chase times performed in Chapter 2. Following this logic, these quiescent neoblasts likely represent 'true' stem cells, while actively dividing neoblasts are the transit amplifying cells (TACs), filling the lower spots on the ladder of the hierarchy. Based on numerous examples of stem cell systems in other organisms, these TACs likely have a more limited potential and responsible for the high rate of cell renewal in *M. lignano*.

Assuming that quiescent neoblasts have the broadest potential within *M. lignano*, they are primary candidates to test pluripotency of individual cells in *M. lignano*. In the planarian

flatworm *S. mediterranea*, tangible evidence for pluripotency of individual neoblasts, so-called clonogenic neoblasts or cNeoblasts, was demonstrated only very recently by Wagner et all (2011). These cNeoblasts had a body wide distribution. Unfortunately, the cell cycle dynamics of cNeoblasts in normal conditions are so far not known. Hence, precise data are absent to evaluate how these pluripotent neoblasts in *S. mediterranea* relate to the quiescent neoblasts in *M. lignano*. However, worth mentioning is that these cNeoblasts were selected based on their higher irradiation tolerance compared to other neoblasts, which might be linked to cell cycle inactivity (and thus possibly cellular quiescence).

Nevertheless, although the cell cycle dynamics of quiescent and active neoblast subpopulations fit the hierarchy-hypothesis, it is too early to jump to conclusions, given that the relation between both subpopulations, and the potential of the cells within, is still obscure. Admittedly, we are still in the starting blocks when it comes to fully understanding how stem cells are regulated to generate distinct lineages in *M. lignano*. However, the clear subdivision in the neoblast pool on the level of cell cycle kinetics, is an intriguing aspect to be reckoned with in future studies.

6.1.4. The cell cycle in *M. lignano*: advances and future prospects

In this study, we were able to determine specific parameters of the cell cycle of the main cycling population. In Chapter 4, the S-phase duration was measured to be approximately 13h. In Chapter 5, based on the progression of an EdU-labelled cohort of cells through the cell cycle, the total cell cycle duration was estimated to be approximately 31h. The G2-phase duration was evaluated in previous studies (Nimeth et al., 2004; Nimeth et al., 2007). It was concluded that the minimal duration of G2 is 2h, but the majority of cells need 4h to traverse the G2-phase and pass from S- to M-phase.

What is the added value of knowing specific phase durations for the study of the neoblast pool in *M. lignano*? Firstly, these parameters serve as a guideline to define experimental designs of future studies that include cell proliferation and cell turnover. Secondly,

knowing the parameters of the cell cycle during normal conditions (homeostasis, and fed *ad libitum*), is pivotal to evaluate changes in the dynamics of cycling cells. This is relevant both from a biological as well as a biomedical point of view. The biological relevance includes (1) the possibility to test the effect of environmental changes, such as regeneration or starvation, and (2) contributing to the study of cell cycle control. For instance, the effect of regeneration (1) on cell cycle dynamics was part of this thesis. In Chapter 3, analysis of S-phase numbers demonstrated an increase, which was highest at 3-5 days after amputation, indicating changes in the dynamics of the neoblast pool. Subsequently, the exact nature of these changes was studied by comparing with the situation during homeostasis. Amputation did not affect the duration of the S-phase (Chapter 4), yet it caused an increased cell cycle activity in the population of quiescent neoblasts and affected the duration of one or both gap phases of the cell cycle (Chapter 5). For cell cycle control (2), the relevance of information on cell cycle parameters was demonstrated by an interesting study in *Drosophila* (Bettencourt-Dias et al., 2004). In this study, the cell cycle function of diverse protein kinases* was evaluated by performing RNAi*-knockdown of these genes, followed by evaluation of the cell cycle phenotype (e.g. delays in the progression through specific cell cycle phases). This example illustrates that knowledge on cell cycle parameters (Chapter 4, 5) will contribute to future studies on the regulation of stem cell proliferation in this flatworm.

From a biomedical point of view, *M. lignano* is a powerful model to test the effect of environmental cues on stem cell proliferation, because its high abundance of cycling adult stem cells and the fact that they can be studied *in vivo*. To this end, the acquired knowledge on cell cycle parameters greatly increases the resolution of such studies since it is possible to pinpoint the disturbance of cell cycle progression.

Although important advances have already been made in the characterization of cell cycle parameters in *M. lignano*, some questions remain unanswered. For example, the M-phase and G1-phase duration could not be determined in our bi-parametric EdU/DAPI experiment in Chapter 5. This, because of the inability to separately distinguish cells in S-phase, a drawback of fixed cell suspensions that are necessary for visualization of the EdU-

label. Hence, future approaches should include one or more antibodies –additional to EdU–to distinguish cells in a particular phase (e.g. mitotic cells, using anti-phos-H3).

Another interesting approach would be to determine the cell cycle duration of quiescent cells that are induced to cycle. So far, this was not possible due to the fact that our label-retention approach does not only result in labelled quiescent neoblasts, but also labelled progeny of these quiescent cells. Therefore, future endeavors should include the use of a marker that allows resolving quiescent neoblasts from their progeny.

6.1.5. Quiescent neoblasts in *M. lignano*: advances and future prospects

The advances on the knowledge of quiescent neoblasts in the current study have already been described in previous paragraphs and will not be repeated here. However, our results suggest a highly important role of these cells as potential 'true stem cells' in *M. lignano* (see 1.1. and 1.2. in this chapter), hence, these cells deserve intensive attention in future *M. lignano* studies. Consideration of other stem cell systems suggests that future progress will require more molecular markers to identify and fractionate subsets of neoblasts (Slack, 2011). Methods based on flow cytometry and FACS have been shown to result in a major breakthrough in a variety of vertebrate and invertebrate stem cell systems (Orford and Scadden, 2008 and references therein; Slack, 2011 and references therein). However, notwithstanding the current absence of appropriate markers, some problems can already be tackled, as described below.

Despite the elaborate pulse scheme that was conducted in Chapter 2, the onset of cellular quiescence could not be pinpointed to one specific developmental window. Instead, all 24-hour pulse-periods that were performed during development resulted in label-retaining neoblasts. It should be mentioned that a pulse-period that results in LRCs does not necessarily overlap with the nascence of quiescence. It merely indicates that at the time of pulsing, these cells were in a proliferative state, possibly after a preceding period of cellular quiescence. Still, our observations in chapter 2 strongly suggest that neoblasts are

set aside in a dormant state, not at one particular moment but at regular time points during development. However, to confirm this hypothesis, information on the kinetics of label-decay is needed. A second consequence of all pulses resulting in label-retaining neoblasts was the impossibility to determine the average size of the quiescent neoblast population. Knowledge on the onset of cellular quiescence as well as the size of the population could easily be answered given the availability of a specific marker for this distinct subpopulation of neoblasts. However, other approaches to distinguish quiescent neoblasts from active neoblasts remain to be tested. For instance, in the planarian flatworm *Dugesia japonica* a subpopulation of neoblasts (so-called type B) was demonstrated based on distinct ultrastructural and morphometrical characteristics (Higuchi et al., 2007). Compared to the majority of neoblasts (so-called type A), type B neoblasts demonstrated a smaller size, fewer chromatoid bodies*, and a heterochromatin* rich nucleus. Higuchi et all (2007) hypothesized that these cells might be a distinct population of cells in G0. This hypothesis could be tested in *M. lignano,* by combining our label-retention assay with electron microscopy. From our Macvasa-LRC experiment in Chapter 2, we have indications that label-retaining Macvasa^{+} cells had, indeed, a lower number of chromatoid bodies, compared to other Macvasa^{+} cells (See Figure 2.4). However, this should be tested in more detail. In a previous study in *M. lignano*, slow cycling or cell cycle arrested neoblasts have been identified using electron microscopy (Bode et al., 2006). But, in the latter, a study of the number of chromatoid bodies was not included. In conclusion, if quiescent neoblasts really differ on ultrastructural level and/or morphometrically from active neoblasts, these characteristics can be used in flow cytometric analysis to distinguish between both types of neoblasts.

Another interesting venue for future research would be to test whether quiescent neoblasts that were induced to divide during regeneration, return to a dormant state afterwards. The fact that these cells are protected by cellular inactivity suggests that they are of special importance to the organism. Therefore, it seems likely that they do resume cellular inactivity in order to provide long-term self-renewal. Our pulse-chase experiments in chapter 2, combined with information on other stem cell systems (Nowak et al., 2008),

strongly suggest that this subset of neoblasts is founded during development. During adulthood, this set-aside population occasionally proliferates to contribute to the cycling neoblast population (chapter 2, 5). Assuming that none of the daughter cells re-enters quiescence seems counterintuitive as it would indicate that self-renewal is not sustained, and these cells become susceptible to stem cell exhaustion (Orford and Scadden, 2008). On the other hand, depletion of the quiescent stem cell pool might be linked to ageing in *M. lignano*. The validity of these hypotheses is definitely an important consideration for future research. One way to tackle this problem could be to 'challenge' the population of LRCs by repeated amputation and regeneration.

6.2. Universal relevance of stem cell research in flatworms

The ability of stem cells to self-renew and to divide, proliferate and differentiate is the key to their therapeutic efficacy (Ho 2005). However, strategies to manipulate stem cell division and differentiation require a clearer understanding of these processes *in vivo* (Cheng, 2004), which can be best obtained through experimentation. Laboratory studies of stem cells enable scientists to learn about the essential properties of these cells and their differences from specialized cell types. Therefore, model organisms are essential for such *in vivo* interrogations, and stand to provide us with better insight to answer fundamental questions (Spradling et al., 2006; Sánchez Alvarado and Tsonis, 2006; Bosch, 2009).

With this in mind, flatworms have gained attention as a powerful and also an intellectually attractive system to study stem cells and their proliferation. The ultimate argument to explain their potential as model organisms is, simply, the significant presence of adult stem cells that seem to be champions at fulfilling their 'job'. Therefore, flatworms provide a unique way to study mechanisms that enable stem cells to generate appropriate numbers and types of differentiated cells during steady state and repair. In combination with the accessibility of these cells for *in vivo* studies, these organisms have shown to be highly

informative in the field of stem cell biology (Gentile et al., 2011). In particular, flatworms have the potential to increase information on human stem cells. For example, analysis of mRNA microarray profiles of planarian neoblasts showed that >75% of their enriched mRNAs (with known mammalian homologs) could be classified into categories of protein biosynthesis, RNA binding, transcription, and DNA binding (Eisenhoffer et al., 2008). All four of these categories represent intracellular processes that have been shown to be enriched in a variety of stem cells isolated from both mouse and human organs and embryos (Doherty et al., 2008). Furthermore, as observed in flatworms, Wnt signaling is required for the patterning of regeneration in the limited regeneration capacity demonstrated in some mammalian organs (e.g. hair follicle regeneration in response to punch biopsy wounds in skin) (Stappenbeck and Miyoshi, 2009). Additional to being informative on human biology, flatworm stem cell research can contribute to improving human health (Sánchez Alvarado et al., 2003; Reddien et al., 2005; Sánchez Alvarado, 2007; Pellettieri and Sánchez Alvarado, 2007; Pearson and Sánchez Alvarado, 2009; Gentile et al., 2011). This promise has been exemplified by the range of planarian genes that are related to human disease (Reddien et al., 2005; Gentile et al., 2011) and tumor suppression (Pearson and Sánchez Alvarado, 2010). For example several of the stem cell genes that have been identified in flatworms (e.g. *piwi, nucleostemin, mi-2*) were found to be ectopically upregulated in human cancers (Grochola et al., 2008; Li et al., 2010; Ye et al., 2008; Fu et al., 2011). However, when comparing stem cell systems between different organisms, and even within organisms, caution is strongly advised. Besides fundamental similarities between flatworm and mammalian stem cells, of which some have been described here, some diverging characteristics have been observed as well (Table 6.1).

Flatworm stem Cells:	Mammalian stem cells:
- Pluripotency in adult	- Pluripotency in embryo, multipotency in adult
- One stem cell compartment as a source for somatic and germ line cells.	- Several stem cell systems in one organism.
- Quiescent stem cells, which are set aside during early stages of development and are long lived (up to the median life span) in the adult worm.	- Cellular quiescence in adult stem cells. No evidence available on entrance into cellular quiescence during such early developmental stages.
- Extreme regeneration capacity, based upon the stem cell system.	- Non-existent to limited (e.g. liver, hair follicles, intestinal crypts) regeneration capacity in some organs.
- Blastema formation (build-up of undifferentiated cells)	- No blastema formation.

Table 6.1

Thus, although a conclusion based on one stem cell system cannot immediately be extrapolated to another one without further research, current knowledge on stem cell biology has been pushed forward by complementary analysis in diverse model systems. Organisms become models when they support sustainable opportunities with uncompromising experimental rigor and ease of use (Bosch, 2009). With this in mind, flatworms can provide a valuable contribution to the field of stem cell biology.

Significant progress has already been made within flatworm stem cell research, spurred on by the genome sequencing of *Schmidtea mediterranea* (Sánchez Alvarado et al., 2003) and *M. lignano* (annotation in progress), and the availability of experimental tools, including immunohistochemical* staining techniques (Newmark and Sánchez Alvarado, 2000; Ladurner et al., 2000; Ladurner et al., 2005) (Chapter 2 and 5), flow cytometry (Chapter 5) (Ermakov et al., 2011), FACS* (Eisenhoffer et al., 2008), irradiation (Salvetti et al., 2009; De Mulder et al., 2010), qPCR* (Plusquin et al., 2011), and RNAi* (Sánchez Alvarado and

Newmark, 1999; Newmark, 2005; Reddien et al., 2005; Pfister et al., 2008; De Mulder et al., 2009). The advances that were made in this study, both on a technical and informative level, add up to the already fascinating field of stem cell research. Undoubtedly, new discoveries await us.

6.3. References

Baguñà J. (1976). Mitosis in intact and regenerating planarian *Dugesia mediterranea* n.sp. 1. mitotic studies during growth, feeding and starvation. J Exp Zool *195*, 53-64.

Bettencourt-Dias M., Giet R., Sinka R., Mazumdar A., Lock W.G., Balloux F., Zafiropoulos P.J., Yamaguchi S., Winter S., Carthew R.W., Cooper M., Jones D., Frenz L., and Glover D.M. (2004). Genome-wide survey of protein kinases required for cell cycle progression. Nature *432*, 980-987.

Bode A., Salvenmoser W., Nimeth K., Mahlknecht M., Adamski Z., Rieger R.M., Peter R., and Ladurner P. (2006). Immunogold-labeled S-phase neoblasts, total neoblast number, their distribution, and evidence for arrested neoblasts in *Macrostomum lignano* (Platyhelminthes, Rhabditophora). Cell Tissue Res *325*, 577-587.

Boorstein R.J., Chiu L.N., and Teebor G.W. (1989). Phylogenetic evidence of a role for 5-hydroxymethyluracil-DNA glycosylase in the maintenance of 5-methylcytosine in DNA. Nucleic Acids Res *17*, 7653-7661.

Bosch T.C.G. (2009). Hydra and the evolution of stem cells. Bioessays *31*, 478-486.

Cairns J. (1975). Mutation selection and natural history of cancer. Nature *255*, 197-200.

Cairns J. (2002). Somatic stem cells and the kinetics of mutagenesis and carcinogenesis. Proc Natl Acad Sci U S A *99*, 10567-10570.

Cairns J. (2006). Cancer and the immortal strand hypothesis. Genetics *174*, 1069-1072.

Cameron I.L. and Cleffmann G. (1964). Initiation of mitosis in relation to the cell cycle following feeding of starved chickens. J Cell Biol *21*, 169-174.

Cheng T. (2004). Cell cycle inhibitors in normal and tumor stem cells. Oncogene *23*, 7256-7266.

Cheshier S.P., Morrison S.J., Liao X.S., and Weissman I.L. (1999). *In vivo* proliferation and cell cycle kinetics of long-term self-renewing hematopoietic stem cells. Proc Natl Acad Sci U S A *96*, 3120-3125.

Darzynkiewicz Z., Traganos F., Zhao H., Halicka H.D., and Li J.W. (2011). Cytometry of DNA replication and RNA synthesis: Historical perspective and recent advances based on "Click Chemistry". Cytometry A *79A*, 328-337.

De Mulder K., Kuales G., Pfister D., Egger B., Seppi T., Eichberger P., Borgonie G., and Ladurner P. (2010). Potential of *Macrostomum lignano* to recover from gamma-ray irradiation. Cell Tissue Res *339*, 527-542.

De Mulder K., Pfister D., Kuales G., Egger B., Salvenmoser W., Willems M., Steger J., Fauster K., Micura R., Borgonie G., and Ladurner P. (2009). Stem cells are differentially regulated during development, regeneration and homeostasis in flatworms. Dev Biol *334*, 198-212.

Doherty J.M., Geske M.J., Stappenbeck T.S., and Mills J.C. (2008). Diverse Adult Stem Cells Share Specific Higher-Order Patterns of Gene Expression. Stem Cells *26*, 2124-2130.

Egger B., Gschwentner R., Hess M.W., Nimeth K.T., Adamski Z., Willems M., Rieger R., and Salvenmoser W. (2009). The caudal regeneration blastema is an accumulation of rapidly proliferating stem cells in the flatworm *Macrostomum lignano*. BMC Dev Biol *9*. doi:10.1186/1471-213X-9-41.

Egger B., Ladurner P., Nimeth K., Gschwentner R., and Rieger R. (2006). The regeneration capacity of the flatworm *Macrostomum lignano* - on repeated regeneration, rejuvenation, and the minimal size needed for regeneration. Dev Genes Evol *216*, 565-577.

Eisenhoffer G.T., Kang H., and Sánchez Alvarado A. (2008). Molecular analysis of stem cells and their descendants during cell turnover and regeneration in the planarian *Schmidtea mediterranea*. Cell Stem Cell *3*, 327-339.

Ermakov A.M., Ermakova O.N., Kudravtsev A.A., and Kreshchenko N.D. (2011). Study of planarian stem cell proliferation by means of flow cytometry. Mol Biol Rep *39*, 3073-3080.

Fu J.J., Qin L., He T., Qin J., Hong J., Wong J.M., Liao L., and Xu J.M. (2011). The TWIST/Mi2/NuRD protein complex and its essential role in cancer metastasis. Cell Res *21*, 275-289.

Fuchs E. (2009). The tortoise and the hair: Slow-cycling cells in the stem cell race. Cell *137*, 811-819.

Gentile L., Cebria F., and Bartscherer K. (2011). The planarian flatworm: an *in vivo* model for stem cell biology and nervous system regeneration. Dis Model Mech *4*, 12-19.

Grochola L.F., Greither T., Taubert H., Moller P., Knippschild U., Udelnow A., Henne-Bruns D., and Wurl P. (2008). The stem cell-associated Hiwi gene in human adenocarcinoma of the pancreas: expression and risk of tumour-related death. Br J Cancer *99*, 1083-1088.

Hanahan D. and Weinberg R.A. (2000). The hallmarks of cancer. Cell *100*, 57-70.

Higuchi S., Hayashi T., Hori I., Shibata N., Sakamoto H., and Agata K. (2007). Characterization and categorization of fluorescence activated cell sorted planarian stem cells by ultrastructural analysis. Dev Growth Differ *49*, 571-581.

Hollenbach J.P., Resch A.M., Palakodeti D., Graveley B.R., and Heinen C.D. (2011). Loss of DNA mismatch repair imparts a selective advantage in planarian adult stem cells. Plos One *6*, e21808.

Kimura S. and Sakaguchi K. (2006). DNA repair in plants. Chem Rev *106*, 753-766.

Ladurner P., Egger B., De Mulder K., Pfister D., Kuales G., Salvenmoser W., and Schärer L. (2008). The stem cell system of the basal flatworm *Macrostomum lignano*. In Stem cells: from Hydra to man, Th.C.G.Bosch, ed. (Berlin - Heidelberg - New York: Springer), pp. 75-94.

Ladurner P., Pfister D., Seifarth C., Schärer L., Mahlknecht M., Salvenmoser W., Gerth R., Marx F., and Rieger R. (2005). Production and characterisation of cell- and tissue-specific monoclonal antibodies for the flatworm *Macrostomum* sp. Histochem Cell Biol *123*, 89-104.

Ladurner P., Rieger R., and Baguñà J. (2000). Spatial distribution and differentiation potential of stem cells in hatchlings and adults in the marine platyhelminth *Macrostomum* sp.: A bromodeoxyuridine analysis. Dev Biol *226*, 231-241.

Lee S.E., Bressan D.A., Petrini J.H.J., and Haber J.E. (2002). Complementation between N-terminal *Saccharomyces cerevisiae* mre11 alleles in DNA repair and telomere length maintenance. Dna Repair *1*, 27-40.

Lentz S.I., Edwards J.L., Backus C., Mclean L.L., Haines K.M., and Feldman E.L. (2010). Mitochondrial DNA (mtDNA) Biogenesis: Visualization and Duel Incorporation of BrdU and EdU Into Newly Synthesized mtDNA In Vitro. J Histochem Cytochem *58*, 207-218.

Li S., Meng L., Zhu C.H., Wu L., Bai X.Y., Wei J.C., Lu Y.P., Zhou J.F., and Ma D. (2010). The universal overexpression of a cancer testis antigen hiwi is associated with cancer angiogenesis. Oncol Rep *23*, 1063-1068.

Lombard D.B., Chua K.F., Mostoslavsky R., Franco S., Gostissa M., and Alt F.W. (2005). DNA repair, genome stability, and aging. Cell *120*, 497-512.

Milyavsky M., Gan O.I., Trottier M., Komosa M., Tabach O., Notta F., Lechman E., Hermans K.G., Eppert K., Konovalova Z., Ornatsky O., Domany E., Meyn M.S., and Dick J.E. (2010). A distinctive DNA damage response in human hematopoietic stem cells reveals an apoptosis-independent role for p53 in self-renewal. Cell Stem Cell *7*, 186-197.

Mohrin M., Bourke E., Alexander D., Warr M.R., Barry-Holson K., Le Beau M.M., Morrison C.G., and Passegue E. (2010). Hematopoietic stem cell quiescence promotes error-prone DNA repair and mutagenesis. Cell Stem Cell *7*, 174-185.

Mouton S., Willems M., Back P., Braeckman B.P., and Borgonie G. (2009). Demographic analysis reveals gradual senescence in the flatworm *Macrostomum lignano*. Front Zool *6*, art nr 15.

Newmark P.A. (2005). Opening a new can of worms: a large-scale RNAi screen in planarians. Dev Cell *8*, 623-624.

Newmark P.A. and Sánchez Alvarado A. (2000). Bromodeoxyuridine specifically labels the regenerative stem cells of planarians. Dev Biol *220*, 142-153.

Nimeth K.T., Egger B., Rieger R., Salvenmoser W., Peter R., and Gschwentner R. (2007). Regeneration in *Macrostomum lignano* (Platyhelminthes): cellular dynamics in the neoblast stem cell system. Cell Tissue Res *327*, 637-646.

Nimeth K.T., Mahlknecht M., Mezzanato A., Peter R., Rieger R., and Ladurner P. (2004). Stem cell dynamics during growth, feeding, and starvation in the basal flatworm *Macrostomum* sp. (Platyhelminthes). Dev Dyn *230*, 91-99.

Nowak J.A., Polak L., Pasolli H.A., and Fuchs E. (2008). Hair follicle stem cells are specified and function in early skin morphogenesis. Cell Stem Cell *3*, 33-43.

Orford K.W. and Scadden D.T. (2008). Deconstructing stem cell self-renewal: genetic insights into cell-cycle regulation. Nat Rev Genet *9*, 115-128.

Orii H., Sakurai T., and Watanabe K. (2005). Distribution of the stem cells (neoblasts) in the planarian *Dugesia japonica*. Dev Genes Evol *215*, 143-157.

Park Y. and Gerson S.L. (2005). DNA repair defects in stem cell function and aging. Annu Rev Med *56*, 495-508.

Passegué E., Wagers A.J., Giuriato S., Anderson W.C., and Weissman I.L. (2005). Global analysis of proliferation and cell cycle gene expression in the regulation of hematopoietic stem and progenitor cell fates. J Exp Med *202*, 1599-1611.

Pearson B.J. and Sánchez Alvarado A. (2009). Regeneration, Stem Cells, and the Evolution of Tumor Suppression. Cold Spring Harb Symp Quant Biol.

Pearson B.J. and Sánchez Alvarado A. (2010). A planarian p53 homolog regulates proliferation and self-renewal in adult stem cell lineages. Development *137*, 213-221.

Pellettieri J. and Sánchez Alvarado A. (2007). Cell turnover and adult tissue homeostasis: From humans to planarians. Annu Rev Genet *41*, 83-105.

Pfister D., De Mulder K., Hartenstein V., Kuales G., Borgonie G., Marx F., Morris J., and Ladurner P. (2008). Flatworm stem cells and the germ line: Developmental and evolutionary implications of macvasa expression in *Macrostomum lignano*. Dev Biol *319*, 146-159.

Pfister D., De Mulder K., Philipp I., Kuales G., Hrouda M., Eichberger P., Borgonie G., Hartenstein V., and Ladurner P. (2007). The exceptional stem cell system of *Macrostomum lignano*: Screening for gene expression and studying cell proliferation by hydroxyurea treatment and irradiation. Front Zool *4*, 9.

Plusquin M., DeGheselle O., Cuypers A., Geerdens E., Van Roten A., Artois T., and Smeets K. (2011). Reference genes for qPCR assays in toxic metal and salinity stress in two flatworm model organisms. Ecotoxicology *21*, 475-484.

Quesenberry P.J. (2006). The continuum model of marrow stem cell regulation. Curr Opin Hematol *13*, 216-221.

Reddien P.W., Bermange A.L., Murfitt K.J., Jennings J.R., and Sánchez Alvarado A. (2005). Identification of genes needed for regeneration, stem cell function, and tissue homeostasis by systematic gene perturbation in planaria. Dev Cell *8*, 635-649.

Rossi L., Salvetti A., Lena A., Batistoni R., Deri P., Pugliesi C., Loreti E., and Gremigni V. (2006). DjPiwi-1, a member of the PAZ-Piwi gene family, defines a subpopulation of planarian stem cells. Dev Genes Evol *216*, 335-346.

Salvetti A., Rossi L., Bonuccelli L., Lena A., Pugliesi C., Rainaldi G., Evangelista M., and Gremigni V. (2009). Adult stem cell plasticity: Neoblast repopulation in non-lethally irradiated planarians. Dev Biol *328*, 305-314.

Sancar A., Lindsey-Boltz L.A., Unsal-Kacmaz K., and Linn S. (2004). Molecular mechanisms of mammalian DNA repair and the DNA damage checkpoints. Annu Rev Biochem *73*, 39-85.

Sánchez Alvarado A. (2007). Stem cells and the planarian *Schmidtea mediterranea*. C R Biol *330*, 498-503.

Sánchez Alvarado A. and Newmark P.A. (1999). Double-stranded RNA specifically disrupts gene expression during planarian regeneration. Proc Natl Acad Sci U S A *96*, 5049-5054.

Sánchez Alvarado A., Reddien P.W., Newmark P.A., and Nusbaum C. (2003). Proposal for the sequencing of a new target genome: White paper for a planarian genome project. http://www.genome.gov/Pages/Research/Sequencing/SeqProposals/PlanarianSEQ.pdf

Sánchez Alvarado A. and Tsonis P.A. (2006). Bridging the regeneration gap: genetic insights from diverse animal models. Nat Rev Genet *7*, 873-884.

Sato K., Shibata N., Orii H., Amikura R., Sakurai T., Agata K., Kobayashi S., and Watanabe K. (2006). Identification and origin of the germline stem cells as revealed by the expression of nanos-related gene in planarians. Dev Growth Differ *48*, 615-628.

Sekelsky J.J., Brodsky M.H., and Burtis K.C. (2000). DNA Repair in Drosophila. J Cell Biol *150*, F31-F36.

Shapiro H.M. (1983). Multistation multiparameter flow cytometry: a critical review and rationale. Cytometry *3*, 227-243.

Slack J.M. (2011). Planarian pluripotency. Science *332*, 799-800.

Spradling A., Ganetsky B., Hieter P., Johnston M., Olson M., Orr-Weaver T., Rossant J., Sanchez A., and Waterston R. (2006). New roles for model genetic organisms in understanding and treating human disease: Report from the 2006 Genetics Society of America Meeting. Genetics *172*, 2025-2032.

Stappenbeck T.S. and Miyoshi H. (2009). The role of stromal stem cells in tissue regeneration and wound repair. Science *324*, 1666-1669.

Trumpp A., Essers M., and Wilson A. (2010). Awakening dormant haematopoietic stem cells. Nat Rev Immunol *10*, 201-209.

Verdoodt F., Bert W., Couvreur M., De Mulder K., and Willems M. (2012). Proliferative response of the stem cell system during regeneration of the rostrum in *Macrostomum lignano* (Platyhelminthes). Cell Tissue Res *347*, 397-406.

Wagner D.E., Wang I.E., and Reddien P.W. (2011). Clonogenic neoblasts are pluripotent adult stem cells that underlie planarian regeneration. Science *332*, 811-816.

Ye F., Zhou C., Cheng Q., Shen J., and Chen H. (2008). Stem-cell-abundant proteins Nanog, Nucleostemin and Musashi1 are highly expressed in malignant cervical epithelial cells. Bmc Cancer *8*, 108.

Zeng C., Pan F., Jones L.A., Lim M.M., Griffin E.A., Sheline Y.I., Mintun M.A., Holtzman D.M., and Mach R.H. (2010). Evaluation of 5-ethynyl-2'-deoxyuridine staining as a sensitive and reliable method for studying cell proliferation in the adult nervous system. Brain Res *1319*, 21-32.

7. Appendix

7.1. Glossary

- **Cell turnover:** a cycle of cell death and cell renewal that contributes to an organ's normal tissue homeostasis (Pellettieri and Sánchez Alvarado, 2007).

- **Chromatoid body:** a structure similar to nuage, which is found in the stem cells (somatic + germ line) of flatworms. Nuage is described in a broad variety of species as an evolutionary conserved, germ line specific, perinuclear organelle. During the process of cell differentiation, the number of chromatoid bodies is progressively reduced. Molecular biological studies have shown that chromatoid bodies contain RNA. Their function is unclear. (Pfister et al., 2008)

- **FACS:** fluorescence activated cell sorting. A method designed to analyze cell suspensions, allowing the physical separation of subpopulations of cells (on single cell level) based on structural or fluorescent characteristics of cells.

- **Heterochromatin:** condensed form of DNA (as opposed to euchromatin, which is less tightly packed).

- **Immunohistochemistry:** a laboratory technique, mostly performed on tissue sections, that uses antibodies that target specific antigens in cells/tissues via specific epitopes. These bound antibodies can then be detected using different methods (e.g., enzyme-, or fluorochrome mediated detection).

- **Parenchym:** other name for 'mesenchym' in flatworms.

- **PCNA:** proliferating cell nuclear antigen. PCNA, or cyclins are a group of proteins, which accumulate progressively through interphase (G1, S, and G2) and disappear at the end of mitosis. These proteins are now known to be components of DNA replication machinery, and are essential for completion of the cell cycle.

- **Planarian**: freshwater triclad flatworm.

- **Protein kinases:** a well defined family of proteins, characterized by the presence of a common kinase catalytic domain and playing a significant role in many important cellular processes, such as proliferation, maintenance of cell shape, apoptosis.

- **qPCR:** quantitative real time PCR (Polymerase Chain Reaction). A laboratory technique, based on polymerase chain reaction (PCR), which is used to amplify and simultaneously quantify a targeted DNA molecule.

- **RNAi:** RNA interference. A laboratory technique, based on the biological mechanism by which double stranded RNA (dsRNA) induces gene silencing by targeting complementary mRNA for degradation.

- **Simultaneous hermaphrodite:** an adult organism that has both male and female reproductive organs at the same time (as opposed to sequential hermaphrodites).

- **Stem cell exhaustion**: a decline in the production of new cells.

- **Stem cell niche**: a concept that is used to describe the microenvironment in which stem cells reside. Stem cell niches are composed of microenvironmental cells that nurture stem cells and enable them to maintain tissue homeostasis.

- **Tissue homeostasis:** the maintenance of normal tissue morphology and function.

7.2. List of abbreviations

Anti-phos-H3	Anti phosphorylated histone H3
ASC	Adult stem cell
ASW	Artificial Sea Water
BrdU	Bromodeoxyuridine
BSA	Bovine Serum Albumin
CldU	Chlorodeoxyuridine
CMF-SW	Calcium- and magnesium-free artificial sea water
EdU	Ethynyldeoxyuridine
FACS	Fluorescence activated cell sorting
IdU	Iododeoxyuridine
LRC	Label-retaining cell
p-a	Post-amputation
PBS	Phosphate Buffered Saline
PFA	Paraformaldehyde
RNAi	RNA interference
TAC	Transit amplifying cell
Tc	Cell cycle duration
Ts	S-phase duration

7.3. Curriculum vitae

7.3.1. Publication list

- Stem cells propagate their DNA by random segregation in the flatworm *Macrostomum lignano*. (2012) **Verdoodt F**, Willems M, Mouton S, De Mulder K, Bert W, Houthoofd W, Smith III J, and Ladurner P. PLoS One, 7(1):e30227.

- Proliferative response of the stem cell system during regeneration of the rostrum in *Macrostomum lignano* (Platyhelminthes). (2012) **Verdoodt F**, Bert W, Couvreur M, De Mulder K, and Willems M. Cell and Tissue Research, 347(2):397-406.

- Establishing a flatworm ageing model. (2010) Mouton S, **Verdoodt F**, Willems M, Dhondt I, Crucke J, Braeckman BP, Houthoofd W. Belgian journal of zoology, 140:195-197.

- Measuring S-phase duration of neoblasts in the flatworm *Macrostomum lignano* by double replication labelling and quantitative colocalization analysis. **Verdoodt F**, Willems M, Dhondt I, Houthoofd W, Bert W and De Vos WH. In preparation.

- Cell cycle parameters of adult stem cells in *Macrostomum lignano* (Platyhelminthes) during homeostasis and regeneration: studying actively cycling and label-retaining stem cells using flow cytometry. **Verdoodt F**, Couvreur M, Bogaert P, De Meyere K, Mouton S, Meyer E, Bert W, Willems M. In preparation.

7.3.2. Active contribution to international conferences

- 4th International Macrostomum Meeting, Basel, Switzerland (2010). Oral presentation: "Estimation of S-phase duration during homeostasis and regeneration in *Macrostomum lignano* (Platyhelminthes)." Freija Verdoodt, Ineke Dhondt, Winnok De Vos, Stijn Mouton, Wouter Houthoofd and Maxime Willems

- 17th Benelux Congress of Zoology, Ghent, Belgium (2010). Oral presentation: "Segregation mode of DNA-strands during stem cell division in the flatworm *Macrostomum lignano."* Verdoodt F, Willems M, Mouton S, Houthoofd W, Ladurner P

- 11th International Symposium on Flatworm Biology, Hasselt, Belgium (2009). Oral presentation: "Does non-random segregation of DNA-strands occur during stem cell division in *Macrostomum lignano*?" Verdoodt F, Willems M, Mouton S, Borgonie G, Houthoofd W, Ladurner P

- 2nd International Macrostomum Meeting, Basel, Switzerland (2008). Poster: "Does non-random segregation of DNA-strands occur during stem cell division in *Macrostomum lignano*?" Verdoodt F, Willems M, Mouton S, Borgonie G, Houthoofd W, Ladurner P

8. Summary / Samenvatting

8.1. Summary

The potential of stem cells in regenerative medicine relies upon removing them from their natural habitat, propagating them in culture, and placing them into foreign tissue environment. Prior to effectively and safely using stem cells for therapeutic applications, it is essential to fully understand the mechanisms that regulate when and how to proliferate and, particularly, when to stop proliferating. Given that the microenvironment of stem cells is a controlling factor in this process, the need for *in vivo* research is clear. Nevertheless, relatively little is known about population dynamics of stem cells in steady-state, during growth, or during regeneration. Studying stem cells *in vivo* is impeded by the relative experimental inaccessibility of these cells in most models, and technical constraints imposed by *in vivo* cell imaging. Therefore, flatworms have been described as promising models for stem cell research, given that many of the limitations linked to *in vivo* research, are overcome in these organisms. Most importantly, they possess a large population of adult stem cells (ASCs), so-called neoblasts, which are accessible for experimental manipulation. Neoblasts are the only cells in the organism that have the capacity to divide, and are responsible for the remarkable plasticity of flatworms upon, for instance, regeneration and starvation. Vast advances have been made in the molecular characterization of neoblasts. However, this information will be truly useful if more information on the behavior of neoblast populations under a variety of conditions were to be acquired. However, currently, cellular dynamics in flatworms are relatively understudied, and, therefore, this study focuses on the *in vivo* dynamics of stem cells in the flatworm *Macrostomum lignano* (Macrostomorpha, Rhabditophora), during homeostasis and regeneration.

In **Chapter 1**, a general introduction is given, focused on the dynamics of stem cells in general, and more specifically in flatworms. Two topics are evaluated: (1) protection

mechanisms in stem cells, and (2) the organization of the stem cell pool in subpopulations and the distinct cell cycle dynamics during homeostasis, as well as regeneration.

In **Chapter 2**, label-retaining cells (LRCs) were established in *M. lignano*. We sought to address by which means *M. lignano* neoblasts protect themselves against the accumulation of genomic errors, by studying the exact mode of DNA-segregation during their division. Non-random segregation of DNA-strands has been hypothesized as a protective mechanism to protect genomic integrity in stem cells. To date, this remains a controversial theory. In this study, four lines of *in vivo* evidence have failed to prove non-random segregation in *M. lignano*. Instead, clear evidence was conducted in favor of profound cellular quiescence within the neoblast population. Firstly, performing BrdU pulse-chase experiments, we localized 'Label-Retaining Cells' (LRCs). Secondly, EDU pulse-chase combined with Vasa labeling demonstrated the presence of neoblasts among the LRCs, while the majority of LRCs were differentiated cells. We showed that stem cells lose their label at a slow rate, indicating cellular quiescence. Thirdly, CldU/IdU double labeling studies confirmed that label-retaining stem cells showed low proliferative activity. Finally, the use of the actin inhibitor, cytochalasin D, unequivocally demonstrated random segregation of DNA-strands in LRCs. Altogether, our data unambiguously demonstrated that the majority of neoblasts in *M. lignano* distribute their DNA randomly during cell division, and that label-retention is a direct result of cellular quiescence, rather than a sign of co-segregation of labeled strands.

In **Chapter 3**, the proliferative response of the stem cell pool was studied upon regeneration of the rostrum (the region anterior to the eyes) in *M. lignano*. Firstly, a morphological study is performed to evaluate wound closure and the duration of the regeneration process. Subsequently, the proliferative response of the neoblast population is evaluated. During the regeneration process, both S- and M-phase cells were present anterior to the eyes, a region which is devoid of proliferating cells during homeostasis. Furthermore, BrdU-pulse experiments revealed a biphasic S-phase pattern. During a first

systemic phase, S-phase numbers significantly increased, both in the region adjacent to the wound (the anterior segment) and the region far from the wound (the posterior segment). During the second, spatially restricted phase, S-phase numbers in the anterior segment rose to a peak at three to five days post-amputation (p-a). A blastema, characterized as a build-up of S- and M-phase cells, was formed one day p-a. Altogether, our data present new insights into the cellular response of the neoblast system upon amputation, clearly demonstrating important differences from the situation known to occur during regeneration of the tail plate.

In **Chapter 4**, the S-phase duration during homeostasis and regeneration was determined in *M. lignano*. A double immunohistochemical technique was performed using the thymidine analogs chlorodeoxyuridine (CldU) and iododeoxyuridine (IdU), which label cells in S-phase. By gradually increasing the chase time between the first (CldU) and the second (IdU) pulse, the rate by which CldU-labelled cells lose the IdU-label is an indication for the maximal S-phase duration. To avoid misinterpretation by cells entering an new S-phase, colchicine was used to block cells in metaphase of the cell cycle. For image analysis, a standardized method was established to evaluate colocalization of both labels. Using this approach we found that the maximal duration of S-phase in the majority of neoblasts was approximately 13 hours. No significant change in the S-phase duration was observed during regeneration.

In **Chapter 5**, cell cycle parameters of neoblasts were studied *in vivo* during homeostasis and regeneration in the flatworm *Macrostomum lignano*. To this end, three flow cytometry methods were established. First, the distribution of ASCs within the cell cycle was tested, performing DNA-content analysis (DAPI), both during homeostasis and regeneration. Changes in cell cycle distribution upon amputation, were attributed to an increased number of cycling cells, combined with an adjustment of one or both of the gap phases. Second, the total duration of the cell cycle is determined, by monitoring the progress of EdU-labeled cells through the cell cycle. Using this method, the total cell cycle duration was

estimated to be 30 hours. Third, the cycling activity of a special subset of quiescent ASCs is evaluated, demonstrating activation of these cells during regeneration. Taken together, being rapid, reproducible, and highly informative, the methods that were established in this study are promising to generate further knowledge on stem cell heterogeneity and cycling dynamics in *M. lignano*.

In **Chapter 6**, the results of previous chapters were bundled, discussed, and a general picture of the cellular dynamics in the stem cell pool of *M. lignano* was proposed. Based on the existing knowledge, and on the studies presented here, the neoblast population was concluded to consist of (at least) three subpopulations with diverse cellular dynamics: (1) quiescent cells, (2) a main population of actively cycling cells (with an S-phase and total cell cycle duration of 13 h and 30 h, respectively) and (3) fast-cycling cells. Furthermore, a hypothesis was formulated on the organization of the neoblast pool in a hierarchical structure, with the quiescent cells occupying the highest spots, and the actively cycling cells, the lower spots in the hierarchy. Finally, potential future venues were discussed to further unravel the neoblast population in *M. lignano* and potentially other organisms.

8.2. Samenvatting

De rol van stamcellen binnen de regeneratieve geneeskunde situeert zich in het verwijderen van deze cellen uit hun natuurlijke habitat om ze vervolgens in een vreemde omgeving te plaatsen. Echter, vooraleer deze cellen op een efficiënte en veilige manier een therapeutische toepassing kunnen vinden, is het noodzakelijk om de mechanismen die stamcelproliferatie reguleren, volledig te begrijpen. Aangezien de micro-omgeving van stamcellen hierbij een bepalende rol speelt, is de noodzaak voor *in vivo* onderzoek duidelijk. Toch is er tot op heden onvoldoende kennis over de *in vivo* populatiedynamiek van stamcellen tijdens homeostase, groei of regeneratie. Dergerlijk stamcelonderzoek is voornamelijk gehinderd door de lage experimentele toegankelijkheid van stamcellen in vele modelorganismen en technische beperkingen van stamcelvisualisatie in veel modelorganismen. In platwormen, echter, kunnen deze beperkingen vermeden worden, waardoor hun enorme potentieel voor stamcelonderzoek duidelijk wordt. Het belangrijkste voordeel van platwormen (phylum Platyhelminthes) is ongetwijfeld de aanwezigheid van een grote populatie van adulte (pluripotente) stamcellen die daarenboven toegankelijk zijn voor experimentele manipulatie. Die stamcellen, of ook wel neoblasten genoemd, zijn uitsluitend verantwoordelijk voor de vervanging van alle cellen in het lichaam, inclusief die van de germinale lijn. Bovendien staan de neoblasten in voor de opmerkelijke ‘plasticiteit’ die platwormen vertonen als reactie op bijvoorbeeld amputatie of uithongering. Met de opkomst van functionele genomica, heeft stamcelonderzoek in platwormen een enorme vooruitgang gekend. Deze informatie zal echter pas ten volle benut kunnen worden indien kennis over de dynamiek van stamcellen tijdens homeostase en andere condities hieraan toegevoegd kan worden. Toch is dit tot op heden een onderzoeksgebied dat ondervertegenwoordigd is binnen het stamcelonderzoek in platwormen. Tijdens dit project werd de dynamiek van stamcellen bestudeerd tijdens homeostase en regeneratie in de platworm *Macrostomum lignano* (Macrostomida, Rhabditophora).

In **hoofdstuk 1** een werd een algemene introductie weergegeven over de stand van zaken binnen het stamcelonderzoek, eerst algemeen, later toegespitst op platwormen. Hierbij werd de nadruk gelegd op celdeling binnen stamcelpopulaties, met 2 focuspunten: (1) mechanismen die stamcellen beschermen tegen de schade die kan optreden bij celdeling, en (2) de dynamiek van stamcellen en specifieke parameters van de celcyclus tijdens homeostase en regeneratie.

In **hoofdstuk 2** werd het behoud van label, na pulsen met een thymidine-analoog geëvalueerd in *M. lignano*. Er werd getest op welke manier stamcellen zichzelf beschermen tegen de accumulatie van fouten in hun genoom, door de exacte manier waarop stamcellun hun DNA-strengen verdelen bij celdeling. Er is namelijk een hypothese die stelt dat stamcellen hun DNA-strengen niet willekeurig, maar gericht verdelen over de dochtercellen. Dit zou een manier zijn om de kwaliteit van het DNA in de stamcellen te bewaren. Tot op heden echter is deze hypothese controversieel. In dit onderzoek konden verschillende onafhankelijk experimenten deze hypothese niet bevestigen in neoblasten in *M. lignano*. De uitgevoerde testen toonden echter wel aan dat een subpopulatie van neoblasten zich in een vergevorderde staat van celcyclus-inactiviteit (quiescentie) bevinden. Het uitstellen van celdeling wordt algemeen beschouwd als een manier om de integriteit van het genoom te vrijwaren.
Eerst werd met behulp van BrdU pulse-chase experimenten een populatie van 'Label-Retaining Cells' (LRCs), ofwel label-behoudende cellen, aangetoond. Vervolgens, bevestigden EdU pulse-chase experimenten gecombineerd met Vasa labeling, de aanwezigheid van gelabelde neoblasten binnen de populatie van LRCs. De meerderheid bleken echter gelabelde gedifferentieerde cellen. Er werd aangetoond dat binnen de LRC-populatie, het label verdwijnd aan ee trage snelheid, een observastie die wijst op quiescentie. Een derde reeks van experimenten, bevestigde een lage proliferatie-activiteit met behulp van een CldU/Idu dubbele labelingtechniek. Uiteindelijk werd met behulp van cytochalasin D, de random verdeling van DNA-strengen bevestigd. Samengevoegd toonden de uitgevoerde testen aan dat de meerderheid van neoblasten hun DNA random verdelen

tijdens celdeling en dat behoud van label het gevolg is van quiescentie in plaats van non-random verdeling van DNA-strengen.

In **hoofdstuk 3** werd het regeneratieproces na amputatie van het rostrum (de regio anterieur van de ogen) in *M. lignano*, beschreven. Vooreerst werd dit proces morfologische bestudeerd en werd wondheling en de duur van regeneratie beschreven. Vervolgens werd de proliferatieve respons van het stamcelsysteem geëvalueerd, met behulp van een thymidine-analoog (BrdU) en een merker voor mitotische cellen (anti-phos-H3). Tijdens regeneratie werden zowel S- als M-fase cellen opgemerkt in het rostrum, een regio waarin tijdens homeostase geen celproliferatie optreedt. Verder kon, met behulp van BrdU-experimenten, een snelle respons van de neoblastpopulatie worden aangetoond die opgebouwd was uit 2 fasen. Tijdens de eerste systemische fase, steeg het aantal cellen in S-fase significant in de anterieure regio (dicht bij de wonde) alsook in de posterieure regio (ver van de wonde). Tijdens de tweede gelokaliseerde fase, steeg het aantal S-fase cellen in de anterieure regio tot een maximum, op dag 3 tot dag 5 na amputatie. Een regeneratieblastema, beschreven als een accumulatie van S- en M-fase cellen, was zichtbaar 24 uur na amputatie.
De data die in dit hoofdstuk werden weergegeven creëren nieuwe inzichten in de cellulaire respons van het neoblastsysteem na amputatie en tonen opmerkelijke verschillen aan ten opzichte van de beschreven situatie tijdens regeneratie van the staartregio in *M. lignano*.

In **hoofdstuk 4** werd de duur van de S-fase van neoblasten bepaald in *M. lignano*. Dit werd bewerkstelligd aan de hand van een dubbele kleuringstechniek met chlorodeoxyuridine (CldU) en iododeoxyuridine (IdU), twee thymidine analogen die cellen in de S-fase labelen. Door de chase-tijd tussen de eerste (CldU) en tweede (IdU) pulse gradueel te verlengen, kon de snelheid waarmee CldU-gelabelde cellen hun IdU-label verliezen, gebruikt worden als maat voor de maximale duur van de S-fase. Om foutieve interpretatie van de data, veroorzaakt door cellen die een nieuwe S-fase starten, te vermijden, werd colchicine gebruikt om de cellen te stoppen in de metafase van de celcyclus. Voor de analyse van de

dubbele kleuring werd een methode ontwikkeld die de colocalisatie van beide labels evalueert. Met behulp van deze techniek werd een maximale duur van 13 uur gemeten voor de meerderheid van neoblasten in *M. lignano* tijdens homeostase. Tijdens regeneratie, kon geen significante verandering van deze duur opgemerkt worden.

In **hoofdstuk 5** werden parameters van de celcyclus van neoblasten *in vivo* in *M. lignano* bestudeerd tijdens homeostase en regeneratie. Hiervoor werden verschillende technieken ontwikkeld, die allen gebruik maken van flow-cytometrie. Eerst werd op basis van de precieze hoeveelheid DNA in individuele cellen die gemeten kon worden na DAPI-kleuring, de verdeling van de cellen binnen de celcyclus bepaald, zowel tijdens homeostase als regeneratie. De veranderde verdeling tijdens regeneratie werd verklaard door een verhoogde deelname van cellen in de celcyclus en een aangepaste duur van één of beide intermediaire fasen (G1, G2) in de celcyclus. Als tweede stap werd deze bepaling van de DNA-inhoud gecombineerd met het gebruik van een thymidine-analoog, ethynyldeoxyuridine (EdU). Een populatie S-phase cellen die gelabeld werden met Edu, kon op die manier gevolgd worden tijdens hun verloop doorheen de celcyclus. Op basis van dit experiment werd een totale celcyclusduur van 30 uur gemeten. Ten derde werd de celcyclusactiviteit geanalyseerd van de subpopulatie van neoblasten die een lange celcyclus-inactiviteit vertonen. Deze cellen bleken door amputatie geactiveerd te worden. Door hun snelheid, betrouwbaarheid en reproduceerbaarheid kunnen de technieken die hier ontwikkeld werden, bijdragen aan de verdere studie van het stamcelsysteem in *M. lignano*.

In **hoofdstuk 6** worden de resultaten van de voorgaande hoofdstukken besproken. Deze worden tot een geheel verwerkt om een zo volledig mogelijk beeld te scheppen van de dynamiek van stamcellen in *M. lignano*. Op basis van vooraf bestaande kennis en de resultaten die in voorgaande hoofstukken werden voorgesteld, werd geconcludeerd dat de neoblastpopulatie uit ten minste drie subpopulaties bestaat met een verschillende kinetiek: (1) quiescente neoblasten, (2) actief delende neoblasten (met een S-fase van 13

uur en een totale celcyclusduur van 30 uur) en (3) snel-delende neoblasten. Verder werd een hypothese geformuleerd over de organisatie van deze subpopulaties in een hiërarchische structuur, waarbij hoogste en lagere regionen in de hiërarchie respectievelijk opgevuld worden door de quiescente neoblasten en de actief delende neoblasten. Finaal werden nog enkele mogelijke toekomstperspectieven besproken die kunnen bijdragen aan een verdere uitbreiding van de kennis over het stamcelsysteem in *M. lignano* en mogelijks ook andere organismen.